DEVELOPMENT OF FEA WIDE-BASE TRUCK TIRE AND SOIL INTERACTION MODELS

By

Mehrsa Marjani

A Thesis Presented in Partial Fulfillment

of the Requirements for the Degree of

Master of Applied Science

In

Automotive Engineering

Faculty of Engineering and Applied Science

University of Ontario Institute of Technology

Oshawa, Ontario, Canada

July 2016

ABSTRACT

Tires are considered one of the most important components of ground vehicles as they are the only link between the chassis and ground. They support the vehicle weight and cushion road surface irregularities to provide a comfortable ride. Tires are designed in a way that provide necessary tractive, braking, and cornering forces to form a safe and stable ride for ground vehicles. Recent advancements in computerized and virtual modeling provided an efficient methodology for accurate prediction of tire characteristics. In this thesis Finite Element Analysis (FEA) is employed as a method to accurately construct a new virtual wide-base tire model, validate it, and then study rolling resistance of the tire on a hard surface. This thesis includes tire-soil interaction and effects of soil on tires rolling resistance. To accurately study rolling resistance on soft soil, various soil models are created by using FEA and Smoothed Particle Hydrodynamics (SPH), as a representative of dry sand soil. Soil models are calibrated by using shear-displacement and pressure-sinkage simulation tests. The simulation results are then compared to published data. Also, the created soil models are compared to each other to determine the optimum one based on computational time efficiency and accuracy. SPH, as the accurate current method for soil modeling, has long computational solving time. In this thesis FEA/SPH hybrid soil models are studied and modified to achieve lower computational solving time while having the desirable accuracy. Rolling resistance of tire on each soil model is carried out through various loads and inflation pressures and the simulation results are compared to physical test results to examine the accuracy of each soil model. The new hybrid soil model created in this thesis reduces the computational CPU time almost by half and slightly increases accuracy compared to full SPH soil model.

TABLE OF CONTENTS

LIST OF FIGURES

LIST OF TABLES

NOMENCLATURE

Symbol	Description	Unit
b	Loading plate radius	m
c	Cohesion	kPa
$c_{2,3}$	Radial/bias tires coefficients	-
$C_{0,1,2,3}$	Material constants	N/mm^2
$C_{4,5,6}$	Dimensionless material constants	-
C_r	Rolling coefficient	-
E_i	Internal energy	N/mm^2
FEA	Finite Element Analysis	-
f_r	Rolling Resistance Coefficient	-
F_x	Longitudinal force	kN
F_y	Lateral force	kN
F_z	Normal force	kN
k_c	Cohesive modulus of terrain deformation	kN/
k_φ	Frictional modulus of terrain deformation	kN/m
M	Total mass	kN
M_x	Overturning moment	Nm
M_y	Rolling resistance moment	Nm
M_z	Self-aligning moment	Nm
n	Exponent of terrain deformation	-
p	Pressure	MPa
FEA	Finite Element Analysis	-
RRC	Rolling Resistance Coefficient	-
SPH	Smoothed Particle Hydrodynamics	-
V	Velocity	km/h

Symbol	Description	Unit
Z	Sinkage	m
ξ	Critical damping effect	-
Φ	Angle of internal shearing resistance	deg
ρ_0	Initial material density	kg/m^3
ρ	Material density	kg/m^3
μ	$\mu=(\rho/\rho_0)-1$	-
ω	Frequency	Hz

ACKNOWLEDGEMENTS

The author expresses gratitude to Volvo Group Trucks Technology for their continuous support during the course of this study. Also I would like to thank NSERC and Auto21 for the additional funding of this research work.

I am always thankful to Dr. Moustafa El-Gindy for his endless support and guidance during my research work. I would like to thank Dr. Alhossein Mostafa Sharaf, postdoctoral fellow from the Military Technical College in Egypt, for his technical support and editing this thesis.

I would like to express my gratitude to my colleagues, in particular Kristian Lardner and Arnold Odrigo for their kind help and support.

I am forever thankful to my parents Mohsen and Parivash. Everything I am from the very first step I took to the last, it is all due to their love, support and patience along the way.

My deepest appreciation to my brothers Mehrdad, Mehryar, Ashkan, and my sister in-law Shirin who stood by me and supported me in all possible manners through my way.

Finally, I am always thankful to my dearest, Farzad, for lighting up this path with his patience and guidance and for all the love and care he brought to my life during this journey.

CHAPTER 1

INTRODUCTION

This chapter presents the necessary background relevant to the topics of tire soil interaction. Originally, the motivation, objectives and scope of the present work are outlined. Additionally, a critical review to the well published work employing Finite Element Analysis (FEA) method for both tire and soil and Smoothed Particle Hydrodynamics (SPH) for soil are carried out.

1.1 MOTIVATION

Tires can be considered as one of the most important components of ground vehicles since they are responsible for transferring the arising forces from ground in longitudinal, lateral and vertical directions. These forces primarily control the vehicle performance and stability. All main forces and moments which may affect vehicle's motion are applied to the vehicle by tire's contact area [1]. Tires support vehicle weight, provide comfortable ride, and they are acquired to provide adequate braking, traction for driving, and stability in direction. The goal of the presented thesis is to develop a new tire model using FEA with high accuracy that can predict the majority of the tire's characteristics.

Previously in order to examine in-plane and out of plane characteristics of tires, the only accurate method was to conduct field or laboratory tests. Laboratory testing setup, measuring data accurately, and providing the necessary environment for each specific test for various tire characteristics can be extremely expensive and time consuming. Every characteristic of tire to be determined needs a specific laboratory test setup which some was hard to implement. All aforementioned limitations, and the arising computational

power has motivated researchers to pursue for alternative methodologies to overcome such problems.

Numerical simulation has become a popular method for predicting tire characteristics. The effect of numerous parameters such as material characteristics, speed, tire loading, inflation pressure, even tire size and physical dimensions of the tire can be easily evaluated. This capability enables researchers to simply investigate tire characteristics, while considering the effects of each parameter without the necessity for various, expensive, and time-consuming laboratory testing set up.

It has been widely recognized that, the interaction between tire and soft soil is complex and not only dominated by the tire design parameters but also by the soil mechanical properties. Furthermore, the developed theoretical or physical off-road tire models may not be enough to predict a wide range of tire and soil parameters.

1.2 OBJECTIVES AND SCOPE

The main objective of this thesis is to employ Finite Element Analysis (FEA) method for the development of highly sophisticated wide-base tire model with further potential of accurate prediction of tire characteristics. The accuracy of the proposed numerical model has to be verified by comparing the results of the model with that of typical measurements for the same tire and testing conditions. The next step is to determine the tire characteristics on soft soil. To model the soil, FEA, Smoothed Particle Hydrodynamics (SPH), and combinations of both methods are the methodologies employed to create different soil models. In the first steps of soil modeling, the soil is calibrated through two well-known tests, pressure-sinkage relationship and shear strength. The chosen soil for this thesis is dry sand. The goal here is to model the soil correctly to have dry sand characteristics. Once the

soil is verified, soil models are created such that not only they have high accuracy, but also they have low computational time as well. All soil models are then compared to each other under same circumstances. While studying various soil models, tire model characteristics are also examined on soft soil. In the end, an optimum soil model is chosen which is both accurate and efficient.

1.3 THESIS OUTLINE

The work is organised in six chapters. A brief description of the issues discussed in each chapter is given below, in order to provide an overview of the approach followed in the thesis.

CHAPTER 1: INTRODUCTION

The aim and objectives of the investigations are clearly stated and a brief description for the research framework is outlined. An in-depth review of the state of the art in the field of tire modeling is presented. The review covers the aspects of pneumatic tire's construction and forces and moments, rolling resistance, tire and soil modeling methodologies.

CHAPTER 2: WIDE-BASE TIRE MODELING

The development of the wide-base pneumatic tire model using Finite Element Analysis (FEA) method is presented. Furthermore, the validation procedures and results are illustrated including tire tests such as vertical stiffness test, static footprint length and width test and drum-cleat test.

CHAPTER 3: SOFT SOIL MODELING

Different models representing dry sand soil are developed. Both pressure-sinkage and shear strength tests are employed to verify the modeled soil. Additionally, all soil models are examined regarding to computational CPU time efficiency.

CHAPTER 4: ROLLING RESISTANCE TESTS AND SIMULATION ON HARD SURFACE

The facility provided for physical tests of rolling resistance is explained. The modeled tire's rolling resistance is simulated on hard surface and the results are compared to the measurements.

CHAPTER 5: ROLLING RESISTANCE TESTS AND SIMULATION ON SOFT SOIL

Accuracy of the created soil models and tire model are examined. The tire's rolling resistance simulation results on soft soil are compared with measurements received from physical tests

CHAPTER 6: CONCLUSION AND SUGGESTIONS FOR FUTURE WORK

This chapter summarises the major findings of the presented thesis. The main outcomes as well as some suggestions for future research work are outlined.

1.4 LITERATURE REVIEW

The literature review covers the current state of arts on the topic of research presented within this thesis. There are four main topics within this section: pneumatic tires, rolling resistance of tires, tire modeling, and soil modeling.

1.4.1 Pneumatic Tires

Tires can have great influences on diverse aspects of vehicle performance, handling and ride superiority. Tires should be constructed in a way that can provide directional and handling stability, adequate traction for the vehicle and comfortable safe ride for the passenger. Tires should have the tolerance for vehicles weight. The design and structure of tires should enable the tires to cushion vehicle's ride while over irregular surfaces.

Pneumatic tires are normally constructed from different components which can be named as carcass, belt plies, tread, undertread, side wall, and beads. A cross-section of a tire is shown in Figure 1-1. Tires are built from highly complex rubber combination, nylon fibers, steel cords, and other materials to satisfy the aforesaid requirements [2]. Carcass is the most important component in tires since it supports air pressure, vertical load and absorb shocks from road irregularities. It is constructed from coats of flexible cords with high modulus of elasticity covered with low modulus rubber composites. Each layer of cord is developed from fabrics of natural synthetic or metallic compounds. The type of material which is used for tread differs from one tire to another depending on the purpose of tire. Tire sidewalls are made from styrene-butadiene composites in order to be greatly resistant to fatigue and scuffing [1].

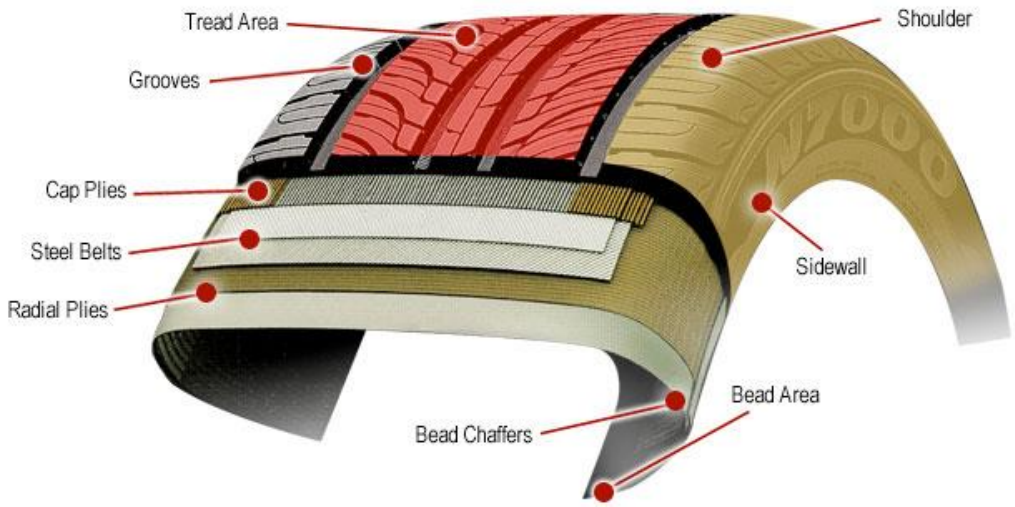

Figure 1-1 Typical radial tire components [3]

The carcass as mentioned above is the most important component in the tire since it is influential on the performance characteristics of tire. The geometric design of cords layers (plies) can define the characteristics of tire. The angle between the cords and center line of the tire, known as crown angle, defines the direction of cords. A tire will have good cornering characteristics but harsh ride when crown angle is low. Meanwhile tires with high crown angle provide comfortable ride and poor handling. In this case tires have been divided in to two categories based on their crown angle, bias-ply and radial-ply tires. Bias-ply tires have cords extended diagonally from bead to bead in carcass with approximately 40° crown angle. The cords in plies (varying from 2-20) run in opposite directions in a diamond shape pattern as shown in Figure 1-2. Radial-ply tires has one or more layers of cords placed radially in carcass with 90° angle. The cords in the belt have low crown angles of approximately 20 degrees. Radial-ply tires had been originally introduced by Michelin in 1948 and they are currently being widely used for passenger cars and among heavy-duty machines while bias-ply tires are still being used in military equipment, motor cycles and agricultural machines [1].

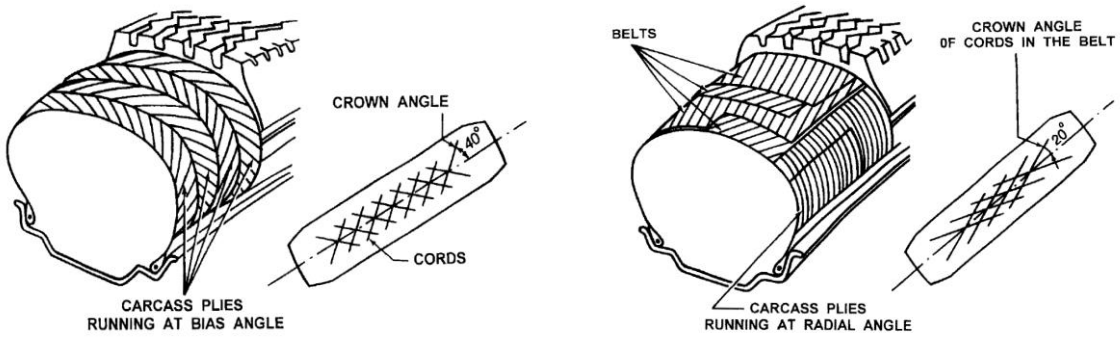

a) b)

Figure 1-2 a) Bias-ply and b) radial-ply tires [1]

1.4.1.1 Wide-Base Tires

Wide-base tires are new to industry and it has not been long that wide-base tire are taking place of dual truck tires. Wide-base tires as a replacement for dual tires on truck tractor pusher axles is being introduces in 2000 [4]. Figure 1-3 is a comparison of wide-base tire and dual tires. Wide-base tire contact patch is the overall contact patch of dual tires. In this case the essential gap between the dual tires space is eliminated and wide-base tires take less space compared to dual tires while having the same cornering and tractive properties [4].

Figure 1-3 Wide-base tire vs dual tire [5]

Wide-base tires have successfully improved fuel efficiency up to 10% and they have saved 740 pounds from truck weight [6]. It has been found that wide-base tires have longer brake life and lower costs [4]. By using wide-base tires, less managing for tires configuration is needed, since there are fewer tires and wheel to cope with [7]. As a new area in tire designing, wide-base tires are interesting subject of research during past decade.

In comparison of dual truck tires versus wide-base tires, Michelin has specified that since wide-base tires have two sidewalls and lower hysteresis, they are having 30% lower rolling resistance compared to dual tires with four sidewalls. Rolling resistance consisting 35% of the fuel consumption. Michelin claims that XOne wide-base tires improve the fuel efficiency by 10% [8].

1.4.2 Tire Forces and Moments

In order to describe forces and moments acting on tire, an axis system should be defined. A well-known axis system, which is widely used, is presented by the Society of Automotive Engineers (SAE) and it can be seen in Figure 1-4.

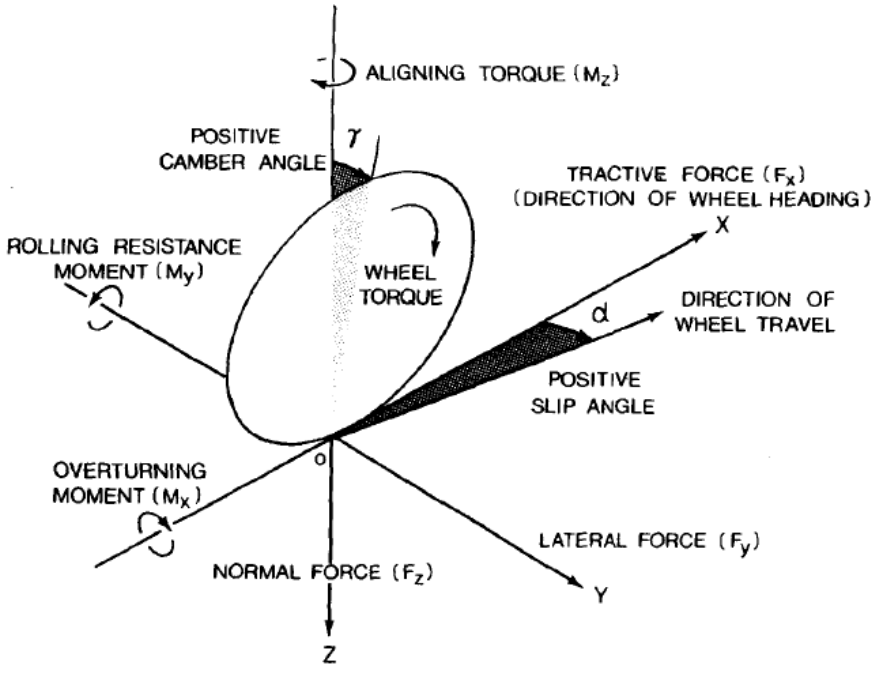

Figure 1-4 SAE tire axis system [1]

The center of tire contact with ground is considered as the origin of axis. As shown on the SAE axis there are three forces and three moments acting on the tire from ground. Forces can be listed as tractive force (longitudinal force) F_x, lateral force F_y, and normal force F_z. Moments acting on the tire also can be named as overturning moment M_x, rolling resistance moment M_y, and self-aligning torque M_z.

Tractive force (longitudinal force), F_x, is the result of the force developed in contact area in x direction; it is divided into three main categories known as the rolling resistance force, longitudinal frictional force, and longitudinal reaction force. The force applied to the tire in the opposite direction of rolling while free rolling is defined as the rolling resistance force, which will be discussed in depth later. Longitudinal frictional force is the force developed in the contact area in the x direction caused by the slip or skid which is resulting from vehicles acceleration and deceleration. The slip is caused by the difference between rolling speed of tire and traveling speed. Longitudinal reaction force is caused by the tire running on speed bumps, stairs, and such surface irregularities. Since the force is applied as a shock, it can be harmful to rim and tire [1].

Lateral force, F_y, is developed in the tire contact area during a cornering maneuver or when an external lateral force is applied such as a cross wind.

Normal force, F_z, is the static force applied to the tire due to gravity. Also when the vehicle is moving there is a vertical acceleration of sprung mass which can increase the vertical force noticeably.

There is a non-symmetric vertical pressure distribution along the width of the tire in the contact area which results an overturning moment M_z. Overturning moment is acting about the x axis on the tire spindle.

Tire rolling resistance moment, M_y, is acting on about y axis and it caused by the uneven vertical pressure in contact area of the loaded tire while rolling.

Tire vertical M_z moment acts about the z axis and on the spindle of the tire. This moment is caused by the non-symmetric force distribution on contact plane; it is called self-aligning moment as well. When a vehicle is taking a cornering maneuver, the cornering force created will be acting with an offset behind the center of the contact area. The vertical moment that is created by the offset and the cornering force, tends to restore the tire into the original position of tire without steering which is the reason why it is called aligning moment.

1.4.3 Rolling Resistance

Among all the forces and moments applied to tire the main purpose of this research is to study tire's rolling resistance which is one of the forces that is applied longitudinally in the opposite direction of rolling tire.

The main reason of rolling resistance is the tire material hysteresis which is caused by the carcass deflection when the tire is rolling. The air circulating around the tire while rolling, which in this case tire is acting as a fan, and the tire/road friction while sliding, are also the secondary reasons of rolling resistance [1].

There are many factors affecting rolling resistance of tires such as temperature, inflation pressure, speed, road surface (smoothness and irregularities), normal load, and etc. While

free rolling, rolling resistance coefficient (RRC) can be calculated by ratio of tractive force f_x to normal load f_z [1]:

$$RRC = \frac{f_x}{f_z} \tag{1-1}$$

Considering primary and basic outlook, rolling resistance coefficient of tires on different surfaces is estimated as shown in Table 1-1.

Table 1-1 Estimated RRC based on surface type [9]

Vehicle Type	Concrete	Medium Hard	Sand
Passenger cars	0.015	0.08	0.3
Heavy trucks	0.012	0.06	0.25
Tractors	0.02	0.04	0.2

As it can be seen in Table 1-1 surface texture and irregularities plays an important part on RRC values. Also, effect of speed and inflation pressure should be considered as well. Due to previous research works, rolling resistance coefficient of truck tires can be estimated up to 100 km/h. Equation (1-2) and (1-3) are presented by Wong, where "f_r" is rolling resistance coefficient (N), and "V" is Velocity (km/h). [1]:

Radial-ply truck tire: $$f_r = 0.006 + 0.23 \times 10^{-6} \times V^2 \tag{1-2}$$

Bias-ply truck tire: $$f_r = 0.007 + 0.45 \times 10^{-6} \times V^2 \tag{1-3}$$

As it can be seen from the formulas and Figure 1-5 by increasing the speed, rolling resistance will be increased both for bias-ply and radial-ply tires. Bias-ply tires have higher rolling resistance compared to radial-ply tires at same speed, which is because of their differences on tire construction and materials that have the most influence on rolling resistance due to tire hysteresis. The greater number of carcass plies and the tread and sidewall's thickness are the reasons for higher rolling resistance.

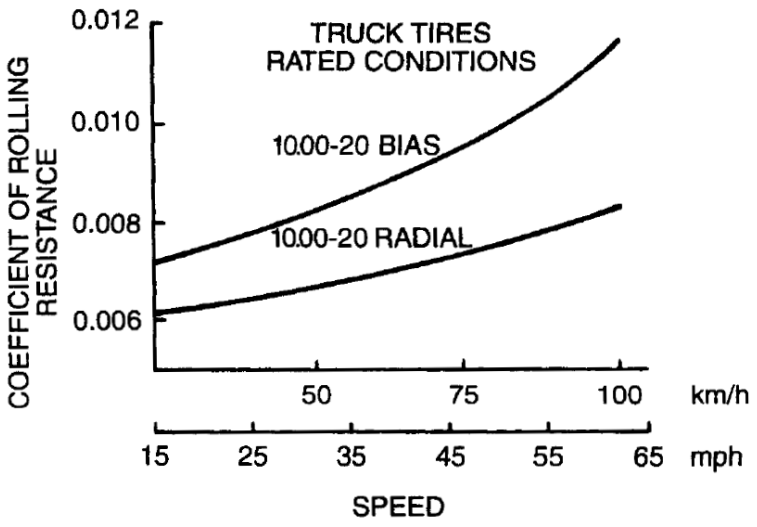

Figure 1-5 The effect of speed on RRC [1]

Based on the rolling resistance model presented by Fitch, 1994, a linear function of rolling resistance is shown in Equation (1-4). As the equation shows, rolling resistance of tires increases with increase in mass and speed [10]:

$$R_r = 9.8066 C_r (c_2 V + c_3) \frac{M}{1000} \tag{1-4}$$

In this equation, "C_r" is surface rolling resistance, "V" stands for speed, "c_2" and "c_3" are radial/bias tires coefficients, and "M" is the total mass.

Studying effects of inflation pressure on rolling resistance is highly dependent on the surface type of the ground that is in contact with the tire. Underinflated and overinflated tires may have different rolling resistances depending on type of surface they are contacting with. While overinflated tires are running on hard surfaces, the tire deflection decreases, which drops tire hysteresis losses as well. However, when the tire is running on soft surfaces such as sand, higher inflation pressures results in higher ground penetration work which will increase rolling resistance in a considerable way as shown in Figure 1-6.

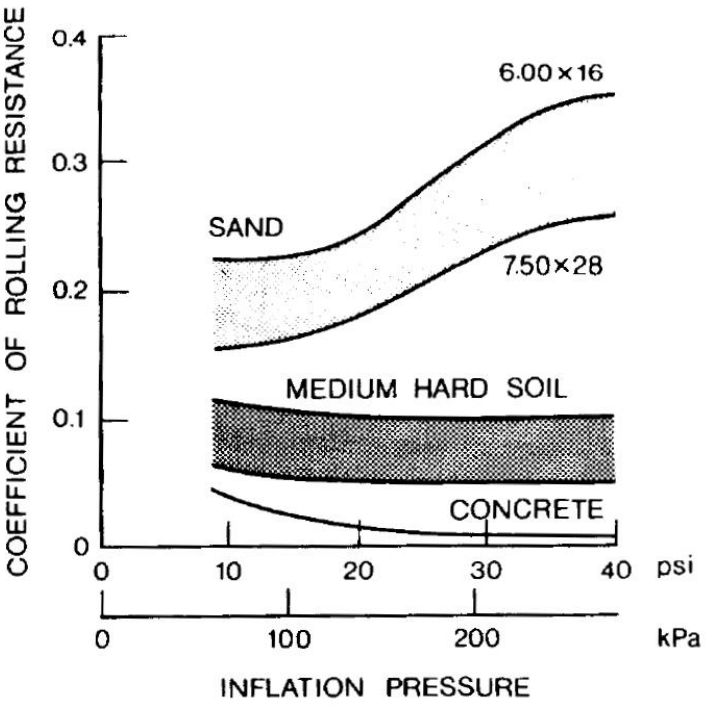

Figure 1-6 Effects of inflation pressure on RRC [1]

1.4.4 Tire Modeling

Ever since the very first pneumatic tire was made, many manufacturers and researchers have created analytical, empirical and virtual tire models in an effort to better understand tire behaviour. Accomplishing physical laboratory tire testing is time consuming and expensive. It requires high amount of considerations, and complicated experiment set-up. By using a combination of analytical models and recreation of laboratory tests in virtual environment, there have been huge developments in virtual tire testing in order to reduce the need for physical experimentation [2].

Due to the highly nonlinear nature of tires, it is difficult to create an experimental model that can describe all of the characteristics of its physical counterpart. As a result, most tire models only focus on incorporating a few specific characteristics of the tire. In the

following topics, analytical tire models and Finite Element Analysis (FEA) tire models will be discussed widely.

1.4.4.1 Analytical Tire Models

Analytical tire models are simplified tire models which are consisted of parameters from tire that can be achieved from physical experiments. The complex nature of a tire may be broken down into simple motion equations. These models are useful tools to predict some tire characteristics such as braking, tractive, cornering forces and vibrations. However, there are difficulties such as complicated experiment setups, validation limits, and being time consuming.

The simplest and most popular analytical tire model is the single point contact mechanism. It has been assumed that the tire is in contact with ground through one point which is the reflection of the wheel center on the ground. A schematic view of a single point contact model is shown in Figure 1-7.

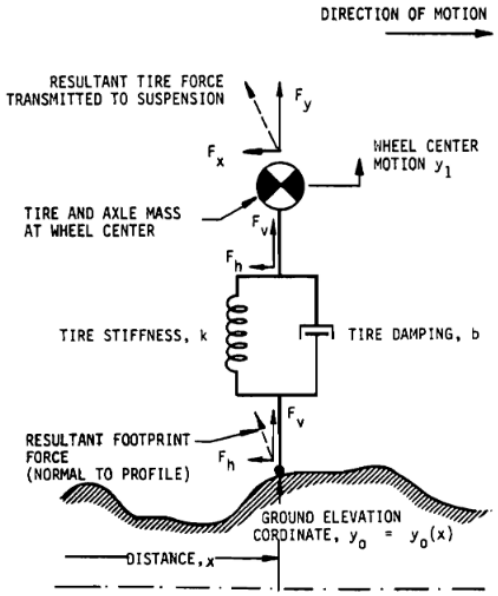

Figure 1-7 Single point contact model [11]

The single point contact models are sensitive to surface irregularities especially regarding to short wave length road profiles, which makes them inefficient for examining dynamic parameters such as rolling resistance. These models are used for long wave profile inputs. This limitation has been solved by using simplified series of linear radial springs connected to the wheel center representing a tire, which is known as equivalent plane tire model. The force that is applied to the center of the tire from spring deformations is equal to the forces that are applied from the road profile. Davis was the first to introduce a model with two-dimensional in-plane radial springs. A schematic view of the model can be seen in Figure 1-8.

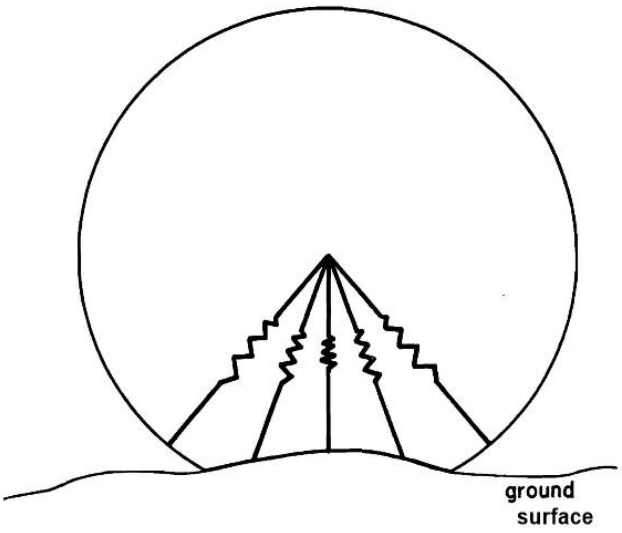

Figure 1-8 Tire model with radial-spring [12]

Although the problems of single point contact model is solved, the equivalent plane tire model has the limitation of predicting out-of-plane parameters.

Zeglaar and Pacejka presented a rigid ring tire model which is a representative of a passenger vehicle tire as shown in Figure 1-9. In this model the tread and steel belts are considered to be a rigid ring. In order to have a representative of tire deformation in contact

area a new parameter is defined as vertical residual stiffness. To represent the tire sidewall the rigid ring is placed on an elastic foundation.

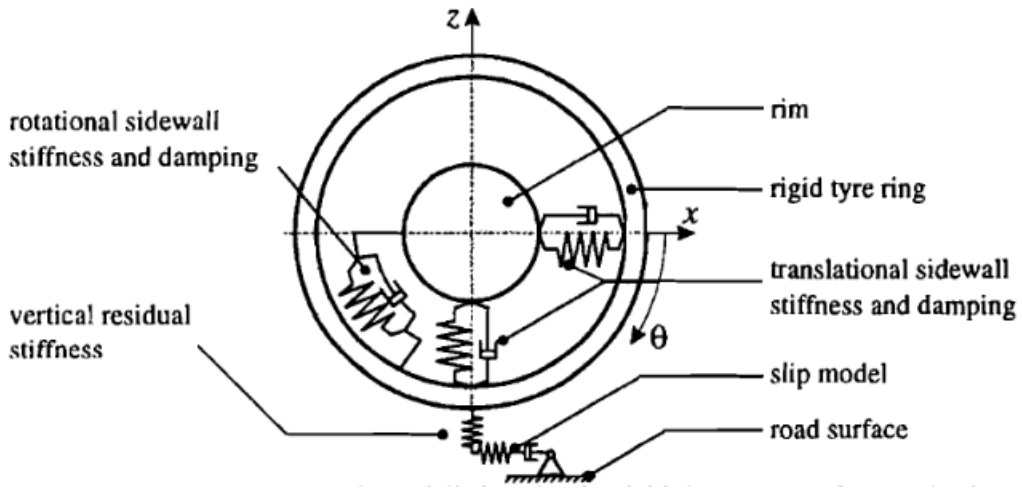

Figure 1-9 The rigid ring model placed on elastic foundation [13]

In continuation of their work, drum-cleat test id used with a drum having diameter of 2.5 m to find tire's frequency response. The resultant frequency response is then used to figure out the required parameters. Drum rotational speed is increased up to 150 km/h. It is then observed that vertical force on tire and effective rolling radius is increased. Test results are in agreement with measurements.

1.4.4.2 FEA Tire Models

Since tires have a very complex construction and various design variables, it is suggested to use computer simulations in order to accurately predict its behaviour compared to analytical models. Finite Element Method (FEM) has proven to have the ability to closely match experimental results while correlating the effect of influencing factors on the tire's characteristics. Finite Element Analysis (FEA) models have been widely used in analyzing stress and strain since 1970 [4].

FEM provides more detailed information about tire responses even inside the tire structure, and it helps to get a deeper perspective about tire characteristics in various situations. It was not until in late 1990s that the complexity of models were increased due to improvement in computational power [4].

By using a combination of physical tests and FEA testing Yong *et al* made a step toward understanding contact relationships of tires and terramechanics [14]. In this experimental-analytical study different inflations had been assigned to the tire rolling on soil. By using series of FEA tests, inflation pressure influences on tractive force and sidewall stiffness had been conducted which showed a good agreement with measured data. His work showed the accuracy and reliability of FEA tire models while describing tire-soil interaction properties under loading [14].

Nakajima and Padovan developed a tire model on an arbitrarily shaped surface. Tire sliding events involving impact with holes and bumps are simulated by finite element simulation software named ADINA [15]. The tread and sidewalls are modeled by a linear viscoelastic ring on an elastic foundation. The vertical and horizontal history of the tire spindle, while the tire is sliding over a bump and a hole has been discussed at different velocities. The computed and experimental results shows that the simulated test results are reliable.

Gelosa found that for FEA simulations for tire testing, it is best to use 3D continuum solid elements rather than shell elements [16]. It is shown that the results with higher accuracy, may take longer solving CPU time. Complex tread geometry and also the behaviour of the tire at tire/road contact area needs FE code to perform the highly non-linear contact conditions. Gelosa also discussed the material properties definition. In the research the cords are kept separate from rubber matrix in order to give material properties to each one

separately. Mooney-Rivlin constitutive law defines the material strain energy function. By considering different 3D Finite Element tire models for tests such as cornering test and cleat test models, the results prove that these models are powerful tools for tire dynamic characteristics [16].Chang and El-Gindy developed a new full nonlinear finite element P185/70R14 passenger car radial-ply tire model for superior dynamic research [17]. The tire consists of reinforced rubber composites and rubber materials modeled as an assembly of three-dimensional Mooney-Rivlin hyperelastic solid finite elements for rubber material. Fiber-reinforced layered membrane finite elements are used for reinforced rubber composites and beam elements for two beads. The tire had run on a 1.7-meter- diameter spinning test drum. The FFT (Fast Fourier Transform) algorithm is applied to examine the transient response information in the frequency domain. The rotating test drum served as an impact input in order to excite the tire in-plane free vibration modes. The simulation is detected as a successful progress.

A good example of FEA tire modeling is a three-groove FEA truck tire model representing radial-ply tire of size 295/75R22.5 developed by Ali *et al.* that is used to predict tire characteristics through different tests [18]. The tire is modeled with PAM-CRASH and is validated through different tests such as a static vertical stiffness, footprint area test, and a free vibration test. Also tire enveloping characteristics and combined camber and cornering characteristics had been considered. Test results corresponds to the published data.

Chae also has a complete analysis about tire modeling and the validation process of truck tire models in his thesis [19]. He modeled a 295/75R22.5 nonlinear three-dimensional FEA truck tire which is created using three-layered membrane elements, hyperelastic solid elements, and beam elements. He validated the tire using various virtual tire tests and

comparing the results with physical responses. After validation process the tire model is ready to predict in-plane and out-of-plane parameters for the rigid ring tire models while using FEA tire model for the first time.

Reid is one of the leads in using FEA using ESI group software, PAM-CRASH, to model a wide-base tire with characteristics of a *Michelin XOne XDA* 445/50R22.5 as shown in Figure 1-10 [4]. He used experimented data received from Volvo group in North Carolina to validate the modeled tire.

a) b)

Figure 1-10 a) Physical *Michelin XOne XDA* tire and b) the modeled tire [4]

The validation results is in good agreement with provided data. Then the rigid ring model parameters on rigid surface is conducted through various tests.

1.4.5 Soil Modeling

Tire modeling and tire-soil interaction has been the focus of many research topics during past years. There are two main reasons for the importance of this research field. In order to predict vehicle characteristics under different operating conditions, it is important to establish a functional relationship between the design characteristics of off-road vehicle and terrain characteristics. Likewise, being able to predict the terrain changes caused by

the passage of an off-road vehicle is also essential [20]. Although there had been remarkable advancement in testing facilities, performing physical tests which can be lead to accurate results regarding to tire forces and tire-soil interaction needs great effort concerning financial issues and experiment set up. Also physical tests are time consuming which can increase the potential occurrence of human error.

1.4.5.1 Terramechanics

There are different properties and characteristics of soil that need definition and explanation, before starting the modeling procedures. Density, shear modulus, pressure-sinkage parameters, and etc need to be defined. There are vast equipment and technologies to measure soil properties such as bevameter, cone-penetrometer, cone-index, pressure-sinkage test.

Two of the chief endeavours regarding to terramechanics mathematical predictions for soil deformation had been accomplished by Bekker in 1950's and 60's [21] [22] [23] and Janosi and Hanamoto in 1961 [24]. Bekker had great achievements regarding to soil modeling. Bekker's model aimed to investigate normal forces interfacing with soil, however, Janosi and Hanamoto created formulation regarding to shear prediction of soil using stress-strain relationships.

Osman has successful achievements regarding to soil shear resistance parameters [25]; He determined cohesion and angle of shearing resistance. There are different available testing techniques to examine different soil techniques; such as the translational shear box, the N.I.A.E shear box, the shear vane, the bevameter, the triaxial test, the weighted sand-coated methods, and the friction trolley method, in order to examine different soil characteristics. In order to measure shear force, translational shear test is being used. In this case

translational shear box filled with soil, contains two halves which are free to move relative to each other, while a constant strain is applied. In this research, the translational shear test is used in virtual environment to validate the created soil. Osman tested clay, dry sand, and wet sand proving that these methods of testing are reliable to accurately predict soil characteristics.

Two traditional methods of determining soil characteristics in civil engineering, known as cone penetrometer, and bevameter technique, are described in next paragraphs.

The Cone penetrometer technique is built by Waterways Experiment Station (WES) of the US Army Corps of Engineers in World War II. It has a 30 degree right circular cone and base area of 0.5 in^2 as shown in Figure 1-11.

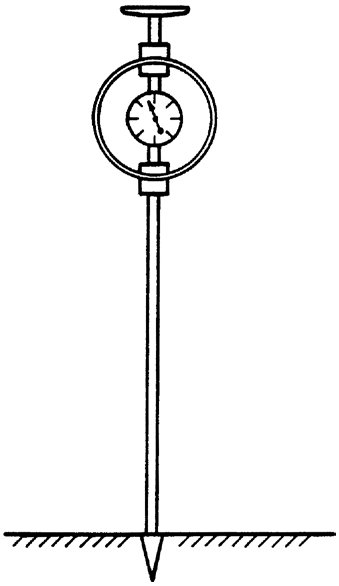

Figure 1-11 WES cone penetrometer [20]

By using penetrometer a parameter is gained which is named as “cone index” and it defines the resistance to penetration into the terrain per unit cone base area. Wismer and Luth used cone index and tire parameters in order to predict pneumatic tire’s tractive performance

[26]. Later on Yong *et al.* compared soil's measurement device results with terramechanic properties and proved that shearing slip may not be determined through the use of a cone penetrometer [27].

The vehicle applies both shear and normal loads on the surface of the terrain. It is very important to have a good understanding regarding to pressure-sinkage test since the total sinkage of tire in soil is highly dependent on it. Bevameter technique is consist of two separate tests to determine both shear and compressive strength of the soil. The Figure 1-12 shows the bevameter originally made by University of Newcastle and modified at Carlton University [20].

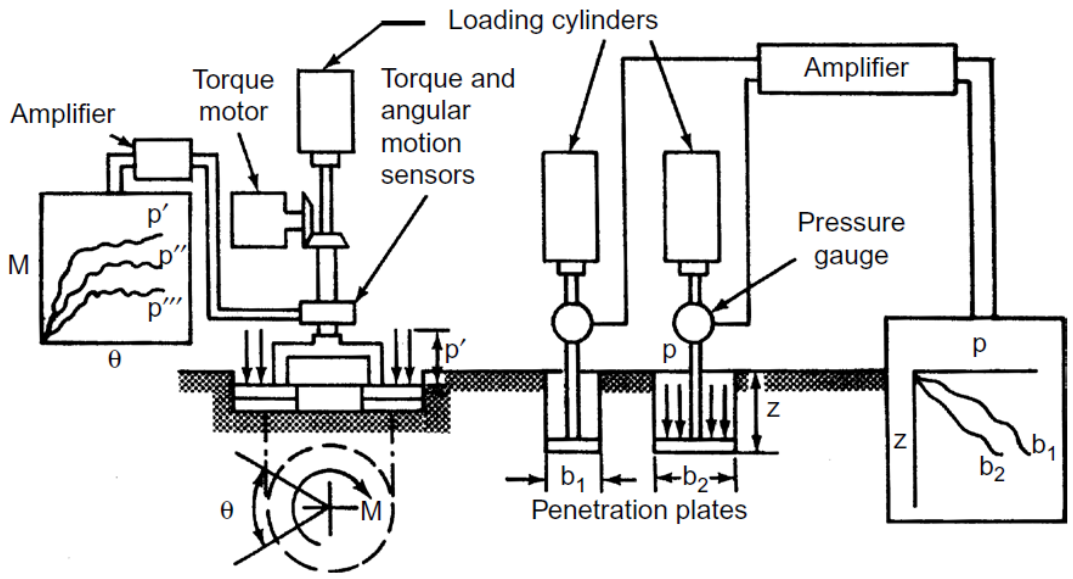

Figure 1-12 Bevameter schematic diagram [20]

As it is shown in Figure 1-12, the right side of the bevameter applies normal load to the sinkage plate in order to implement the pressure-sinkage tests, and on the left side, shear strength can be determined. Via covering the shear plate (on left) by rubber, rubber–train

shear characteristics can be measured. Also slip-sinkage can be measured with potentiometer while applying torque to the shear ring and measuring angular displacement.

1.4.5.2 FEA Soil Modeling Method

In continuation of soil modeling, two recently used FEA, SPH methods and also the combination of two methods, hybrid FEA/SPH soil modeling methods are going to be discussed in following topics.

Among numerous types of methodologies that currently exists to model nonlinear systems, FEA is being widely used in many different fields. FEA is a powerful and useful method of modeling regarding to tire dynamics and internal stresses, however, regarding to soil modeling compared to Smoothed Particle Hydrodynamics it might not be sufficient. In this thesis the differences between FEA and SPH is widely discussed through series of simulations are done to examine the influence each method may have on tire-road interactions.

FEM is being widely used for stress analysis. By implementing FEM in modeling Hiroma *et al.* studied tire-soil stress distribution about the contact patch [28]. To investigate tractive forces viscoelastic soil model is used as a representative of soft soil. The soil mechanical responses is influenced by deformation rate. In this case the FEA tire model is considered rigid and is allowed to first sink into soil and then rolls with constant vertical load, speed, and slip as shown in Figure 1-13.

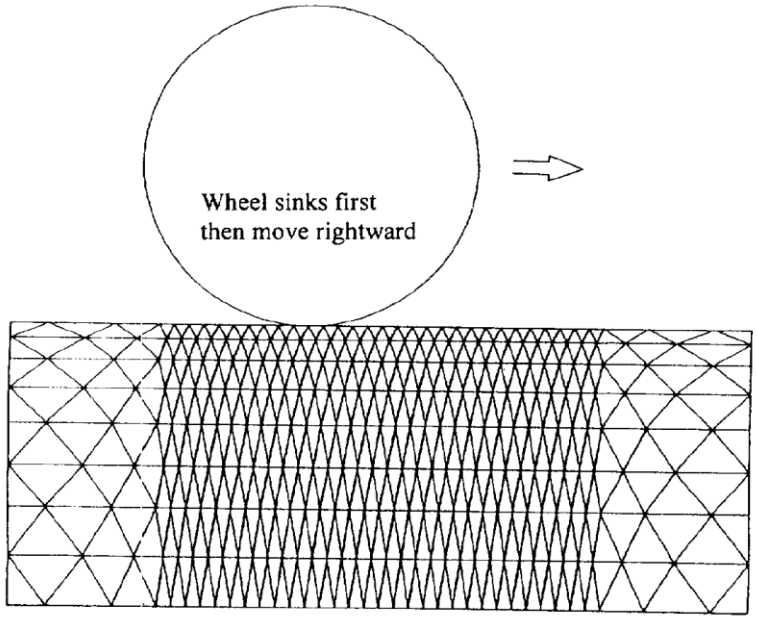

Figure 1-13 Two dimensional FEA tire-terrain interaction model [29]

The soil layer shown in Figure 1-13 is a representation of a sandy loam with a depth of 400 mm and a moister content of 73%. The tractive forces are successfully investigated under several slip levels.

Shoop developed a full three dimensional model in order to simulate tire interaction while rolling on deformable terrain [29]. A rigid wheel, a simplified deformable tire with user-defined sidewall elements, and modal analysis tire models are joined while rolling on deformable terrain. By using critical-state plasticity models, snow and compressed sand are modeled as deformable terrains. The snow model is validated by using pressure-sinkage test in laboratory and field. The measured forces and displacements of the model matched the measured data. The rigid ring wheel on snow is also validated through experiments and the results are satisfying regarding to rolling resistance forces, and snow displacement.

In 2005 Chiroux developed a three dimensional soil model by using ABAQUS and a rigid rotating wheel as shown in Figure 1-14. The soil contains five different regarding to mesh

density; all areas are connected to each other by surface contacts. The parts of soil which the wheel had contact with has smaller mesh compared to the rest of the model. The reason for this modeling approach is to save the amount of time and required storage.

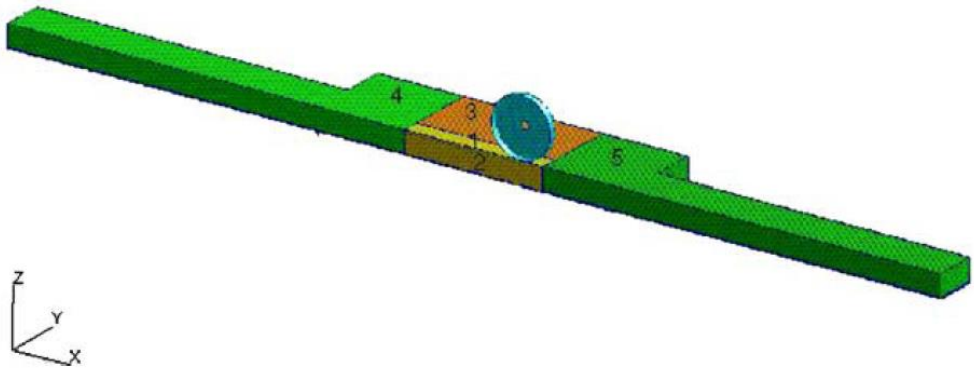

Figure 1-14 Simulation environment of rigid wheel and soil interaction [30]

Norfolk Sandy Loam is the type of soil used in this research. A concentrated load is applied to the center of tire. Friction is considered as 0.6 and it is defined between tire and soil surfaces. The target of the research is to study stress and deflection on soil which is successfully corresponding to experimental and analytical data.

In 2009 Slade modeled and validated a Goodyear 315/80R22.5 RHD FEA truck tire. He also modeled an elastic-plastic FEA soil representing dense sand which is fully validated with the use of material properties from published data. FEA modeling and simulations took place by using ESI software groups, PAM-CRASH. He made a good comparison regarding to tire reaction on soft soil and rigid surface. A new rigid ring model for soft soil is developed. His results showed that rolling resistance on sandy loam is three times higher than rigid surface [31].

1.4.5.3 SPH Soil Modeling Method

There has been numerous research through mathematical modeling of soil which is very complex due to non-homogeneous behaviour of soil even among samples from one source, under same circumstances. FEA in this case, may not be the best option in modeling soil. FEA soil models cannot characterize shear properties of soil and they have sponge like behaviour regarding to pressure-sinkage test. In this case Smoothed Particle Hydrodynamics (SPH) is a better representative aimed at soil modeling in virtual environment. SPH is a meshless modeling method which stated by Schlatter in 1999 [32]. Basically in SPH models the material is modeled as a compact group of particles. It was originally used for galaxy formation investigation. However, in recent advancement SPH is widely used in soft body impacts, fluid dynamics, and soil flow analysis.

Each FEA element is constrained to only interact with their immediate neighbour, However, SPH can interact with all neighbouring particles within a certain defined distance known as smoothing length as shown in Figure 1-15.

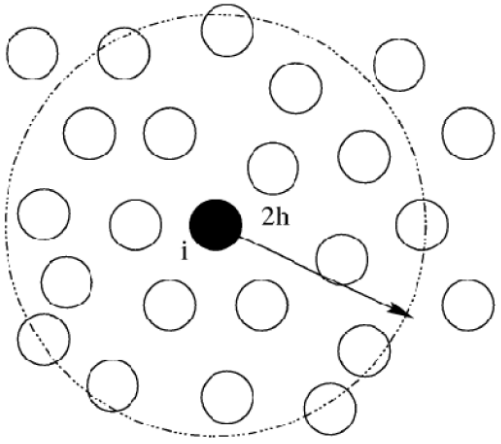

Figure 1-15 Particle i with 2h allowance of interaction distance with neighbouring particles [32]

Bui *et al.* used SPH to simulate soil-water interactions [33]. Dry soil as one phase while using an elastic-perfectly plastic material and saturated soil are modeled as separate phases of water and soil which in this case water is modeled as viscous fluid. Bui *et al*. determined that the SPH model is easily able to solve for problems with large amounts of deformation. Due to the difficulty of the experiment, the results are not compared with numerical results, however, the received results are acceptable based on stability of the calculations.

Later on in 2008 Bui, *et al.* applied an artificial stress method to eliminate SPH numerical unsteadiness in cohesive soil [34]. In order to achieve more realistic simulation results, hydrostatic pressure of soil is calculated precisely from constitutive relations. It is claimed by Bui that SPH particle's performance is similar to atoms. When SPH faces compression, particles repel each other and while stretching, particles attract each other. Bui conducted that through different means, for instance artificial stress method and cracking treatment, tensile instability can be overcome. The gained numerical results shows good correlation with experimental and FEM results, which shows that SPH can be used to resolve general geotechnical problems.

In 2013 Dhillon validated different FEA and SPH soil models through PAM-CRASH using pressure-sinkage and shear tests [2]. The results for pressure-sinkage simulation tests are in agreement with measurements, however, there are room for improvement in regards to the comparable accuracy to physical measurement. In his research a uniformly 25 mm meshed SPH soil is selected which is developed by converting FEA elements to SPH. A series of rolling resistance tests are simulated with results in support of trends presented in published data.

1.4.5.4 SPH/FEA Hybrid Soil Modeling Method

Hybrid soil models are a composition of both FEA and SPH spoil modeling techniques. The exact composition (ratio of SPH/ FEA) of these hybrid models varies depending on the desired simulated test. However, these hybrid models are a new concept. There are various models that are the combination of both methods such as FEA tire rolling on SPH soft soil, however, there is just a few models consisting both SPH/FEA as a hybrid model representing an organisation such as soil.

In order to model 2D and 3D hypervelocity impacts in 1997 Groenenboom used an SPH modeling method via PAM-SHOCK [35]. The results extracted from simulation are adequate while compared with experimental data. Later on Groenenboom used a combination of FEA and SPH creating a model to compare the results of both models. Tied coupling method is used in PAM-SHOCK to link SPH particles to FEA elements. The new model showes less than 0.1% deviation compared to previous model which is considered successful.

Later in 2010, Groenenboom used a coupled FE-SPH model to represent hydrodynamics and fluid-structure interaction (FSI) via ESI software group, PAM-CRASH as shown in Figure 1-16 [36].

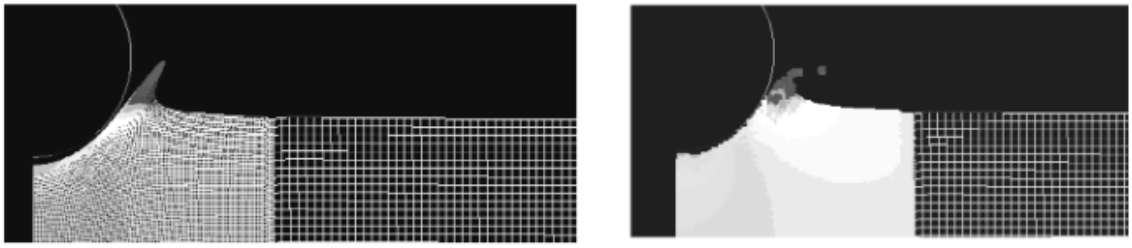

a) b)

Figure 1-16 a) Segment of the FEA and b) coupled FEA-SPH model

The type of link used between coupled FE-SPH is a tied contact which defines virtual spring elements between FE and SPH that acts as a rigid connection between two parts. FE-SPH model represents a deep water wave to study structures responses such as ships and off-shore structures. The FSI results based on FE-SPH model proved the suitability and maturity of this method regarding to hydraulic and hydrodynamic tests in industrial environments.

In 2010 Lescoe had made a vast investigation regarding to soil modeling via ESI group software using PAM-CRASH comparing results from different soil construction such as FEA, SPH, and FEA/SPH hybrid model [37]. He is the first creating Hybrid model for soil in order to examine computational time differences between FEA, SPH, and combined FEA/SPH soil models. The FEA soil model is the first soil model to be constructed. The SPH soil model is then obtained by converting all elements in original FEA soil model to SPH. In order to create combined model, the top portion of FEA soil model is converted to SPH and by using tied link FEA elements are linked to SPH particles. The hybrid model is analysed with varying compositions, altering the depth and density of the SPH component. It has been shown that SPH is much better representative of soil compared to FEA. He examined both rigid and pneumatic tire on soft soil and the results shown higher rolling resistance for both tires while running on SPH [37].

1.5 CHAPTER SUMMARY

Tires are divided into two categories based on the formation of cords plies: bias-ply and radial-ply tires. The forces and moments applied to these tires can be all shown through the use of the conventional SAE axis. One of the main forces examined through this work is the rolling resistance of the tires which is a force developed in the opposite direction of a

rolling tire. The main reason of rolling resistance is the tire material hysteresis which is caused by carcass deflection when the tire is rolling. Investigating the saving in fuel consumption, wide-base truck tries have become increasingly popular due to their reduction in rolling resistance compared to their successor, the dual truck tires.

In order to model tires two methodologies are discussed:

1. Analytical tire models

   Simplified tire models which are obtained from tire parameters extracted from physical experimental testing. The complex construction of the tire is broken down into simple motion equations. The limitation of analytical tire models is their dependant on time consuming and expensive physical laboratory testing and its ability to only investigate a limited number of tire parameters.

2. Finite Element Analysis (FEA) tire models

   FEA has been widely accepted method in analyzing stress and strain since 1970. It provides much more detailed information about tire responses even inside the tire structure and it helps to get a deeper perspective about tire characteristics in different circumstances. FEA methodology overcomes the previous limitations and provides a wide range of possibilities for the future of tire modeling.

Soil modeling has also been studied. Three areas of this subject have been considered:

1. Terramechanics

   The basis of mathematical prediction of soil are from Bekker's model investigating normal forces interfacing with soil, and Janosi and Hanamoto's formulation regarding to shear prediction of soil using stress-strain relationships.

2. FEA soil modeling

   A variety of FEA usage in soil modeling is discussed. FEA is a powerful and useful method of modeling regarding to tire dynamics and internal stresses, however, it may not be a good representative of soil due to lack of penetration.

3. SPH soil modeling

   SPH is a meshless modeling method that the modeled materials are constructed as a group of particles and it is widely used in soft body impacts, fluid dynamics, and soil flow analysis. FEA is more timewise efficient however, SPH represent more accurate results.

4. FEA/SPH hybrid soil modeling

   It is a new modeling combination which has been recently used for various purposes. It can reduce computational solving time and by new modeling methodology it has same accuracy as SPH.

The focus of this research is comparing all four mentioned methods of modeling soil while studying an FEA truck tire model.

CHAPTER 2

WIDE-BASE TIRE MODELING

Tires are one of the most important components of ground vehicles. Tires are the only components that are in direct contact with the road surfaces. They support the vehicle weight and cushion road surface irregularities to provide a comfortable ride. Tires should be designed in a way that can provide adequate tractive, braking, and cornering forces to create safe and stable ride for ground vehicles. There are many experimental tests to be done in laboratories to define tire characteristics. However, experimental analysis requires a large amount of time and financial resources.

Fortunately, a new generation of tire modeling has become more fruitful due to technological advances, which saves a lot of capital and time. Virtual tire testing with high technology computers are becoming more popular due to their wide range of possibilities in design and accurate results.

Effective FEA tire model simulations can duplicate of the experimental tire tests with good accuracy. The main objective of this chapter is to build a nonlinear FEA truck tire model, validate it through different tests and compare the experimental tire test measurements with the results provided by virtual simulations.

In this chapter a *Michelin XOne Line Energy T* tire is modeled through virtual environment and it is validated via different simulation procedures. The findings of this chapter had been presented in the American Society of Mechanical Engineers (ASME) conference in Boston 2015 [38].

2.1 THE PROPOSED FEA TIRE MODEL

Among the well-known software packages, ESI software group is a strong and reliable package regarding to virtual crash testing which is being used by numerous commercial vehicle manufacturers since it can accurately model complex non-linear systems. PAM-CRASH and PAM-MESH are used in this research to model, validate and simulate different test environments. By using explicit solution, PAM-CRASH is a strong software to solve dynamic, non-linear structural mechanics [36].

The UOIT FEA *Michelin XOne Line Energy T*[1] tire model with the size of 445/50R22.5 is developed using PAM-CRASH from ESI Studios. The dimensions and specifications are also shown in Figure 2-1 and Table 2-1.

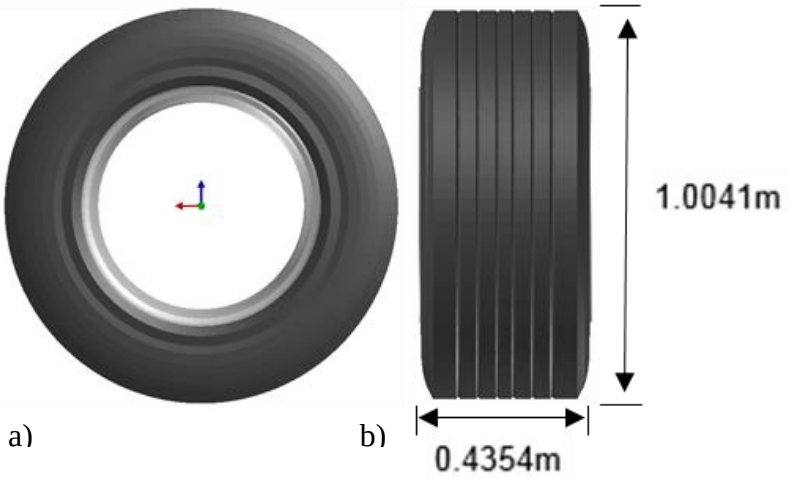

Figure 2-1 a) Side and b) front view of UOIT FEA *Michelin XOne Line Energy T* wide-base truck tire model

[1] Since the material properties of the *Michelin XOne Line Energy T* is unknown in this research, the term "UOIT" is added to the beginning of the FEA tire model name.

Table 2-1 Technical specification of *Michelin XOne Line Energy T* tire

Tire Size	445/50R22.5
Tread Width	371 mm
Tire Overall Weight	160.3 lbs
Maximum Vertical Load	10200 lbs.
Maximum Inflation Pressure	120 psi
Unloaded Tire Diameter	1004.1 mm
Loaded Radius	465.3 mm
Contact Patch Length	231 mm
Contact Patch Width	370 mm

The tire consists of rubber materials and reinforced rubber composites and it is modeled as an assembly of three-dimentional Mooney Rivlin hyperelastic solid elements. It has 212 beam elements, 2014 shell elements, 3,604 membrane elements, 6,360 solid elements, and 11,978 four node tetrahedral elements.

The first step of the modeling started with a footprint of the *Michelin XOne Line Enrgy T* tire received during a visit to the Volvo facilities. The tire's dimensions of the tread and grooves are found through the footprint in Figure 2-2.

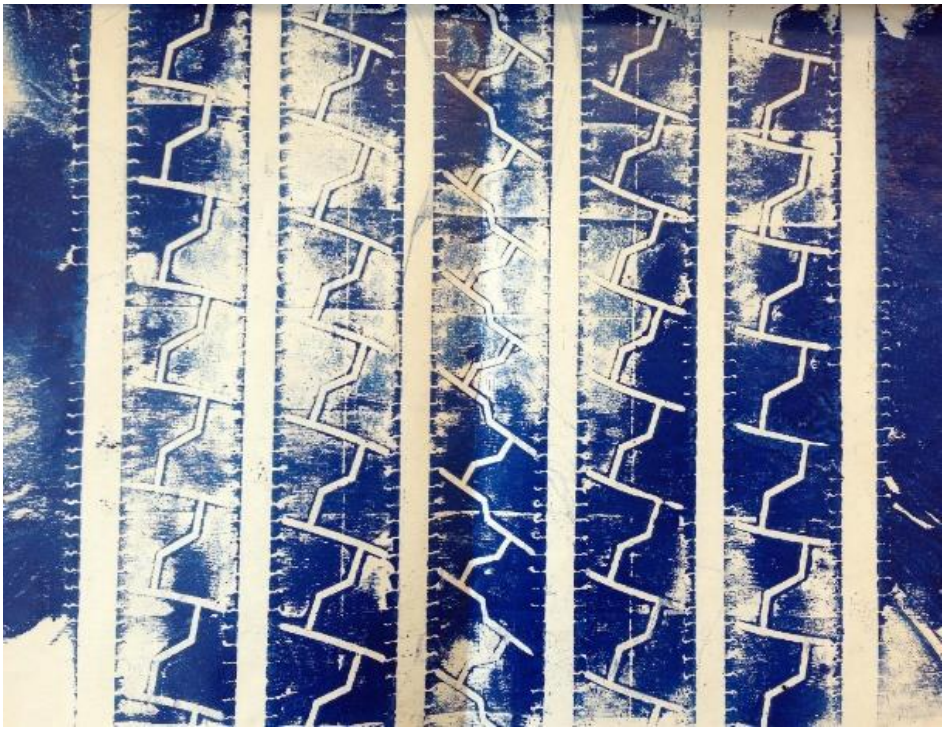

Figure 2-2 *Michelin XOne Line Energy T* tire footprint

The numerical modeling is carried out node by node through PAM-MESH. With a rough sketch of the tread pattern, the more intricate grooves and individual elements could be built next. Based on a published information from Michelin company regarding to tread depths and overall spacing, the tread model is developed, shown in Figure 2-3.

A section cut of the tire is then created which contains all tire parts and the tread is then assembled on the section cut as shown in Figure 2-4. Material properties were available for each part and they are assigned to the section cut through PAM-CRASH.

The sidewall methodology and modeling procedures employed in this thesis are considered as 2D layered membrane owing to the very complex rubber material compounds of tire sidewalls and it was developed through research works done by Chae [19], Slade [31], Dhillon [39], and Reid [4]. Additionally, Sidewall thickness is implemented to model by

directly measuring the real tire section cut provided for this research by Volvo Group in North Carolina as shown in Figure 2-5.

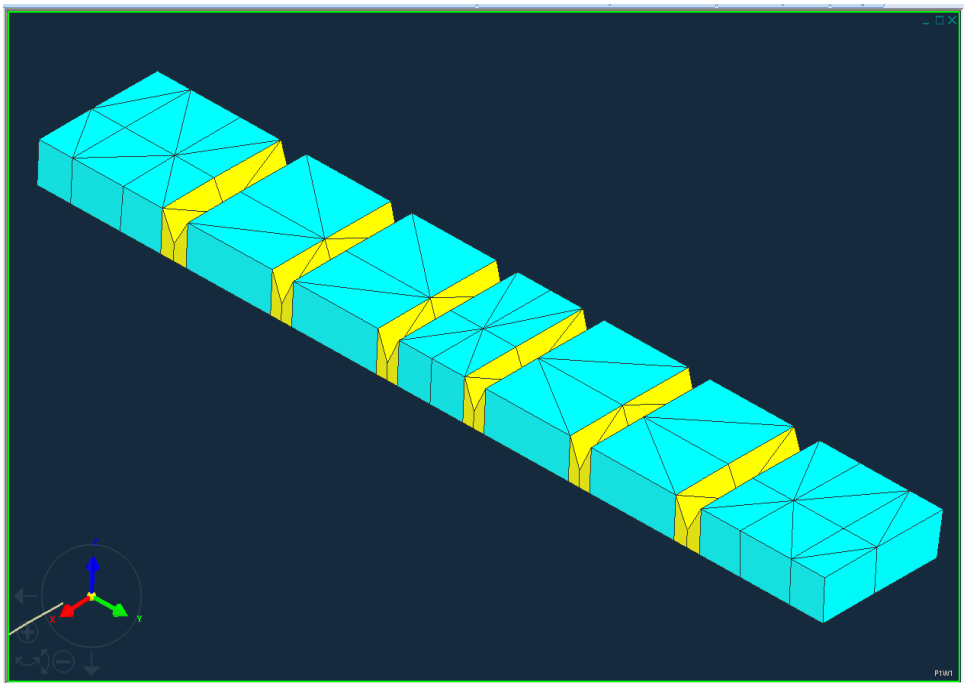

Figure 2-3 UOIT FEA *Michelin XOne Line Energy T* model tread design

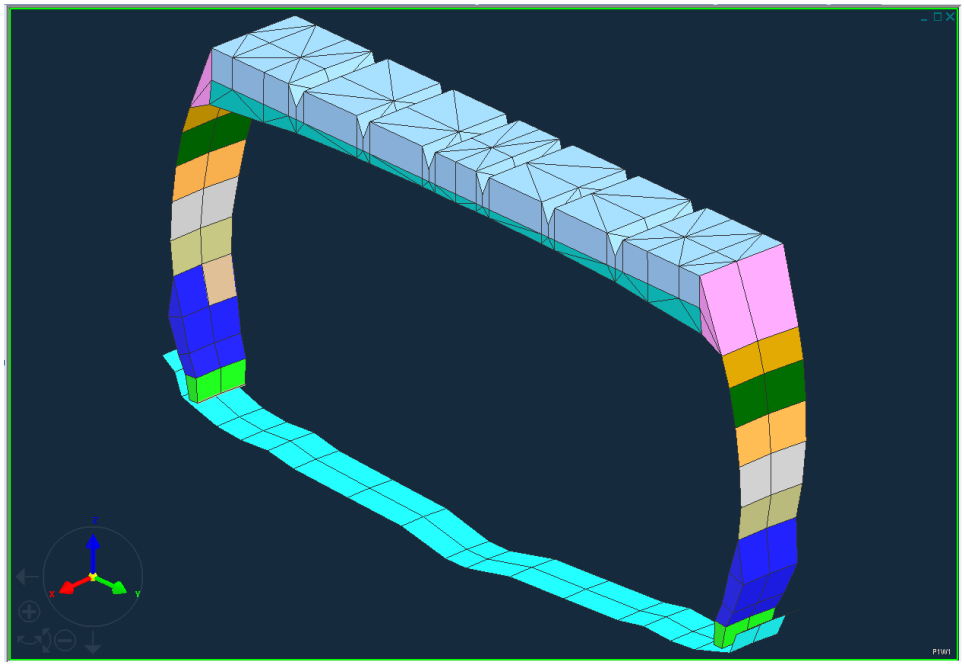

Figure 2-4 Completed UOIT FEA *Michelin XOne Line Energy T* tire model section cut

Figure 2-5 Physical *Michelin XOne Line Energy T* tire Section cut

Based on the number of parts constructing the sidewall in tire model, the physical tire section cut sidewall is divided into different areas. Each area is measured separately with a fine caliber and an artificial thickness is then assigned to each part of sidewall. The section cut is then revolved to make the full tire model, shown in Figure 2-6.

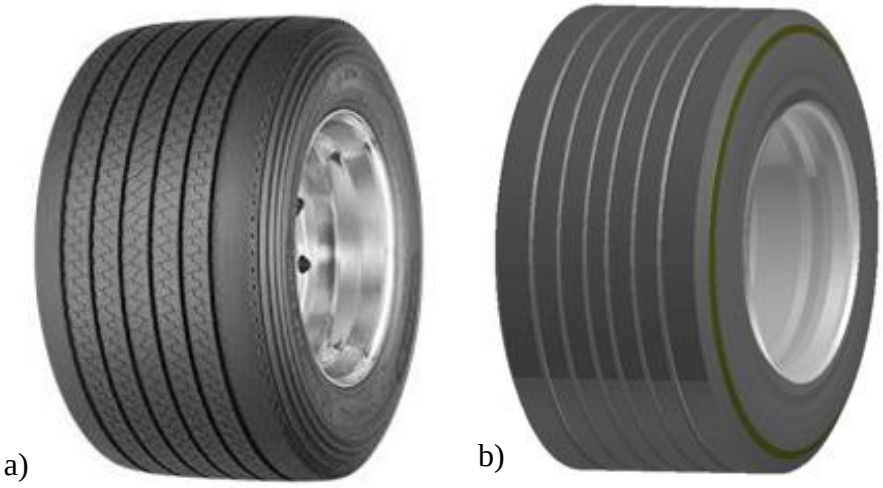

Figure 2-6 a) Actual *Michelin XOne Line Energy T* tire and b) UOIT FEA *Michelin XOne Line Energy T* tire model

Preliminary errors did occur, as to be expected, with small construction discrepancies from the highly-complex structure. They are quickly edited out, and the following full tire model is produced in the same dimensions and properties of the original *Michelin XOne Line Energy T* tire. Preliminary simulations using the UOIT FEA *Michelin XOne Line Energy T* tire model shows promising results in terms of no computational errors.

2.2 TIRE VALIDATION

In order for the tire to be validated some virtual tests had been carried out and the results are compared with published data and the measurements provided from actual tests took place in Volvo facility at North Carolina. Consequently, several numerical simulations have been carried out to virtually validate the tire model such as the vertical stiffness test, static foot print length and width, and drum-cleat test are provided in this research to validate the FEA tire model. Then the model is also validated by comparing the provided RRC values with simulation results in CHAPTER 4.

2.2.1 Vertical Stiffness Test

In order to validate the tire model via PAM-CRASH, vertical stiffness test is applied to the model to calculate tire's spring rate. During this test in simulation environment, the tire is constrained in all directions except for the Z direction which allows the tire to move in the vertical axis which is shown in Figure 2-8. The tire is subjected to a ramp load which caueses the tire to deform. The resultant deflection is then recorded from the coresponding vertical load, and the relationship between load and deflection is calculated. Tire 3D contact patch under ramp load is shown in Figure 2-8. The tire is inflated to 120 psi (0.83 MPa) and the measured results are shown in Figure 2-7.

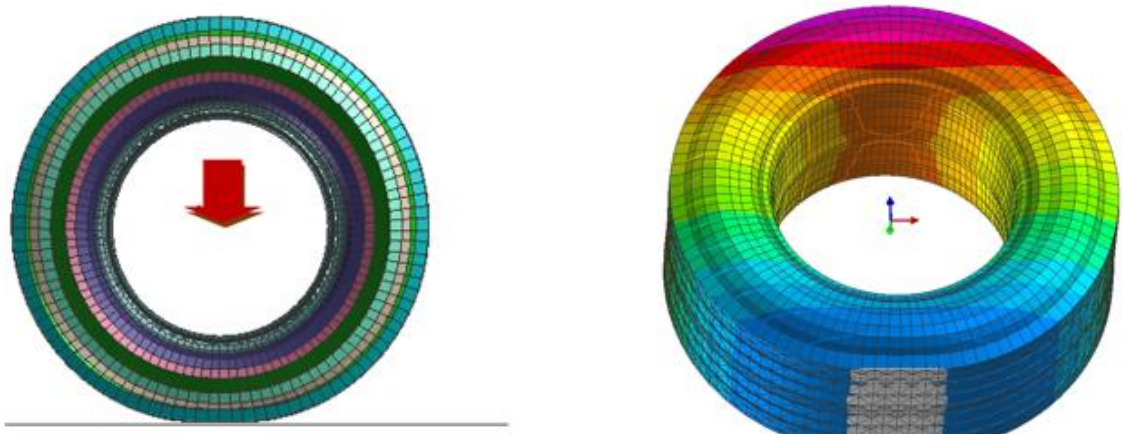

a) b)

Figure 2-7 a) Vertical tire load at the spindle and b) tire 3D contact patch

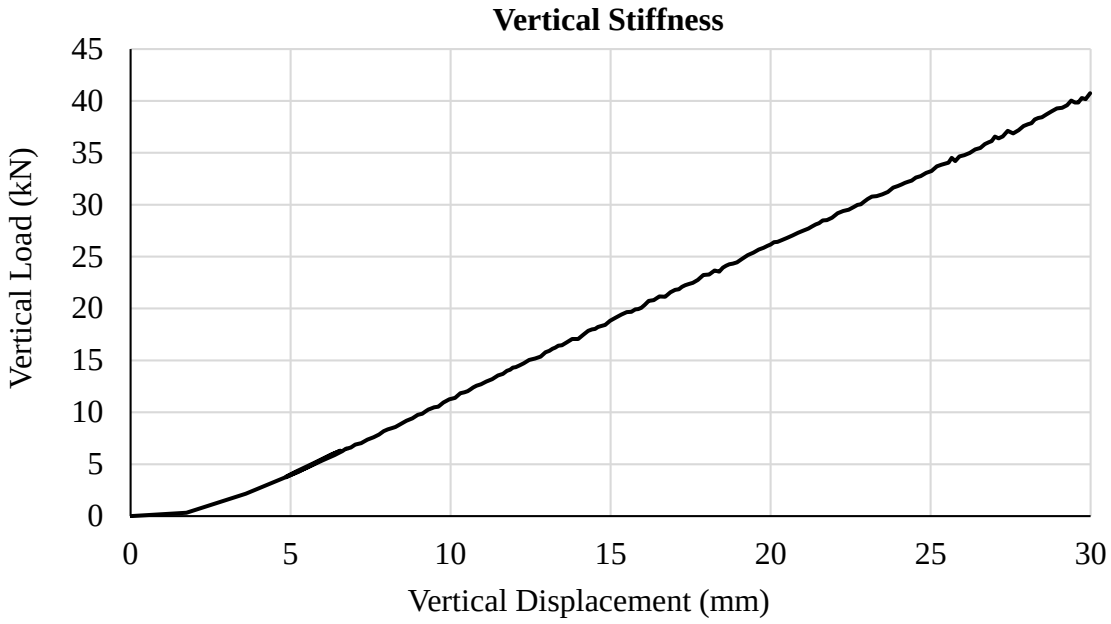

Figure 2-8 Vertical tire load versus deflection

The virtual spring rate is calculated through Equation (2-1) and compared with experimental measurements provided on Michelin's technical characteristics of the *XOne Line Energy T* tire at normal condition brochure. Results are shown in Table 2-2.

$$Spring\ Rate = \frac{Applied\ Vertical\ Load}{Measured\ Deflection} \quad (2\text{-}1)$$

Table 2-2 Measurements and predicted virtual stiffness

	Stiffness	Unites
Calculated Spring Rate	133.45	kg/mm
Measured Spring Rate	140.40	kg/mm
Current Error	4.95%	-

2.2.2 Static Footprint Length and Width

For a given tire vertical weight and inflation pressure, the tire footprint on road surface in terms of length and width can be easilly simulated and validated for different applications as shown in Figure 2-9. It is widlly known that, tires with different footprint areas are stronglly affecting the generated forces at the tire ground contact patch.

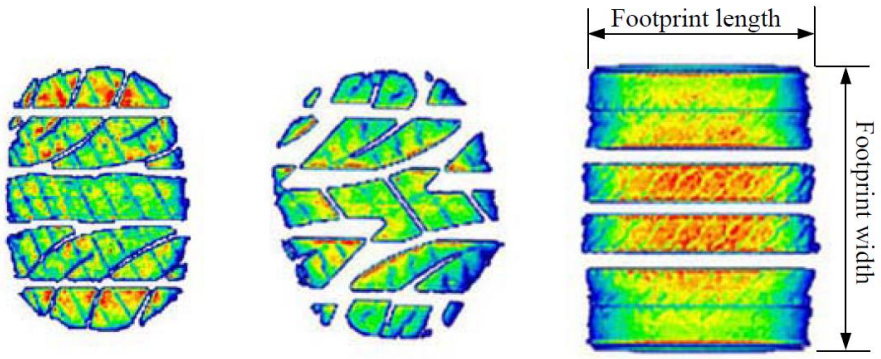

a) Passenger car tire b) Light truck tire c) Commercial truck tire

Figure 2-9 Different footprints resulted from various tires [19]

The footprint of the propsed model of *Michelin XOne Line Energy T* at inflation pressure of 120 psi and vertical load 9000 lbs is ilustrayed in Figure 2-10. Furthermore, a comparison between the results of the proposed tire model and the results obtained from *Michelin XOne Line Energy T*'s brochure is shown in Table 2-3.

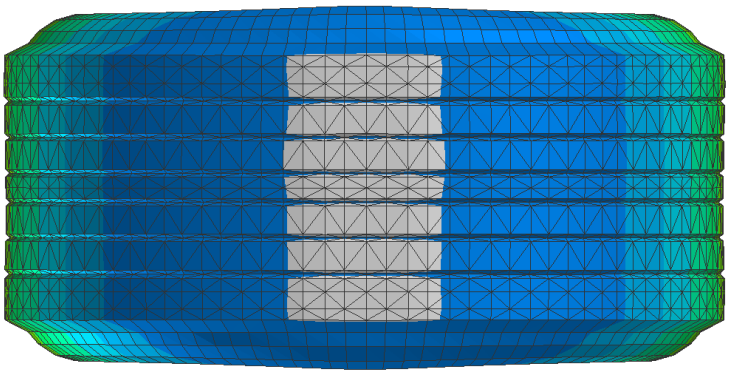

Figure 2-10 Recorded UOIT FEA *Michelin XOne Line Energy T* tire model footprint dimensions

Table 2-3 Comparison between the measurements of the *Michelin XOne Line Energy T* footprint and the simulation

Parameter	Provided data	Measured data	Units
Contact patch width	370	373.1	mm
Contact patch length	231	228.7	mm

As shown above, the results provided by simulations in PAM-CRASH corresponds to the data provided by Michelin's brochure.

2.2.3 Drum-cleat Test

Most of the tire mass is concentrated near the tread, tread base and layers of belt which are composing the outer layer of the tire. The outer layer of the tire is connected to the rim through elastic sidewalls. Due to the radial stiffness of the tire the rolling radius is not constant. The combination of mass and elasticity will allow the tire to vibrate as the tire is facing road irregularities. The vibration of the tire translates a vertical force acting on the spindle of the tire. These vertical forces are measured and converted from a time domain to a frequency domain using an FFT algorithm (PAM-CRASH) thus obtaining the harmonics of the first mode of vibration. This is generated when angular speed harmonic

and the natural frequency of the tire coincide. For the purpose of this experiment, drum-cleat test is virtually simulated in order to determine the first mode of vibration as shown in Figure 2-11 by exciting the tire over a cleat on a circular rigid drum. During this test the tire is loaded under 4,625 kg (45355.8 N) vertical load and inflated to 120 psi (0.83Mpa), then the tire's spindle is fixed in vertical direction (tire drum is not allowed to move vertically during the cleat excitation of the tire). With the tire fixed vertically it is therefore assumed that the vehicle and respective suspension characteristics are negligible. The tire free rolls over the rigid drum with a cleat and diameter of 2.5 m and linear speed of 50 km/h. It is assumed that the rotational speed has no effect on the first mode of vibration. This test is done in order to determine the first mode of vibration of the tire structure from the spindle force which is ploted in FFT diagram based on time history results on tire spindle as shown in Figure 2-12. As it can be seen in Figure 2-12 the first vertical free vibration mode is detected at 74 Hz which falls within the range radial-ply tires [19].

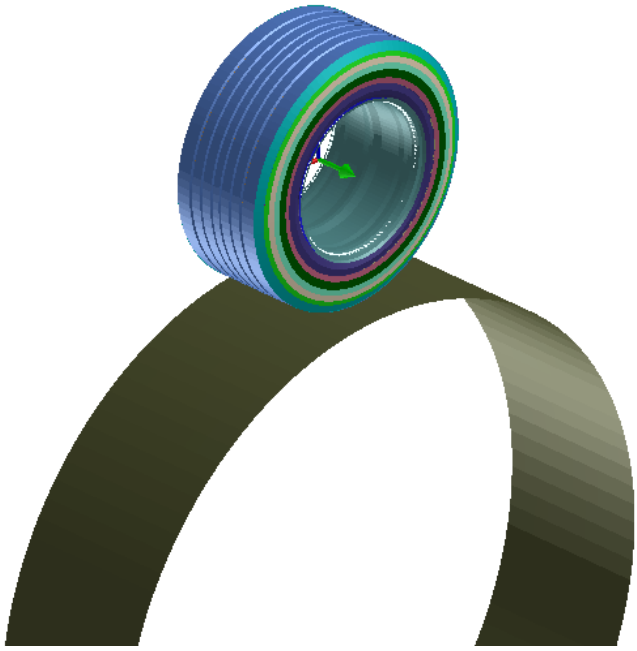

Figure 2-11 Drum-cleat test visual environment

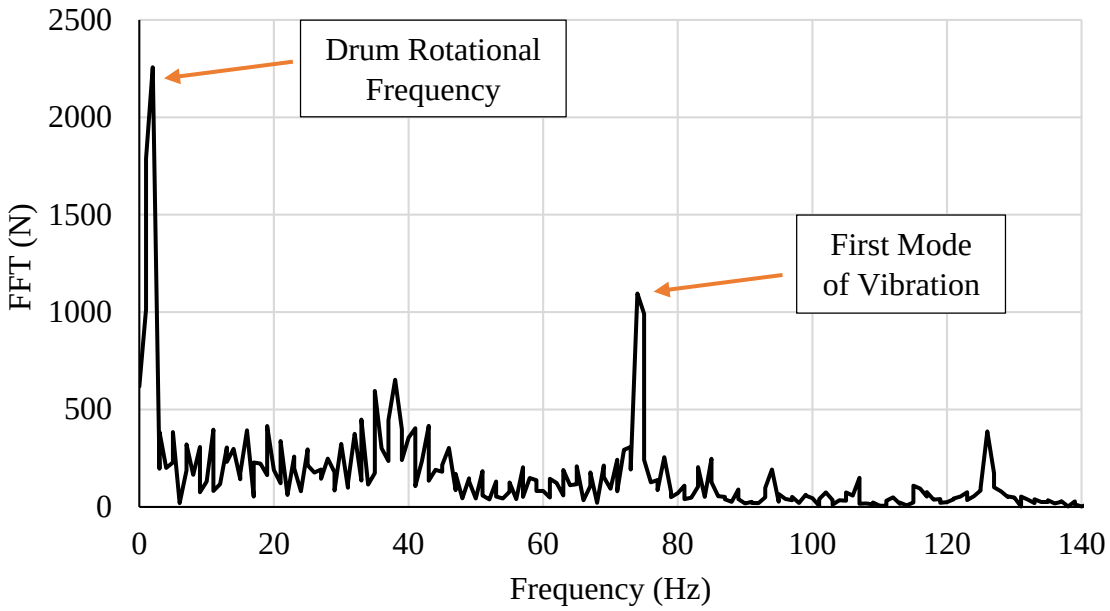

Figure 2-12 FFT result of vertical reaction force at tire spindle

By having the first mode of vibration frequency, 74 Hz, folowing Chae's calculation method, Tire's sidewall damping is calculated by using Equation 2-2 [19].

$$\alpha = \xi 2\omega = 0.05 \times 2 \times (2\pi \times 74) = 46.5 \cong 47 \qquad (2\text{-}2)$$

In this case "α" is sidewall damping, ξ = 5% = 0.05, is 5 percent critical damping effect, and "ω" is considered as first mode of vibration frequency which is 74 as shown in Figure 2-12. Therefore, the tire sidewall damping which is used in all simulations is determined to be 47.

2.3 CHAPTER SUMMARY

In this chapter an FEA tire is modeled via PAM-CRASH and PAM-MESH based on *Michelin XOne Line Energy T* tire with size of 445/50R22.5. The tire is modeled as an assembly of three-dimentional Mooney Rivlin hyperelastic solid elements using:

- 212 beam elements
- 2,014 shell elements
- 3,604 membrane elements
- 6,360 solid elements
- 11,978 four node tetrahedral elements

The modeled tire is validated through 3 tests:

1. Vertical stiffness test

   The error between the calculated and the measured spring rate is 4.95%.

2. Static footprint length and width

   The difference between simulation results and provided data is less than 4 mm.

3. Drum-cleat test

   First mode of vibration detected at 74 Hz.

CHAPTER 3

SOFT SOIL MODELING

In this chapter, different types of models are created representing dry sand soil. In order to ensure that the generated soil models have similar characteristics to dry sand, pressure-sinkage and shear strength tests are applied and discussed in soil calibration section. This chapter is part of an article accepted in International Journal of Vehicle Performance.

3.1 SOIL CALIBRATION

Series of tests are conducted in North Carolina at the Volvo Group Trucks Technology facility in order to measure the rolling resistance of the *Michelin XOne Line Energy T* tire on soft soil. The desired simulated soil should have characteristics close to dry sand to match the soil used in the measurement tests.

In order to calibrate the modeled soil as mentioned above, two types of tests are done: Pressure-Sinkage relationship and Shear Strength. Both FEA and SPH are enrolled in pressure-sinkage relationship test, however, regarding to shear test only SPH is enrolled. Since FEA soil has its inherent limitations due to penetration, it may not be possible to apply a shear test on it [37].

3.1.1 Pressure-Sinkage Relationship

Sinkage is the outcome of vehicle's normal force, applied to the soil through the tires. Pressure sinkage test is applied to determine the normal pressure distribution at the tire-soil contact area [40]. In this case the response of the soil to the normal load can be calculated through mathematical relationship shown on Equation (3-1) [21].

$$p = (\frac{k_c}{b} + k_\varphi)z^n \tag{3-1}$$

Where "k_c", "k_φ", and n are pressure-sinkage parameters, "p" stands for the load which is applied to the loading plate, "b" is the loading plate radius, and "z" is the sinkage in meters. In this research, dry sand material parameters are obtained from published data which can be seen in Table 3-1.

Table 3-1 Empirical properties of dry sand [1]

	Moisture	***n***	k_c	k_φ	***c***	***Φ***
	%	**Constant**	**kN/m^{n+1}**	**kN/m^{n+2}**	**kPa**	**deg**
Dry Sand	0	1.1	0.99	1528.43	1.04	28

In this research, to find pressure-sinkage relationnship, series of simulations are defined which consist of a FEA box that has the dry soil material assigned to it. A known pressure is applied to a plate with 300 mm diameter on the box with width×length of 800×600 mm shown in Figure 3-1.

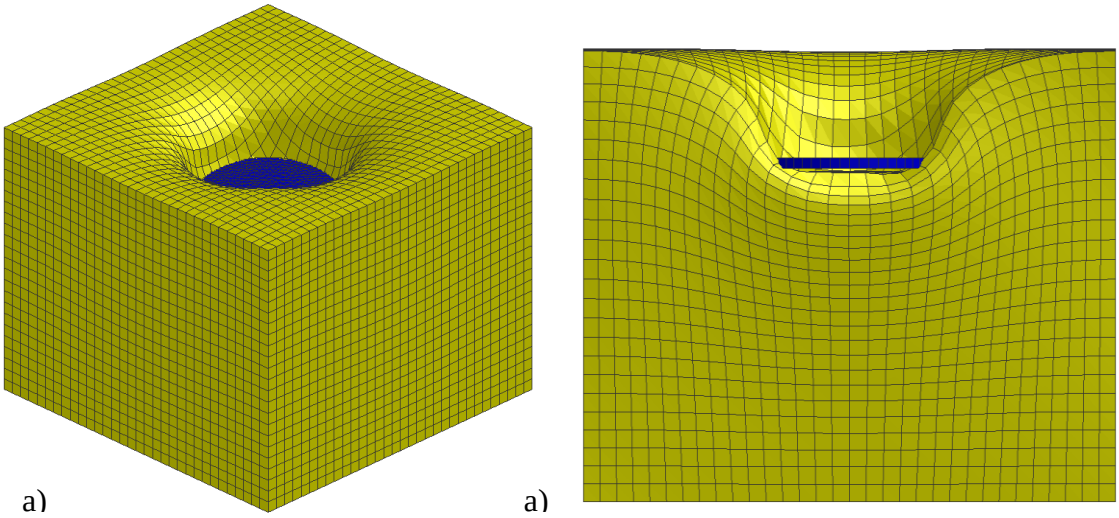

a) a)

Figure 3-1 a) FEA dry sand pressure-sinkage model and b) the model's section cut

The simulation consists of six different pressures varying from 0 to 200 kPa. Simulation result is compared with measurements gained from Bekker's Equation (3-1). Results are shown in Figure 3-2.

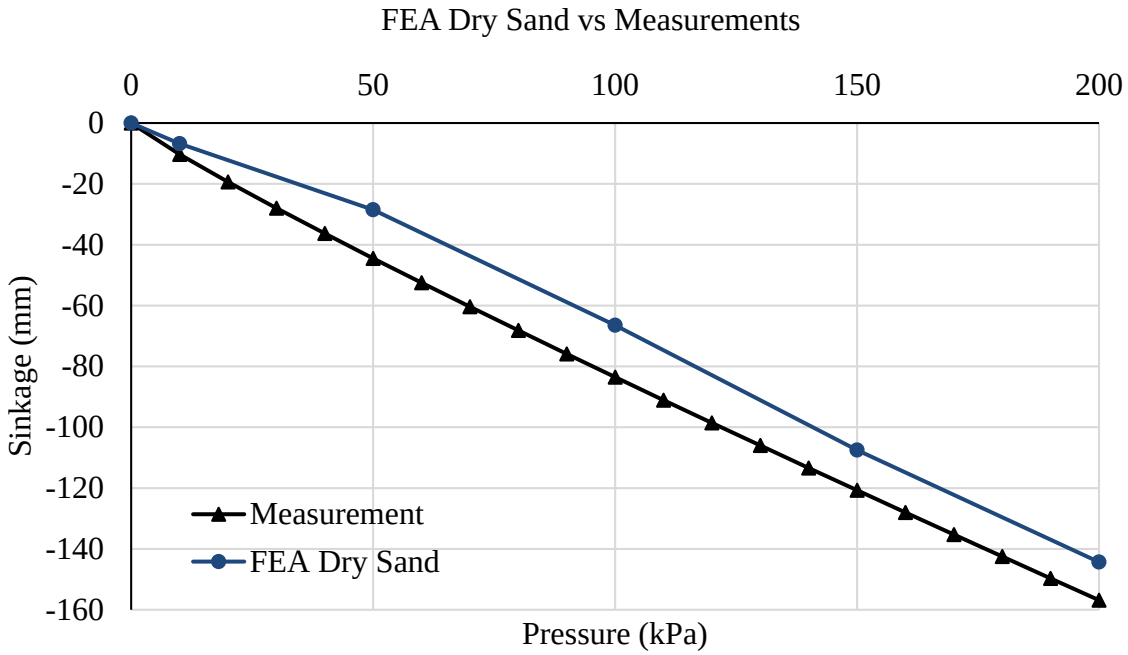

Figure 3-2 Pressure-sinkage relationship

In the FEA soil model every solid element shares nodes with neighbouring elements in regards to transferring forces, energies and moments. A sponge effect is observed in the FEA model, which does not accurately replicate soil characteristics since it cannot penetrate. To compensate for the limitations of the FEA model, the simulations are repeated using SPH soil to simulate soil characteristics as penetration can occur, allowing for a more realistic representation.

Smoothed Particle Hydrodynamics (SPH) is compiled from a finite collection of particles. Every single element of FEA soil is converted to SPH through PAM-MESH as shown in Figure 3-3. SPH soil is modeled in a container FEA box which is defined as a rigid body.

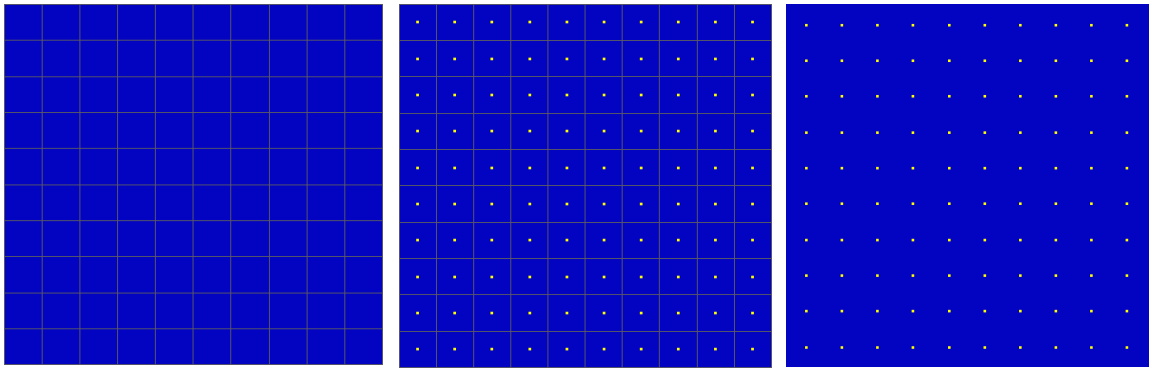

a) b) c)

Figure 3-3 a) Meshed FEA, b) mapping from FEA to SPH and c) SPH particles

After converting all elements to SPH, the pressure-sinkage test is repeated to validate the SPH soil. The material type in PAM-CRASH selected for SPH is Hydrodynamic Elastic-Plastic, with dry sand characteristics is assigned to it. The material uses an equation of state (EOS) in order to control pressure-volume relationship which is shown in Equation (3-2). [41]

$$p = C_0 + C_1\mu + C_2\mu^2 + C_3\mu^3 + (C_4 + C_5\mu + C_6\mu^2)E_i \qquad (3\text{-}2)$$

In this equation, "$\mu = (\rho/\rho_0) - 1$" where "ρ" is the current material density and "ρ_0" is the initial material density, "C_i" is the material constant which needs to be determined, and "E_i" is the internal energy. In this research all C_i's are considered as zero except for "C_1" in order to represent a dilatational elastic material with bulk modulus of "C_1".

In the definition of SPH module, the minimum and the maximum smoothing length for each element is studied and considered as 1 and 100 due to the initial ratio defined by PAM-SHOCK and the particle density. The Ratio must be between 1.21 and 2.1 [37].

The pressure-sinkage model and relationship for dry sand using SPH model is shown in Figure 3-4 and Figure 3-5 respectively. It can be seen that the SPH model overcomes the limitations of FEA soil penetration. The advantage of SPH is that elements do not share

nodes, which removes constraints placed on each element from neighbouring elements and enables unrestricted movement. The freedom of SPH elements thus eliminates the sponge-like effect observed in the FEA model. Because SPH allows penetration unlike FEA, the model is capable of demonstrating a more realistic representation of soil behaviour under pressure.

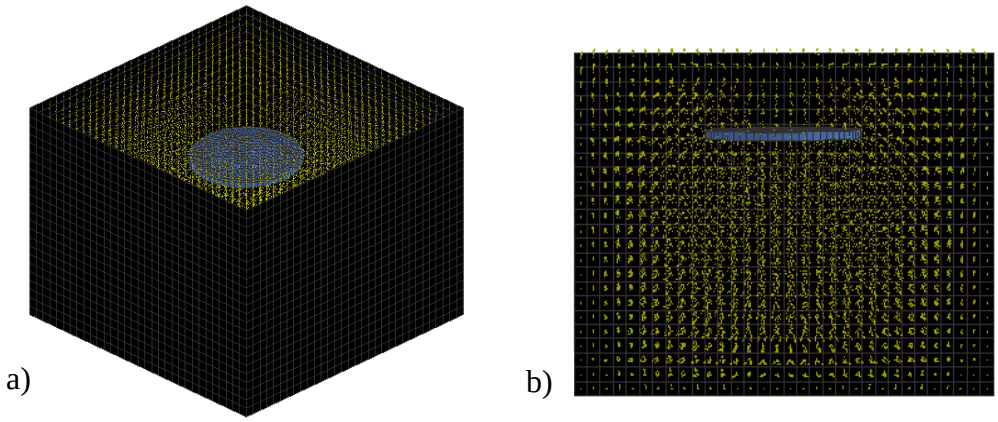

Figure 3-4 a) SPH dry sand pressure-sinkage model and b) the model's section cut

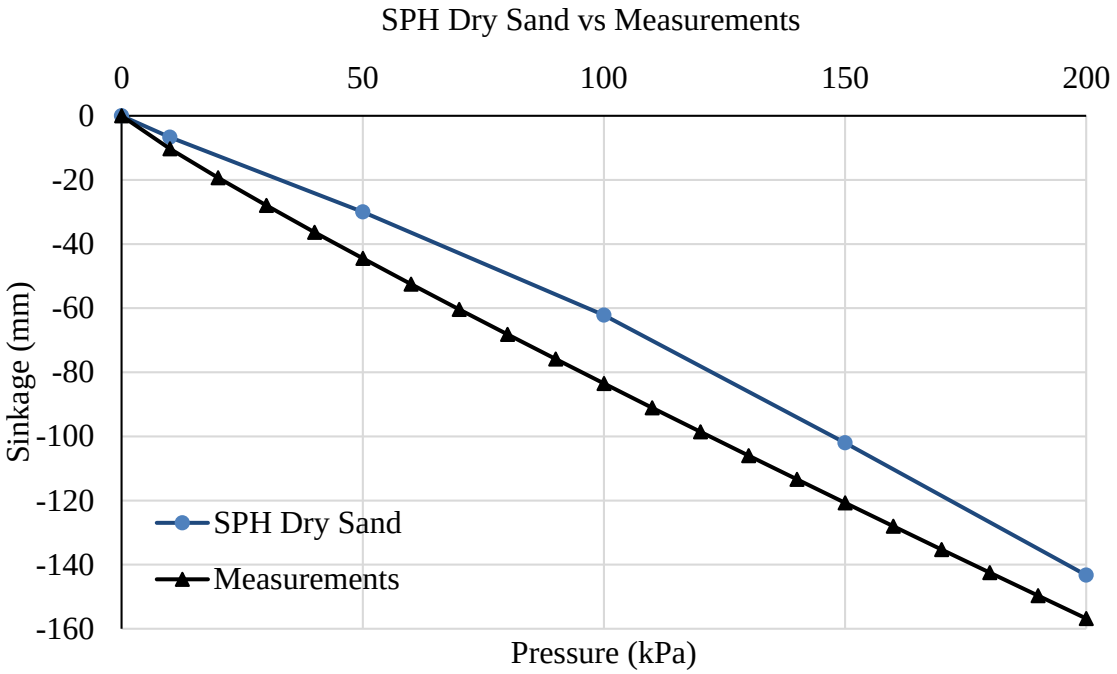

Figure 3-5 Pressure-sinkage relationship

The sinkage results obtained from the SPH soil model are mostly similar to the FEA soil model results. The key difference however, is that SPH presents a better and more realistic simulation results regarding to soil characteristics due to penetration.

3.1.2 Shear Strength

When a tire is rolling on rigid surface, longitudinal slip is due to tread flexure. However, when rolling on soft soil, while the vehicle is accelerating, slip is mostly affected by soil layer shear, which causes vehicles to experience less traction as the tire interacts with the soil. In order to have a better understanding of tire's behaviour on soft soil, it is of a great importance to study the relationship between shear stress and shear displacement under various normal pressures. Maximum shear strength "τ_{max}" can be determined through Mohr-Coulomb failure criterion [40]:

$$\tau_{max} = c + p.tan\varphi \tag{3-3}$$

Where "φ" is the soil internal friction angle and "c" is soil cohesion. In this thesis the dry sand had been calibrated regarding to shear strength by comparing the simulation results with dry sand properties shown in Table 3-1. The direct shear method is used in the simulations which is known as shear box test. In this test a closed box filled with dry sand is used that has separated two halves. Top of the box is open and there is a loading plate placed on it which can be variously loaded. A fixed displacement is assigned to the middle horizontal plane. By measuring the generated shearing force, the peak value of the force right before it decreases is obtained and by dividing it by cross-sectional area of the shear box, shear strength is calculated. Figure 3-6 shows the shear box used in simulations.

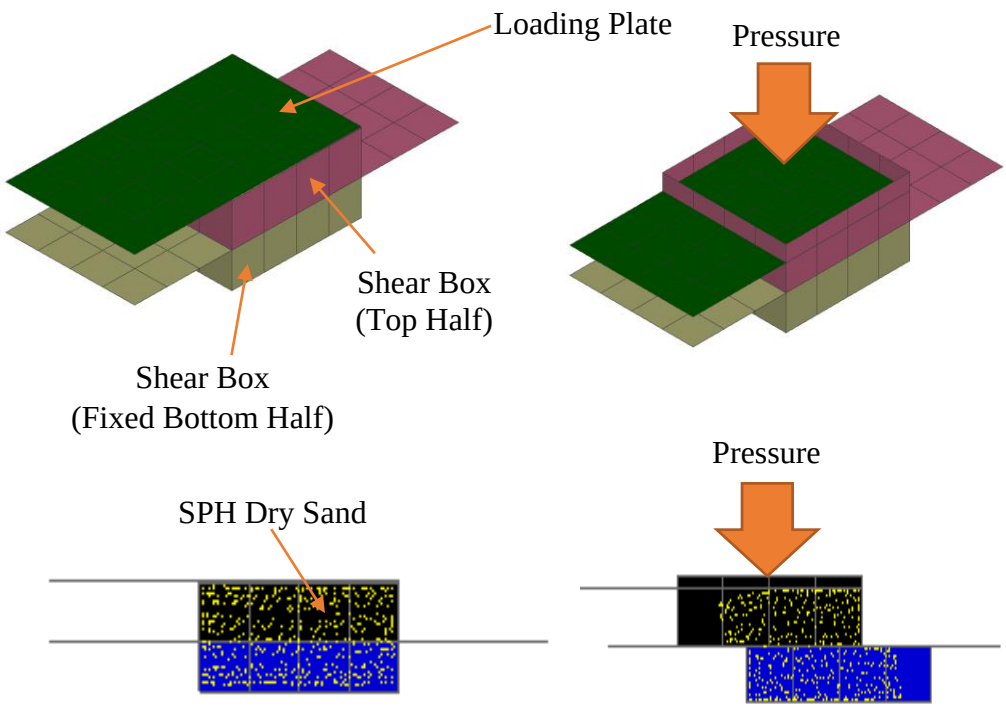

Figure 3-6 Shear box simulation

In the simulation, the shear box cross-sectional area is 0.15 m^2. Different loads varying from 10 to 200 kPa are applied to the loading plate. The shear box is moved by a distance of 70 mm in 80 seconds in order to represent more realistic test as signified previously [42]. Shear test results are shown in Table 3-2 and Figure 3-7.

Table 3-2 Shear strength results

Soil Shear Strength	Cohesion (c)	Internal Friction (Φ)
Dry sand - Simulation	5.516	24.8
Dry sand - Measurement	1.04	28

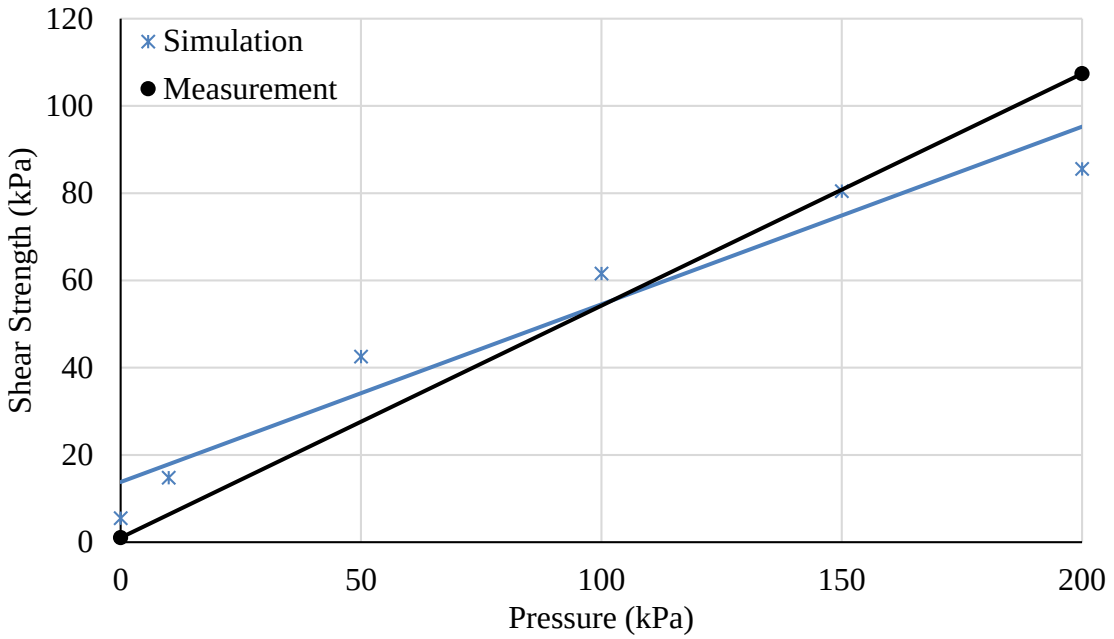

Figure 3-7 Shear strength simulation vs measurement

By applying the shear test, "Φ", which is the angle of internal friction, can be calculated from the angle of the shear curve in Figure 3-7 and also "*c*", which is cohesion, can be determined from the intersection of the curve and shear strength axis. Table 3-2 shows the shear strength test values compared to the measurements from Table 3-1.

3.2 SOIL MODELS

Full FEA, full SPH, hybrid half SPH/FEA, and hybrid quarter SPH/FEA have been modeled as a representative of dry sand while using different methodologies to determine the most accurate and efficient one. Each model is individually discussed in this section. In all simulations, 0.6 is used as the friction coefficient. Soil parameters and SPH factors are kept constant and each simulation's length is 1 second. The dimensions of the soil box are such that they have negligible effect on soil performance. For all soil models discussed in this section, the box has a width 780 mm, length of 7180 mm, and depth of 585 mm.

3.2.1 Full FEA Soil Model

The soil modeling employs a traditional FEA soil model for dry sand as shown in Figure 3-8. Similar to the pressure-sinkage calibration box, the FEA soil box uses a 25-mm mesh size which is the most efficient mesh considering the results and time consumption of FEA and SPH soil models [37]. The full FEA soil model has 8897 thin shell elements and 204631 solid elements. The bottom nodes of the box are defined as rigid body nodes and the outer edges are constrained to prevent motion in the x and y directions in order to simulate a stationary plot of soil. Elastic-Plastic solid material is chosen to represent soil characteristics for FEA soil. Dry sand characteristics are assigned to the elastic plastic solid material type in PAM-CRASH.

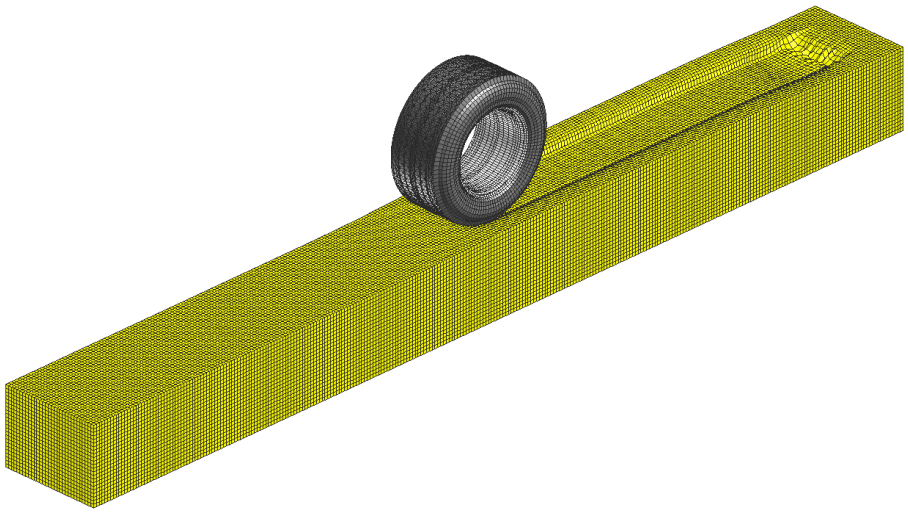

Figure 3-8 Full FEA dry sand soil model

3.2.2 Full SPH Soil Model

Following the soil calibration procedures, all solid elements of the soil model are converted from FEA to SPH. A soil box is developed around SPH soil which is considered as rigid body. SPH elements are produced in the center of a solid FEA element, and are separated

by a 25-mm distance. The full SPH soil model has 15257 thin shell elements, and 204631 SPH elements. The tire is in contact with soil by friction of 0.6. The full SPH soil model is shown in Figure 3-9.

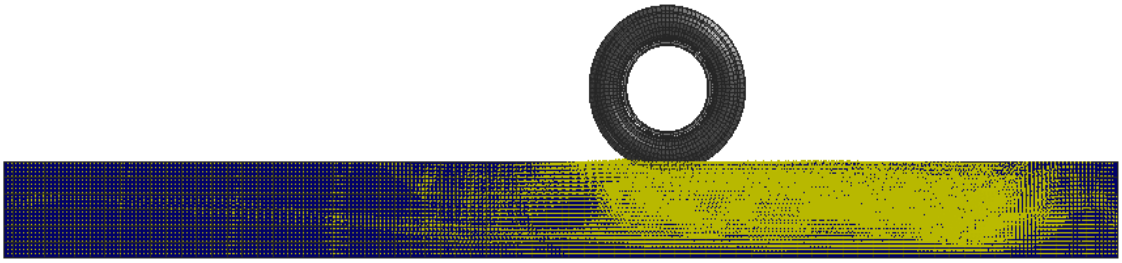

Figure 3-9 Full SPH dry sand model

3.2.3 Original Hybrid SPH/FEA Soil Model

In order to complete this research while comparing SPH and FEA modeling methods, hybrid soil models are also proposed in order to study the its effects on the final results as well as CPU time consumption of the simulation. In this case, the full FEA dry sand soil model is converted to a quarter SPH and a half SPH model to observe the effects of different combinations. The FEA and SPH material parameters are kept consistent to those used in the aforementioned, respective models. FEA and SPH elements are linked together with a tied link feature assigned in PAM-CRASH. Both models are shown in Figure 3-10.

In this case a 3D solid element sidewall is created around the SPH soil, which sits on top of the FEA soil that can be seen in Figure 3-11. The FEA sidewalls have the same mesh sizing of the FEA soil (25 mm) and the same material is assigned to them. Half SPH/FEA soil model has 112587 solid elements, and 106764 SPH elements. Quarter SPH/FEA soil model has 165969 solid elements, and 53382 SPH elements. The use of 3D solid element sidewalls allows for a realistic representation of the soil box, ensuring that the results are

accurate. However, since solving 3D solid element in FEA models with a fine mesh is computationally expensive, new modeling methods are investigated which will be discussed.

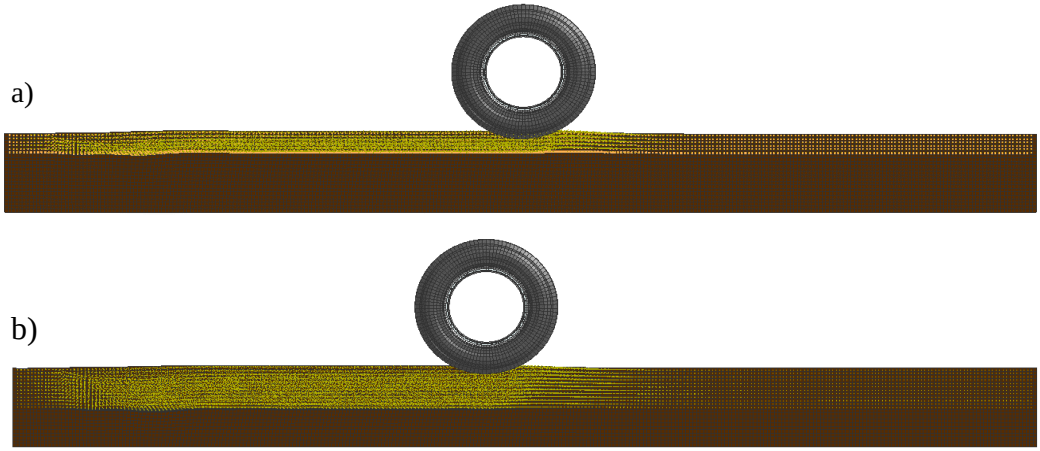

Figure 3-10 a) Quarter SPH/FEA hybrid model and b) half SPH/FEA hybrid model

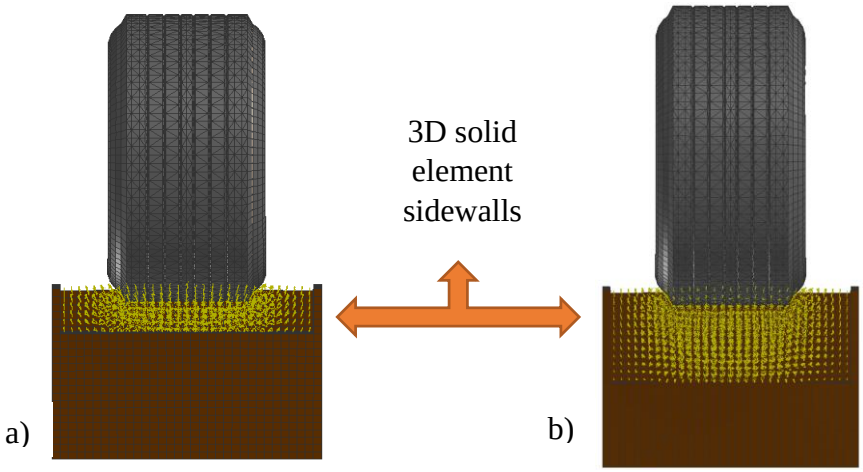

Figure 3-11 Hybrid a) quarter and b) half FEA/SPH model with FEA sidewalls

3.2.4 Modified Hybrid SPH/FEA Models

The hybrid FEA/SPH had been used previously while having 3D solid elements as SPH sidewalls. In this research the 3D solid elements are replaced with 2D elements defined as rigid bodies, which can be seen in Figure 3-12, to reduce the computational time. This has

been successfully done without affecting the final results and increasing the simulation speed. The mesh size used in this model is consistent with aforementioned models, at 25 mm. The modified half SPH soil model has 3180 thin shell elements, 97867 solid elements, and 106764 SPH elements. The modified quarter SPH soil model have 1272 thin shell elements, 151249 solid elements, and 53382 SPH elements.

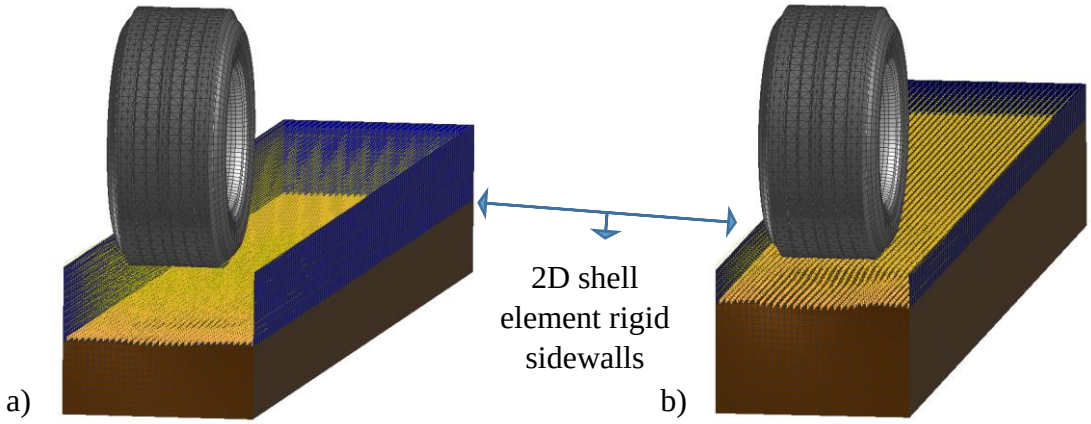

Figure 3-12 Modified hybrid models with 2D shell element rigid sidewalls a) half SPH and b) quarter SPH

3.3 SOIL MODELS COMPUTATIONAL EFFICIENCY

One of the most important aspects of the soil models that need to be investigated is the computational efficiency of each dry sand soil model, which can be listed as full FEA, full SPH, hybrid half SPH, and hybrid quarter SPH. The comparison of efficiency is done through measuring CPU, or computational time, which is how long the simulation solver loads the CPU. Since the CPU time of modeled *Michelin XOne Line Energy T* tire is high, comparison of the simulation time of the soil models is done using a simplified rigid tire model. This was previously used by Lescoe to compare the computational times of dense sand/sandy loam soil models [37]. The tire used in his research is modeled from the

Goodyear G357, 295/75R22.5 G by Chae [19]. This tire has 9200 nodes, 1680 layered membrane elements, 4200 solid elements, and 120 beam elements. The pneumatic three groove Goodyear tire model is then converted by Lescoe to rigid tire as shown in Figure 3-13 by removing tread and increasing the width by 20%.

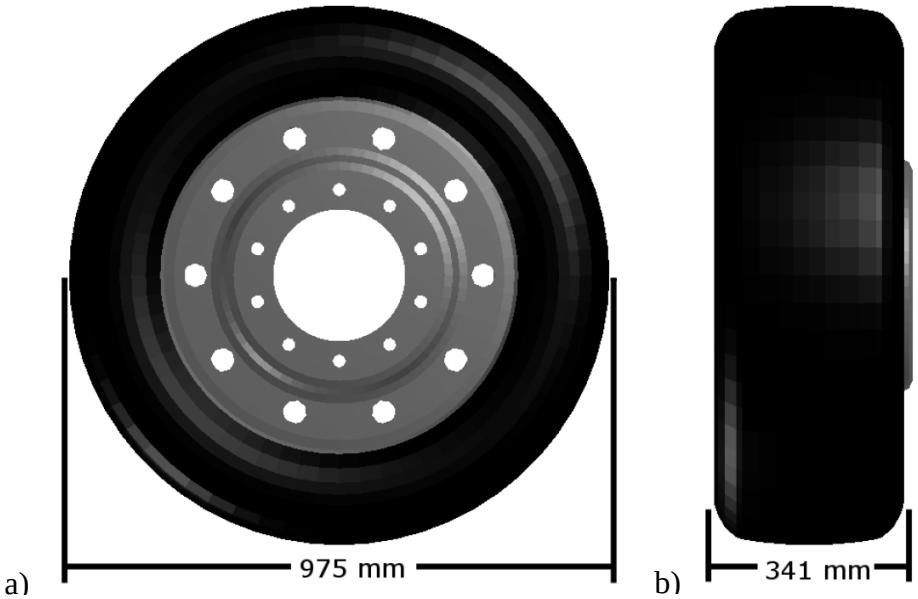

Figure 3-13 a) Side view and b) front view of treadless rigid tire model [37]

In the case of treadless rigid tire model, the tread is removed to reduce computational time by eliminating several solid elements and all other tire parts are defined as a rigid body. Tire is then settled on soil with the same setup as pneumatic tire. Friction is considered as 0.6. Simulation time is set to 1 second. Every model parameter is maintained the same throughout all models to ensure a compatible, fair comparison. All simulations are solved on hardware with two Intel processors (12M Cache, 2.53 GHz, 5.86 GT/s, 6 cores) which are fully utilized for one solver. Figure 3-14 shows the hybrid soil models (with rigid sidewall surrounding SPH), and FEA model, with rigid tire rolling on it.

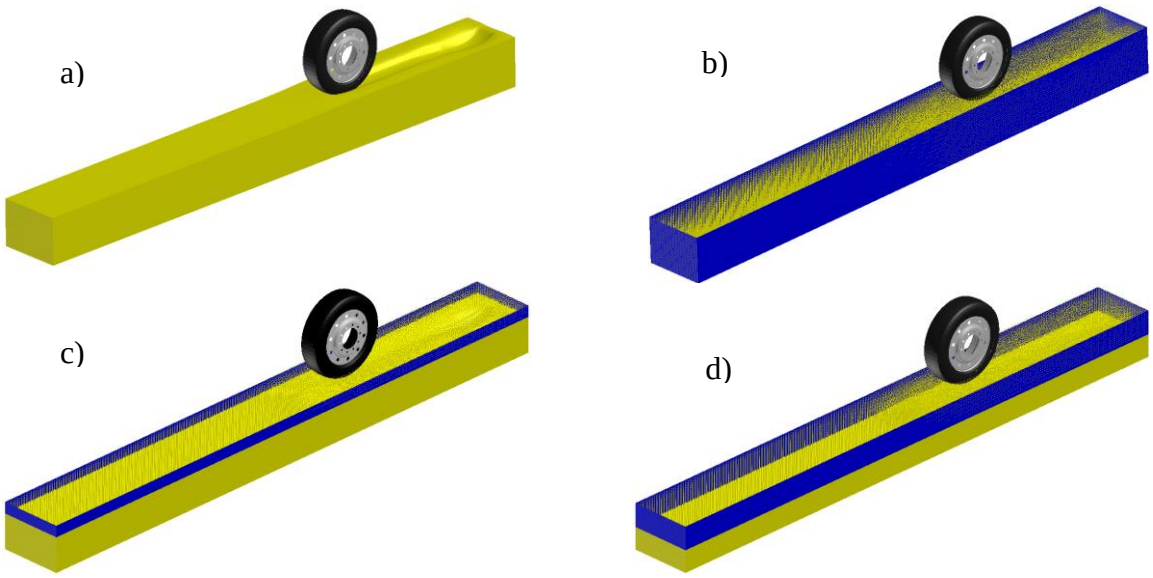

Figure 3-14 a) Full FEA, b) full SPH, c) quarter SPH, and d) half SPH soil models with treadless rigid tire model

This experiment environment is set up with rigid tire to examine computational time efficiency of models to each other and also to the original soil models. As shown in Table 3-3, SPH takes the longest time compared to the others which is in agreement with previous published data. Since SPH has the highest computational time and has been proved to be a better representative of soil compared to FEA, hybrid models have also been tested. It can be seen in Table 3-3 and Figure 3-15 that hybrid models reduce the computational time considerably compared to SPH. In CHAPTER 5, *Michelin XOne Line Energy T* tire model is validated using modified soil models due to equal accuracy compared to original models and lower computational time.

Table 3-3 CPU time comparison between modified and original soil models

TREADLESS RIGID TIRE SIMULATIONS		
Soil Models	**CPU Time (s)**	
	Modified	**Original**
FEA Model	2.79E+04	2.79E+04
Full SPH	8.28E+04	8.29E+04
Half SPH	5.59E+04	5.98E+04
Quarter SPH	4.69E+04	5.12E+04

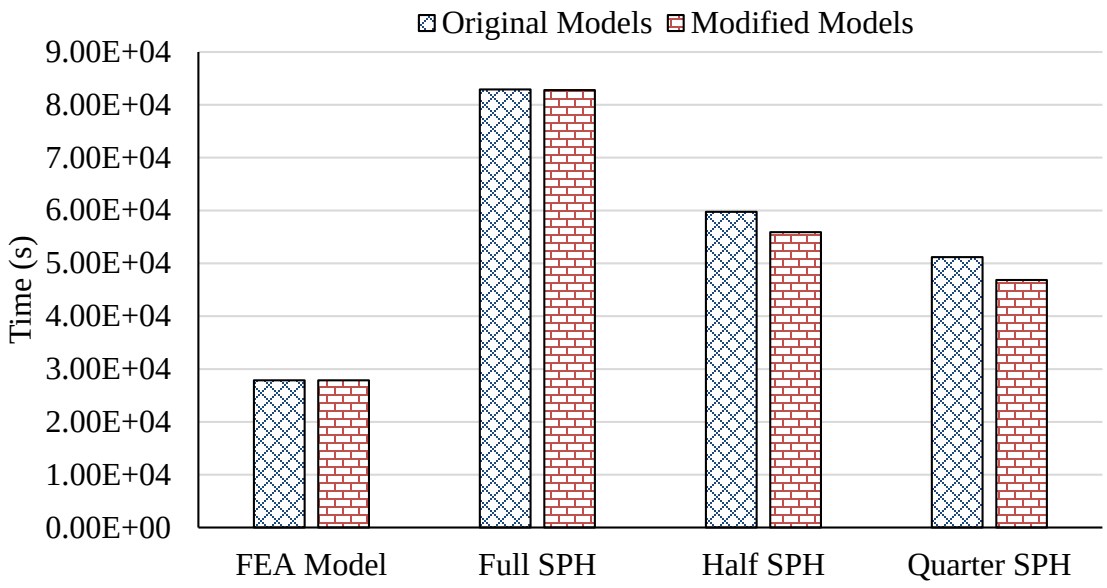

Figure 3-15 Modified and original models CPU time comparison

The wide-base tire model is also converted to rigid body to be studied regarding to CPU time on different soil models. Wide-base tire results are then compared to the treadless rigid tire results to ensure the size and the absence of tread does not affect computation time. Table 3-4 shows the computational time trend of different soil models for both wide-base rigid tire and treadless rigid tire. Figure 3-16 shows the rigid wide-base tire rolling on modified soil models.

Table 3-4 Wide-base and teadless rigid tire CPU time comparison

Soil Models	CPU Time (s)	
	Wide-Base Rigid Tire	Treadless Rigid Tire
FEA Model	7.15E+05	2.79E+04
Full SPH	6.96E+05	8.28E+04
Half SPH	4.53E+05	5.59E+04
Quarter SPH	3.61E+05	4.69E+04

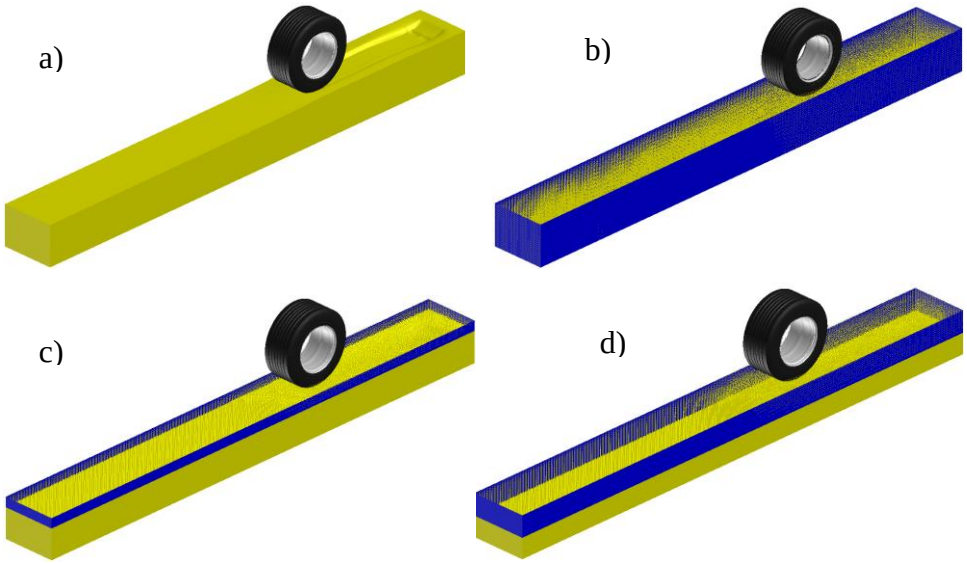

Figure 3-16 a) Full FEA, b) full SPH, c) quarter SPH, and d) half SPH soil models with wide-base rigid tire model

Referring to Table 3-4, the highest computational time for each type of tire is different. In general, wider tires take longer to solve for all soil models due to the complexity of the tire model and the larger number of elements. For the wide-base rigid tire, the tread and shoulder are not removed and due to contact between the large number of solid elements (the tread and soil) the contact solving time has increased in a considerable way which caused the CPU time of FEA soil model and wide-base rigid tire increase significantly. However, for the treadless tire, full SPH is taking the longest CPU time because the tire has no solid elements, less number of membrane and shell elements, simpler model, and no tread. In other words for treadless tire only membrane elements of undertread are in contact with soil. This trend of time for wide-base tire is same for pneumatic tire as well. Table 3-5 shows CPU time comparison for different soil models with pneumatic wide-base tire.

Table 3-5 CPU time for pneumatic tire rolling on different soil models

Pneumatic Tire-Dry Sand-1775 lbs-5 mph - 110 psi		
Soil Models	**CPU Time (s)**	**Time Reduced Compared to Full SPH (%)**
FEA Model	3.33E+06	-
Full SPH	3.00E+06	-
Half SPH	2.03E+06	32.33%
Quarter SPH	1.63E+06	45.67%

As shown in Table 3-5, full FEA is taking the longest. The newly developed hybrid half SPH and hybrid quarter SPH had successfully reduced the CPU time up to 32.33% and 45.67% respectively. In continuation of this thesis, the soil models will be examined regarding to accuracy as well and the optimum soil will be selected.

3.4 CHAPTER SUMMARY

Series of soil models are created which are known as full FEA, full SPH, half SPH, and quarter SPH. To make sure the modeled SPH and FEA soil models accurately represent dry sand characteristics they are examined through two calibration processes.

1. Pressure-sinkage relationship

   Both FEA soil and SPH soil are examined. The simulation results for both modeling methods are in agreement with measured data. A sponge-like effect is observed in the FEA model due to lack of penetration, which is overcome using SPH modeling method.

2. Shear strength

   It is only applicable for SPH soil model. By having less than 4 degrees difference in the angle of internal friction, the model corresponds well to measured data. The intersection of the curve and shear strength axis represents cohesion.

Four different soil models are then created, known as: full SPH, full FEA, hybrid quarter SPH, and hybrid half SPH. The hybrid models are then modified from having 3D solid element sidewalls to rigid body 2D sidewalls to reduce computational time.

Later the computational efficiency of each soil model is examined and compared by using a rigid tire. By converting the *Michelin XOne Line Energy T* tire model to a rigid tire and rolling it under the same conditions on all four soil models, it is determined that the quarter SPH soil model is the most efficient soil model. The hybrid quarter SPH soil model had reduced the computation time up to 45.67% compared to full SPH.

CHAPTER 4

ROLLING RESISTANCE TESTS AND SIMULATIONS ON HARD SURFACE

In this chapter the physical experimental determination of the *Michelin XOne Line Energy T* tire's rolling resistance is explained as it is conducted at Volvo Group Technologies Inc in North Carolina U.S.A.. It is proved that the simulations of UOIT FEA *Michelin XOne Line Energy T* tire model produces characteristic results accurately comparable to the physical results. This chapter had been presented in ASME conference in Boston 2015 [38].

Fundamentally, rolling resistance is a force developed against the direction of the motion, applied to wheel, while a force is requaired to overcome this unwanted force and move the wheel forward. Rolling resistance is an important area of study because it is an influencal factor on a vehicle's fuel economy, the tire wear, and ride comfort.

Rolling resistance is measured using a tractor pusher axle (non-driven axle) equipped with the same wide-base tire model used in this research, *Michelin XOne Line Energy T*. Simulation environment can be seen in Figure 4-1. The vehicle is towing varios trailers producing various vertical loads of the instrumented tires. Volvo truck tractor is outfitted with wheel force transducers from Michigan Scientific to record the three dimentional forces and moments at left and right tires spindles on the pusher axle. The transducer has been designed in a way that all the forces and moments must pass through it before being transferred to vehicle. The transducers specification is shown in Table 4-1 and the tire equiped with tranceducers is shown in Figure 4-2.

Table 4-1 Wheel load measurement system specifications from [43]

MSCLW-2T-50K/MSCLW-2T-100K-S 6-Axis Single or Dual Wheel Load Transducer Stainless Steel		
Capacities		
Maximum Force Capacity	**[Fx, Fz]**	50,000 lb (222 kN)
At Tire Patch	**[Fy]**	25,000 lb (111 kN)
Maximum Torque Capacity	**[Mx, My, Mz]**	50,000 lb-ft (67.8 kN-m)
Full Scale Output (before amplifier)		1mV/V nominal
Transducer		4 arm strain gage bridges
Nonlinearity		Less than 1% of full-scale output
Hysteresis		Less than 1% of full-scale output
Repeatability		Less than 1% of full-scale output
Zero Balance Prior To Installation		Less than 2% of rated output
Radial Sensitivity Variation		<1% of radial load
Temperature Range		-40 to 125 C (-40 to 257 F)
Excitation Voltage		10 VDC
Insulation Resistance From Bridge To Case		Exceeds 1000 M-ohm
Vehicle Power Input Voltage		10 to 36 VDC

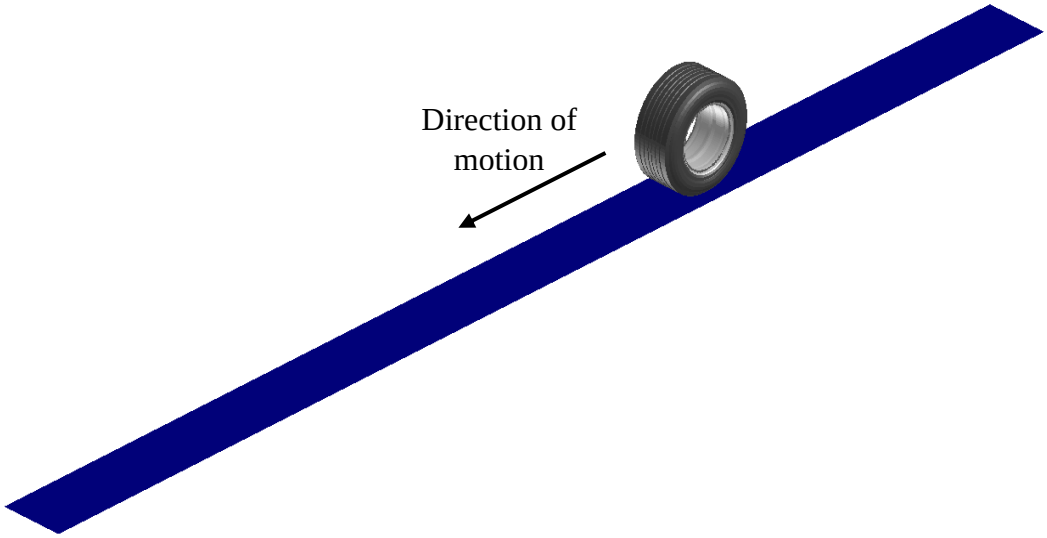

Figure 4-1 Rolling resistance virtual test environment

Figure 4-2 Wheel forces and moments transducers

The measured vertical loads and speeds at the center of the left-middle tire are used in the virtual tests. The modeled tire is tested through all measurement conditions and the rolling resistance of the modeled tire is compared with the provided data from experimental tests. Meanwhile in Figure 4-3, stress pressure distribiution for the modeled tire can be seen. The pressure distribiution has been studied under one of the testing conditions, at 80 psi, 8 mph speed and 8,917 lbs vertical load. As it can be seen while the tire is rolling the stress pressure is the highest at the contact patch, especially close to the shoulders.

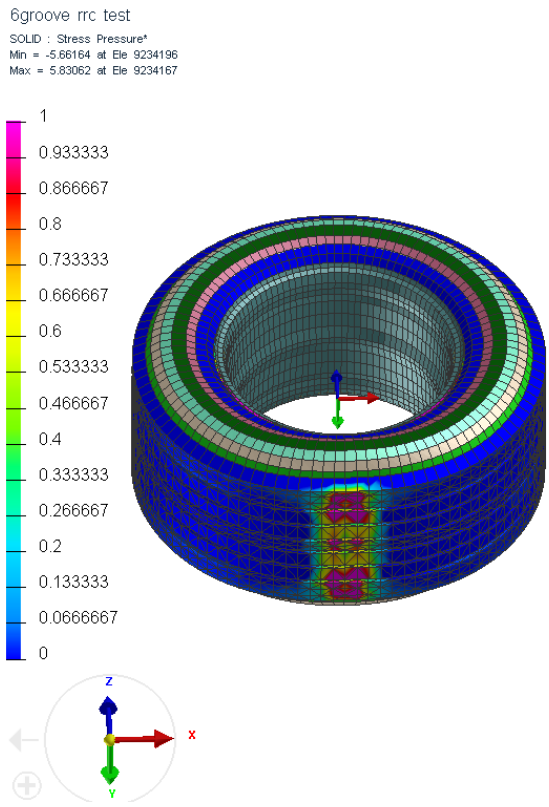

Figure 4-3 Stress-pressure distribution of rolling tire

4.1 ROLLING RESISTANCE TEST RESULTS:

During the testing procedure, left middle tire of the truck is studied and all the experimental tests are simulated in PAM-CRASH in order to validate the modeled tire. The friction coefficient of the road is 0.8 due to warm weather condition of the testing environment. Also by using a rigid surface model with roughness as the road, surface irregularities in experimental tests are considered in the simulations by using road model with roughness. The vertical force and the speed are varying with time as measured by the force transducers. All the collected data regarding to speed and load are implemented in simulations precisely. During the experimental tests, the truck moved on an oval track for three full cycles at constant speed. In order to get the most accurate results for the rolling resistance coefficient, data from the parts that the truck is taking a cornering maneuver is omitted and

only the straight motions segments are considered and implemented to simulations. The results are obtained from six simulations during six stable time segment (the segments that the truck is moving in straight line). Results for each pressure, load and speeds are conducted and shown in different sections based on the changes in vertical load.

4.1.1 Bobtail (Tractor only)

The simulations are considered for the desired tire of the truck without trailer. The average tire load is 866 lbs, average speed is 15 mph, and the inflation pressure is 110 psi. Vertical load and speed used from measurements are considered as the inputs of the simulations. The total measured data during one complete cycle are shown in Figure 4-4 and Figure 4-5. Then the parts that the truck is taking a cornering manuver are omitted and six segments are selected as shown in Table 4-2.

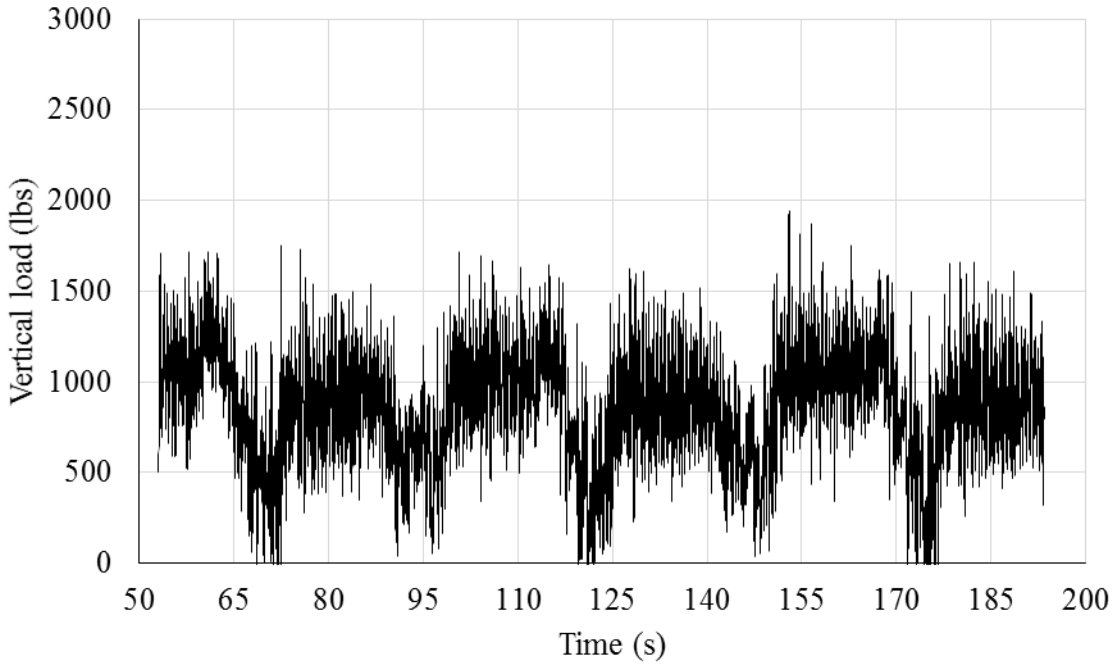

Figure 4-4 Measured tire vertical load

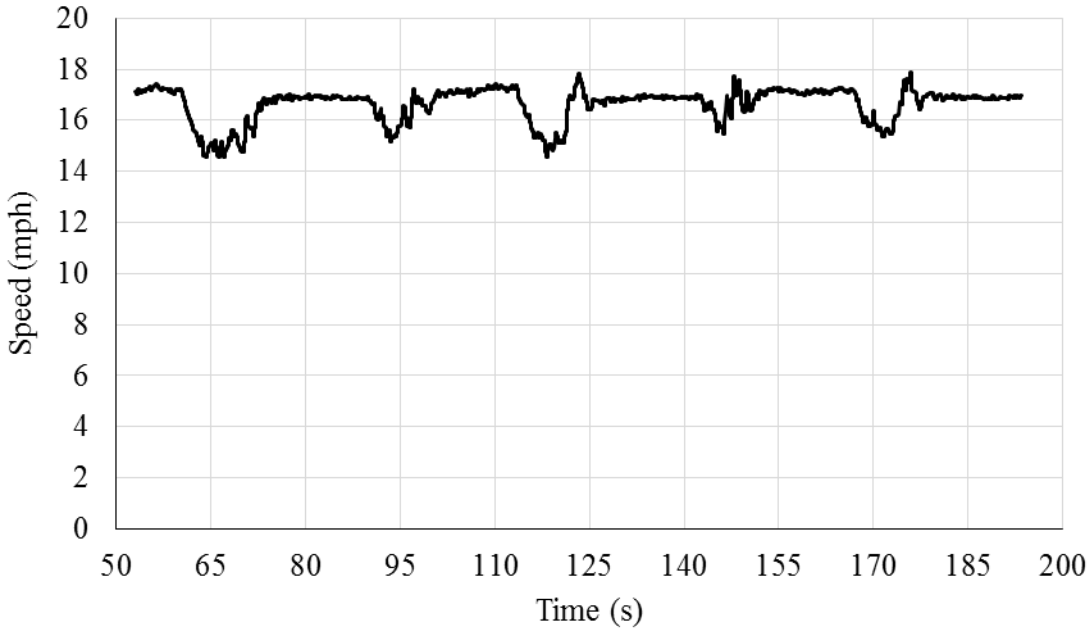

Figure 4-5 Measured speed vs. time

Table 4-2 Bobtail time segments

Time Segments	
1	55-60
2	80-85
3	105-110
4	130-135
5	160-165
6	185-190

Each segmant is five seconds and the duration of each simulation is considered the same. During each one of these six segmants, the truck is moving straight. Figure 4-6 and Figure 4-7 show the first segment of vertical load and speed on the desired tire. Table 4-3 and Figure 4-8 compare the measured RRC via simulation results. In this case it can be seen

that there is a difference between the simulation results and measurement which it is eliminated as the loading increases in the next tests.

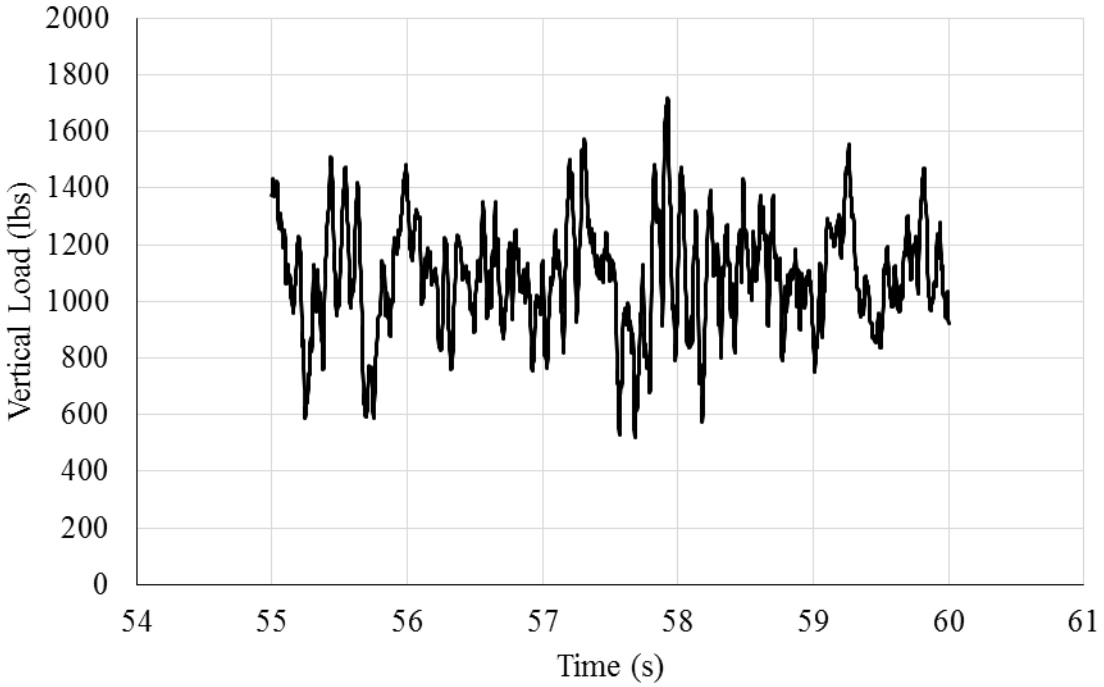

Figure 4-6 First segment of tire vertical load

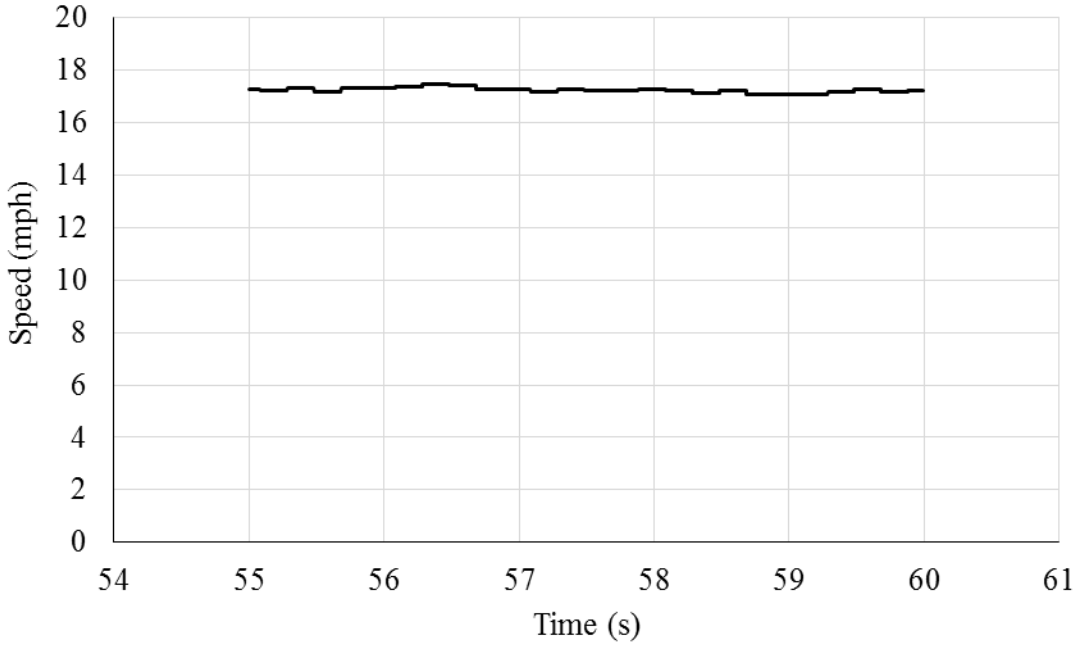

Figure 4-7 First segment of speed

Table 4-3 RRC comparison in six segments

Average Tire Load 866 lbs - Average Speed 15 mph - 110 psi		
RRC Results	**Virtual tests**	**Measurements**
First Segment	0.0050759	0.0021997
Second Segment	0.0049082	0.0025736
Third Segment	0.0048023	0.0027807
Fourth Segment	0.0047257	0.0024031
Fifth Segment	0.0046122	0.0023776
Sixth Segment	0.0046415	0.0016800

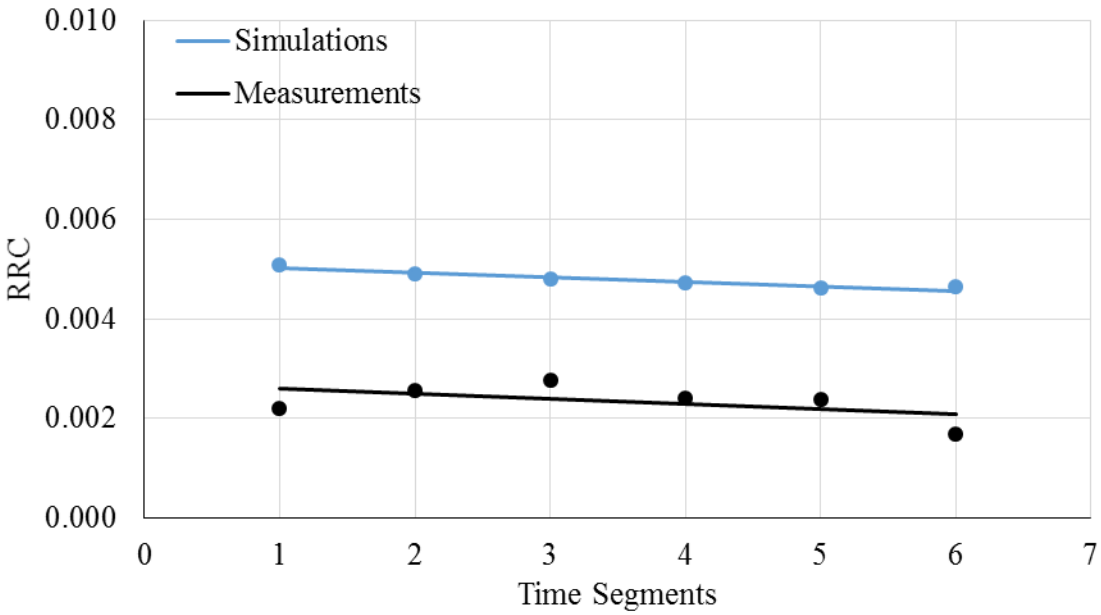

Figure 4-8 RRC comparison for each time segment between measurements and simulations

4.1.2 Tractor- First Trailer

First trailer has the average tire load of 8,723 lbs. The left middle tire for first trailer is tested both for 110 psi and 80 psi inflation pressure. Also it is tested through two different speeds with the averages of 8 mph and 15 mph. In continiuation, all consitions are listed into separate cathegories.

4.1.2.1 80 psi Inflation Pressure and Average Speed of 8 mph

The total measured data for load and speed are shown in Figure 4-9 and Figure 4-10 respectively. The six five seconds segment of the truck's straight motion are shown in Table 4-4. Figure 4-11 and Figure 4-12 show the first segment for vertical load and speed respectively.

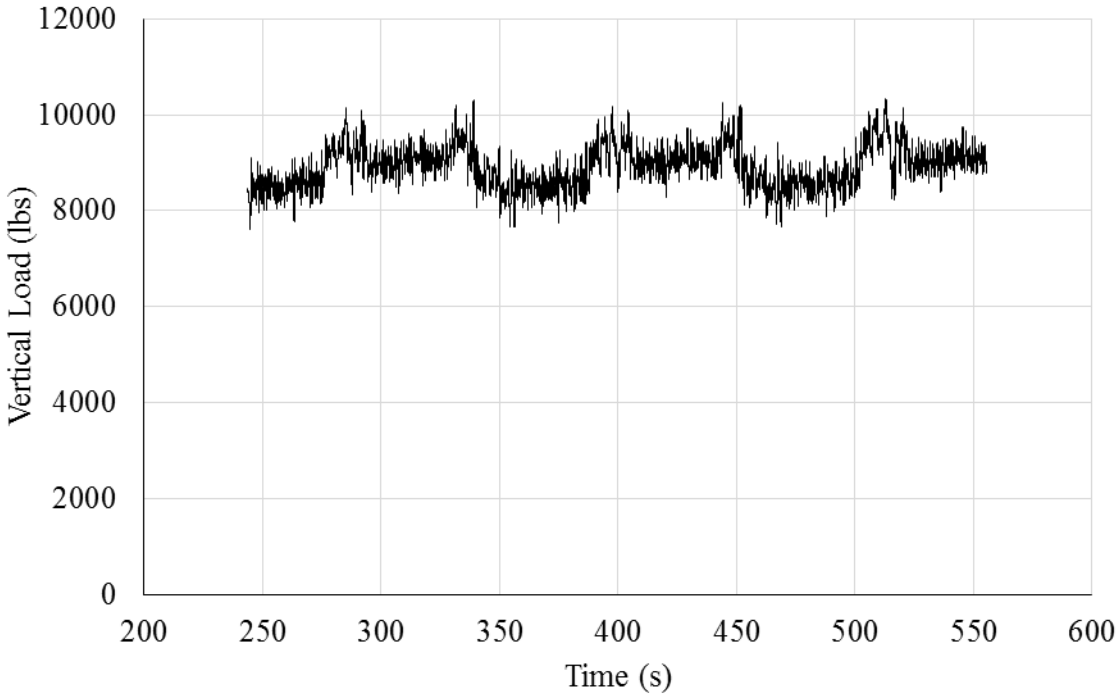

Figure 4-9 Measured tire vertical load

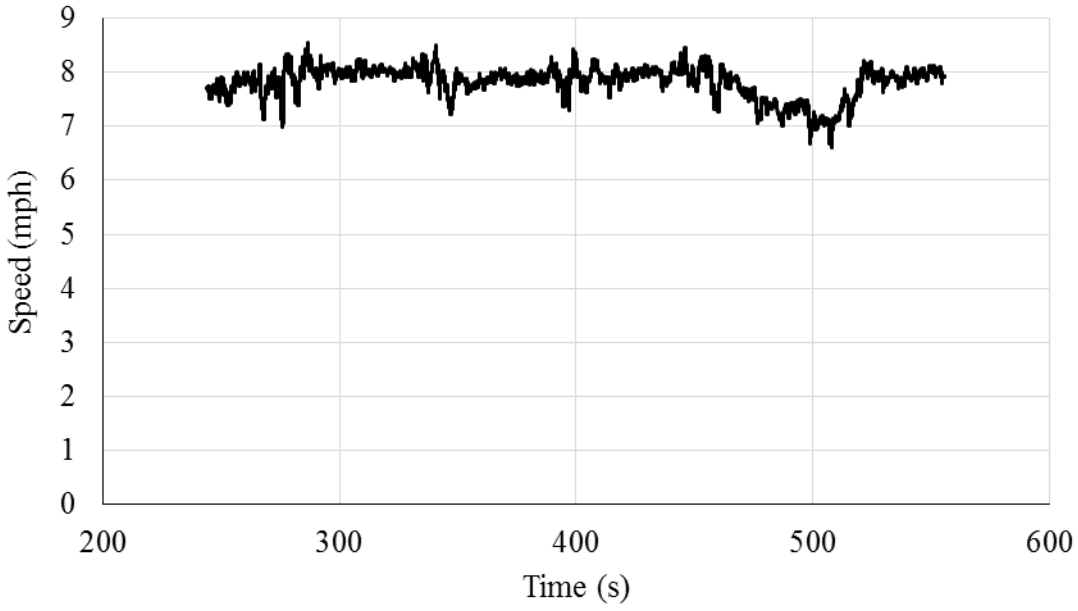

Figure 4-10 Measured speed vs. time

Table 4-4 First trailer time segments (80 psi, 8 mph)

Time Segments	
1	260-265
2	310-315
3	360-365
4	420-425
5	480-485
6	540-545

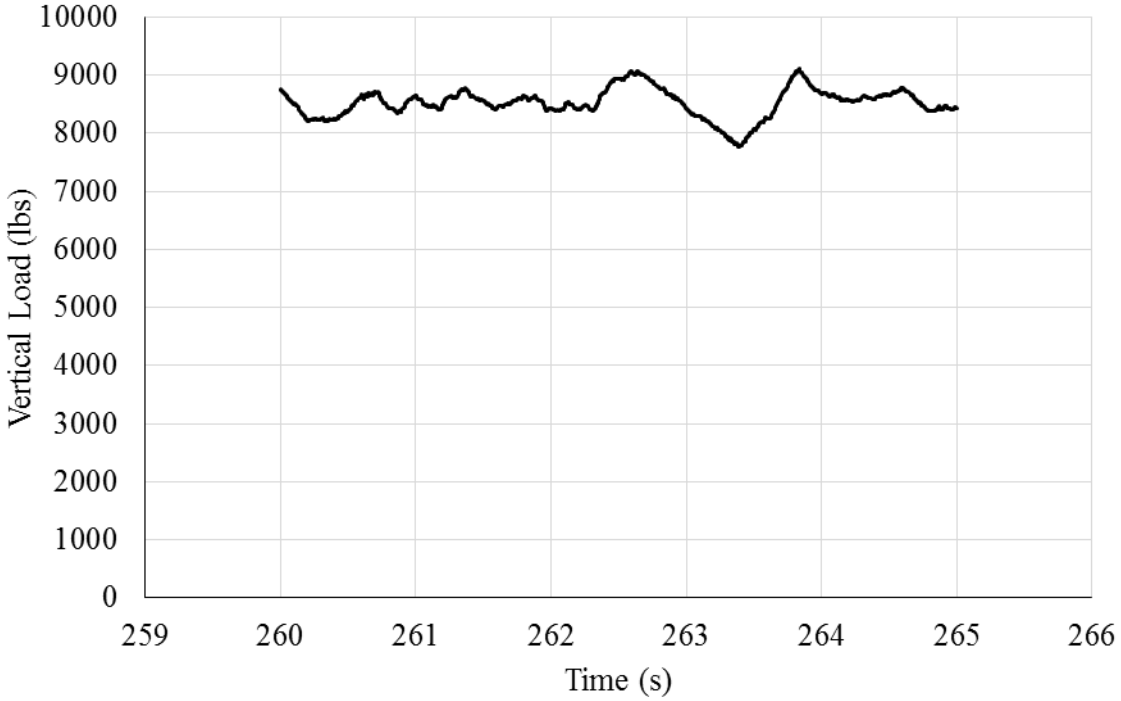

Figure 4-11 First segment of tire vertical load

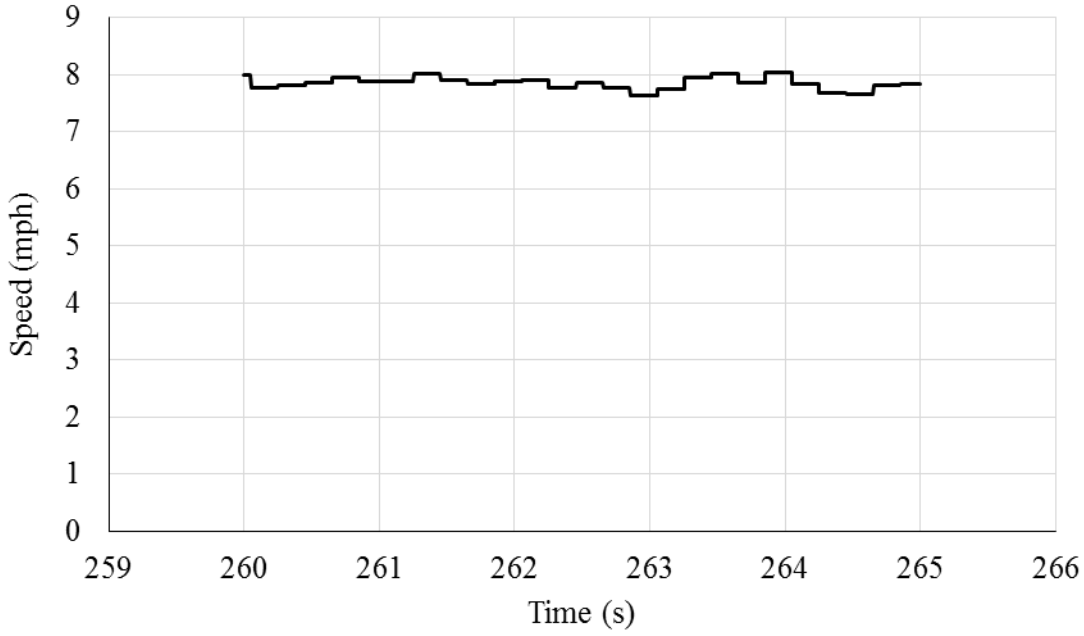

Figure 4-12 First segment of speed

Table 4-5 and Figure 4-13 compare the measured RRC via the simulations. It can be seen the simulation results are almost in complete agreement with the measured RRC.

Table 4-5 RRC comparison in six segments

Average Tire Load 8,917 lbs - Average Speed 8 mph - 80 psi		
RRC Results	**Virtual tests**	**Measurements**
First Segment	0.0006771	0.0010185
Second Segment	0.0006548	0.0006050
Third Segment	0.0006406	0.0005262
Fourth Segment	0.0006304	0.0007499
Fifth Segment	0.0006153	0.0011644
Sixth Segment	0.0006192	0.0005698

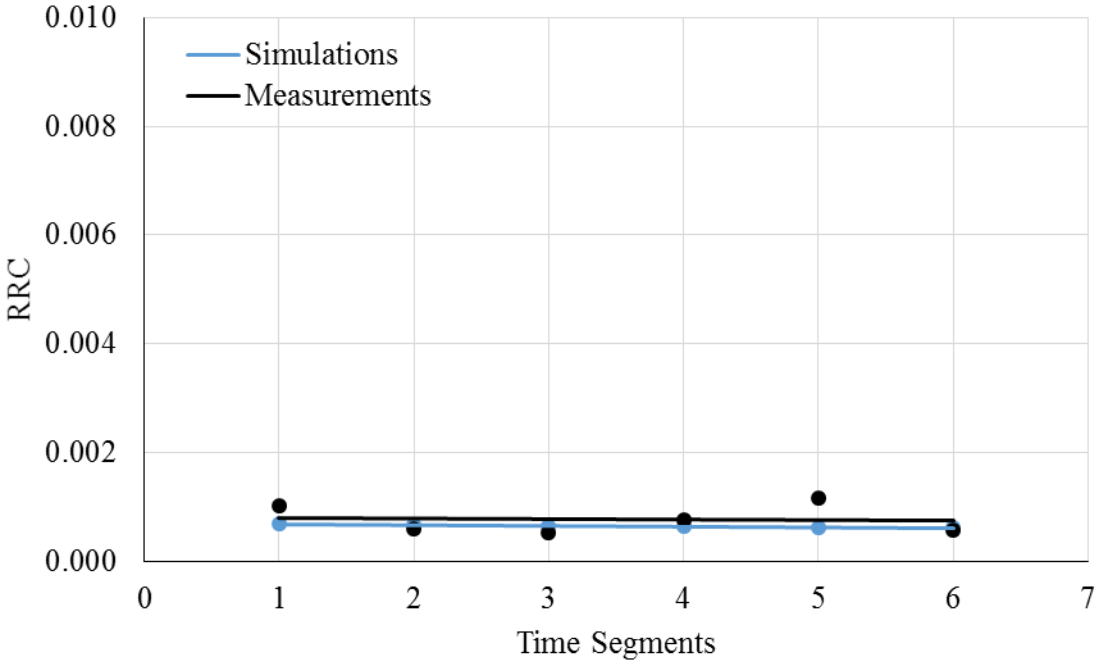

Figure 4-13 RRC comparison for each time segment between measurements and simulations

4.1.2.2 80 psi Inflation Pressure and Average Speed of 15 mph

The total measured data for vertical load and speed are shown in Figure 4-14 and Figure 4-15 individually, and the six segment of the straight truck's straight motion under the mentioned cicumstances are shown in Table 4-6. Figure 4-16 and Figure 4-17 show the first five second segment of recorded vertical load and speed.

Table 4-7 and Figure 4-18 compare the measured RRC via simulations. It can be seen the simulation results are in agreement with the measured RRC.

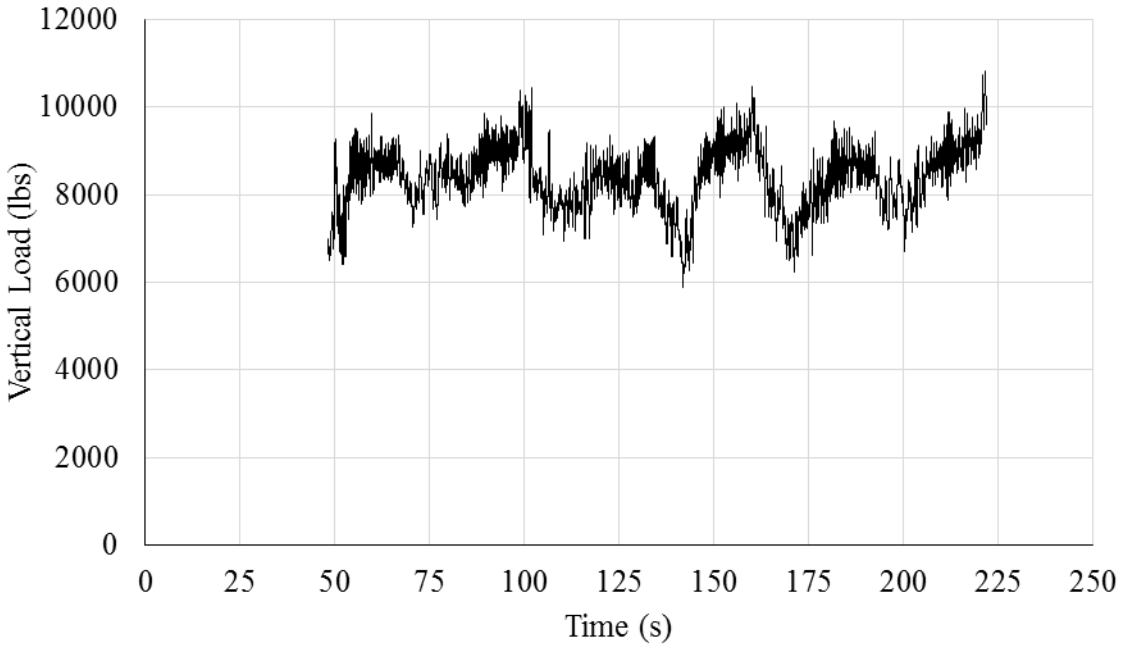

Figure 4-14 Measured tire vertical load

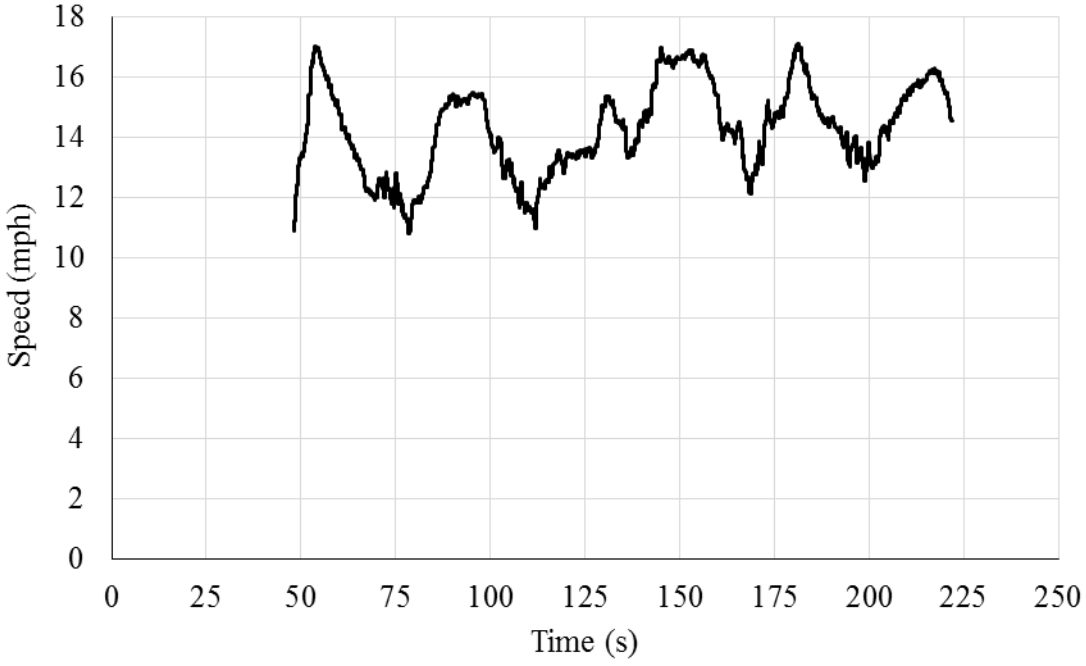

Figure 4-15 Measured speed vs. time

Table 4-6 First trailer time segments (80 psi, 15 mph)

Time Segments	
1	60-65
2	90-95
3	120-125
4	155-160
5	185-190
6	210-215

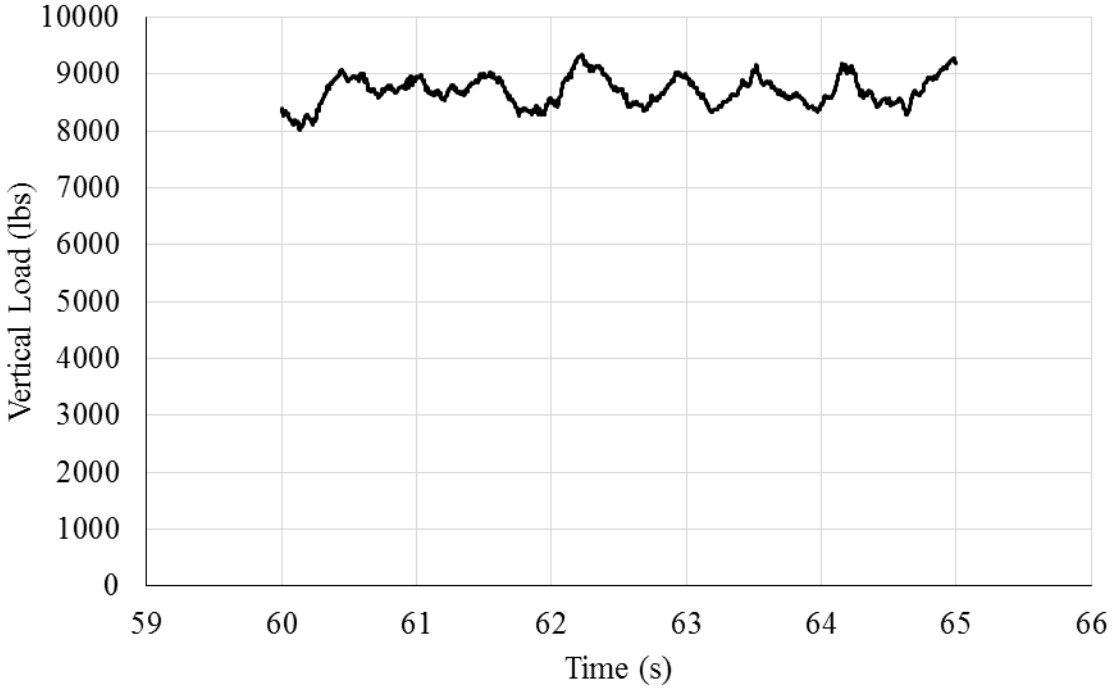

Figure 4-16 First segment of tire vertical load

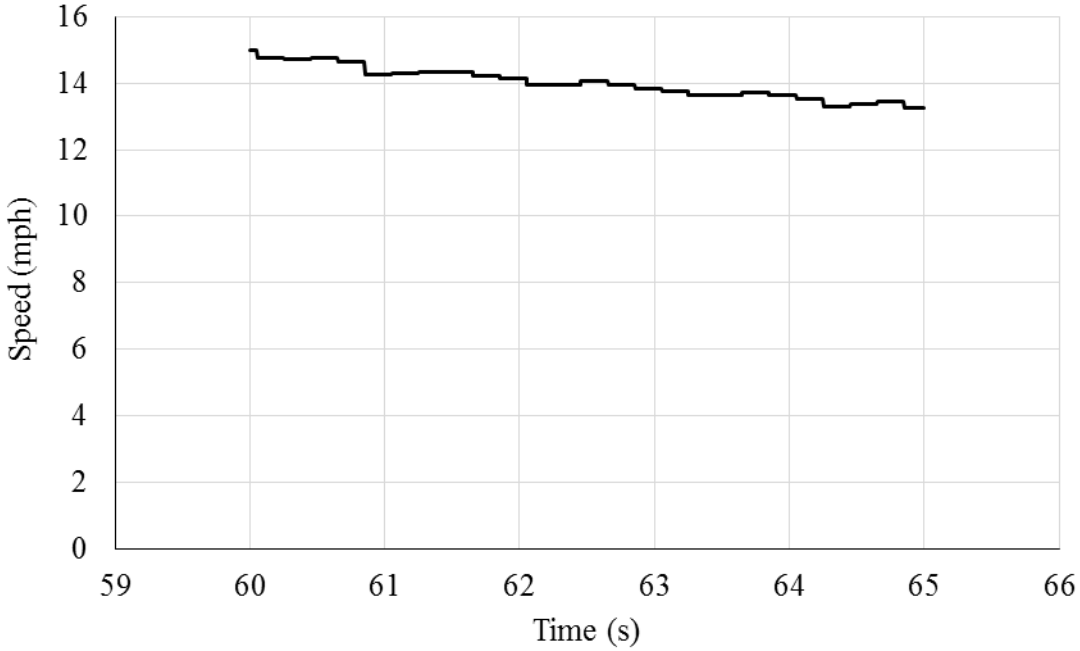

Figure 4-17 First segment of speed

Table 4-7 RRC comparison in six segments

Average Tire Load 8,380 lbs - Average Speed 8 mph - 80 psi		
RRC Results	**Virtual tests**	**Measurements**
First Segment	0.0007000	0.0004935
Second Segment	0.0006769	0.0005386
Third Segment	0.0006623	0.0007248
Fourth Segment	0.0006517	0.0003326
Fifth Segment	0.0006361	0.0004818
Sixth Segment	0.0006401	0.0002471

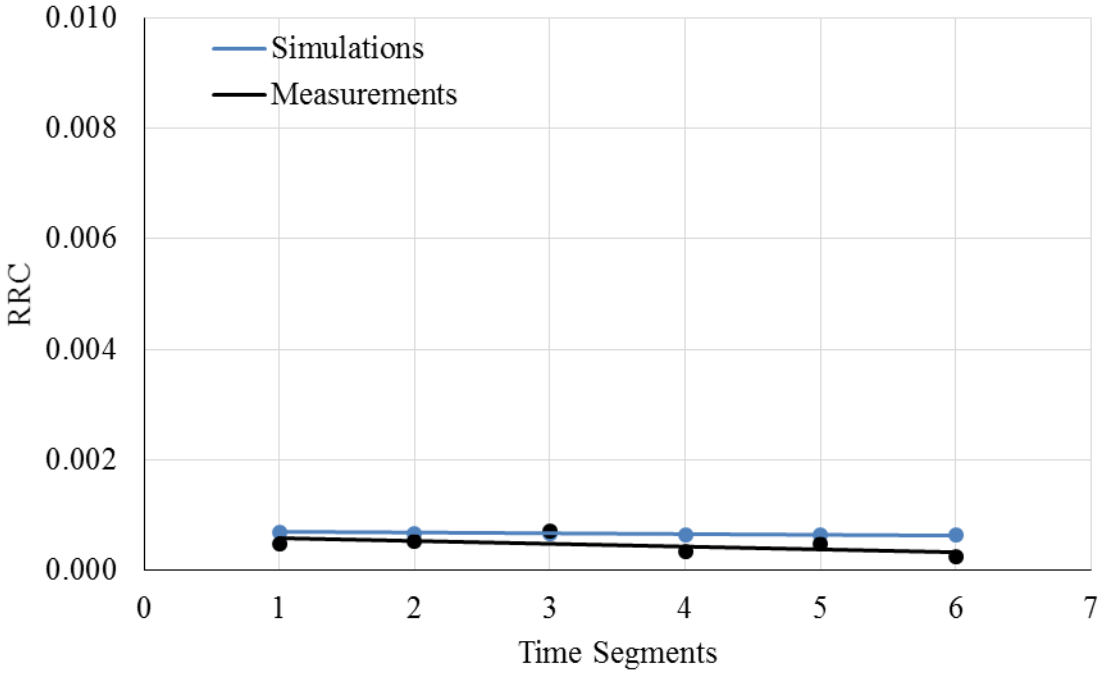

Figure 4-18 RRC comparison for each time segment between measurements and simulations

4.1.2.3 110 psi Inflation Pressure and Average Speed of 8 mph

The simulations are then continiued under same load for 110 psi inflation pressure. The full measured data of loading and speed are shown in Figure 4-19 and Figure 4-20.

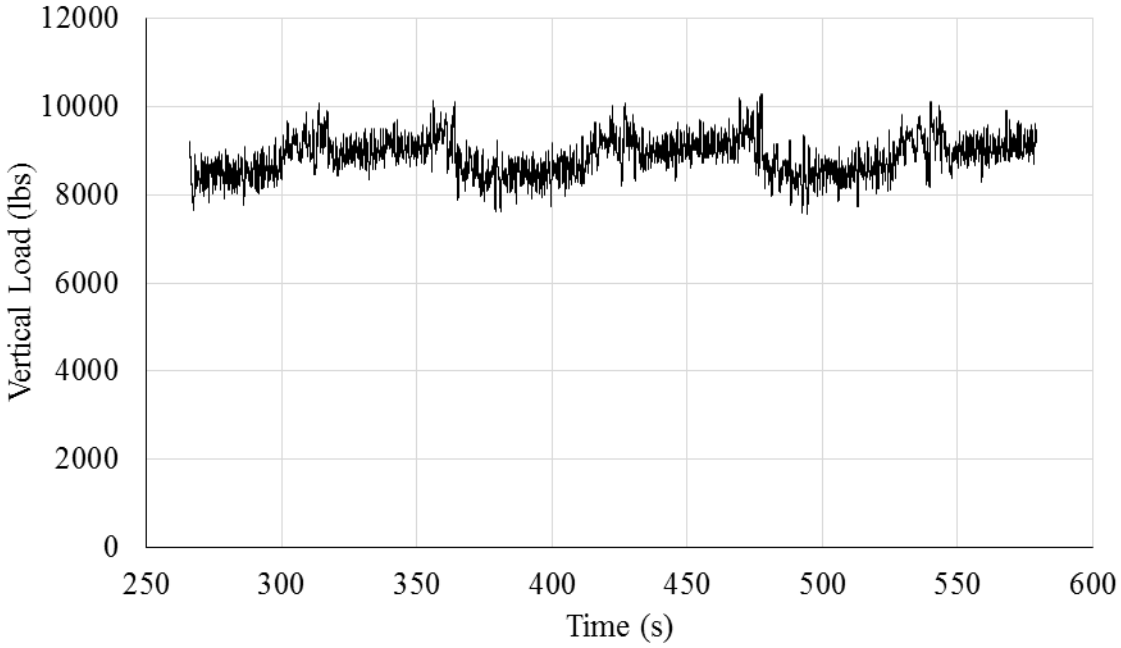

Figure 4-19 Measured tire vertical load

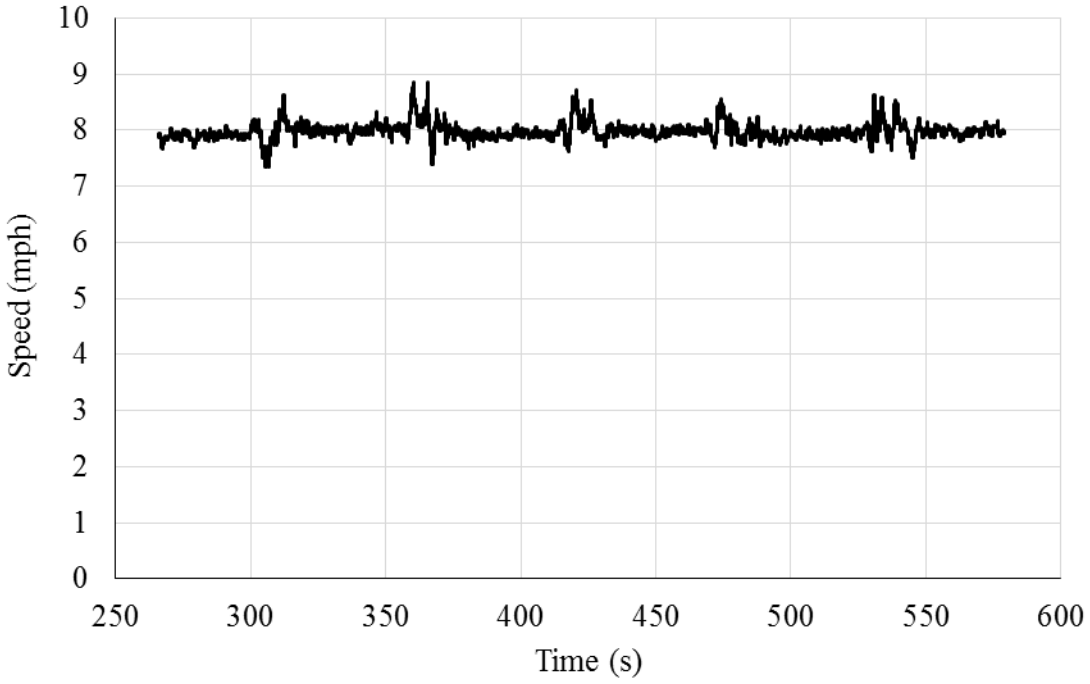

Figure 4-20 Measured speed vs. time

The six segment of the straight movement of the truck, are shown in Table 4-8. Each one of the segmants is considered five seconds. Figure 4-21 and Figure 4-22 show the first segment of vertical load and speed from the six segments.

Table 4-8 First trailer time segments (110 psi, 8 mph)

Time Segments	
1	280-285
2	330-335
3	390-395
4	440-445
5	500-505
6	560-565

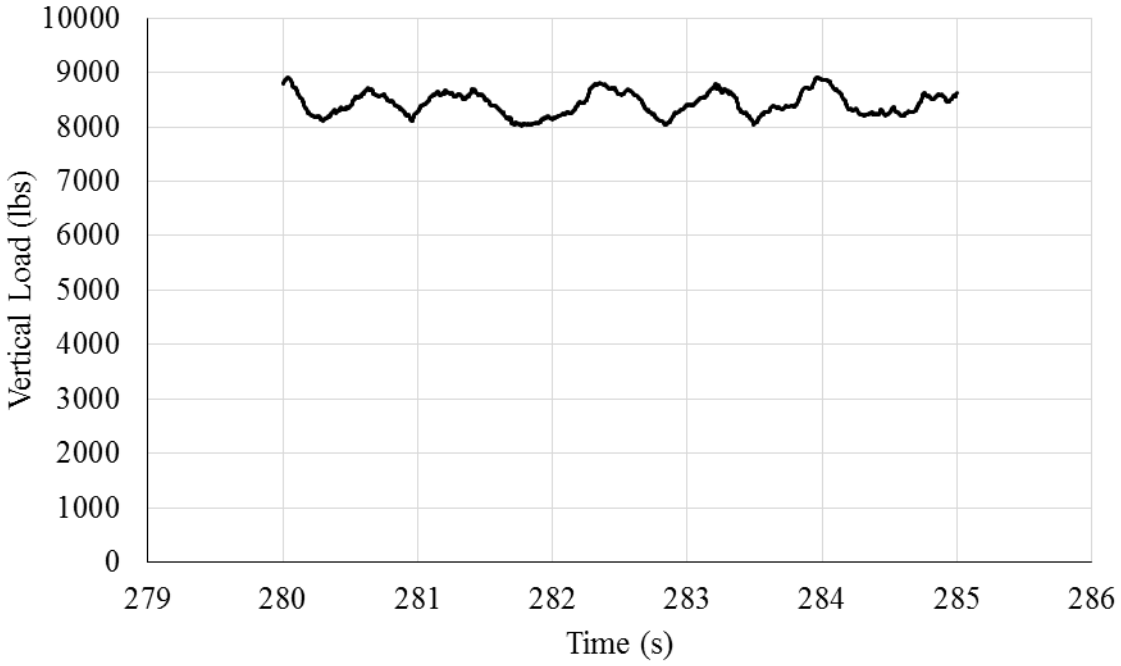

Figure 4-21 First segment of tire vertical load

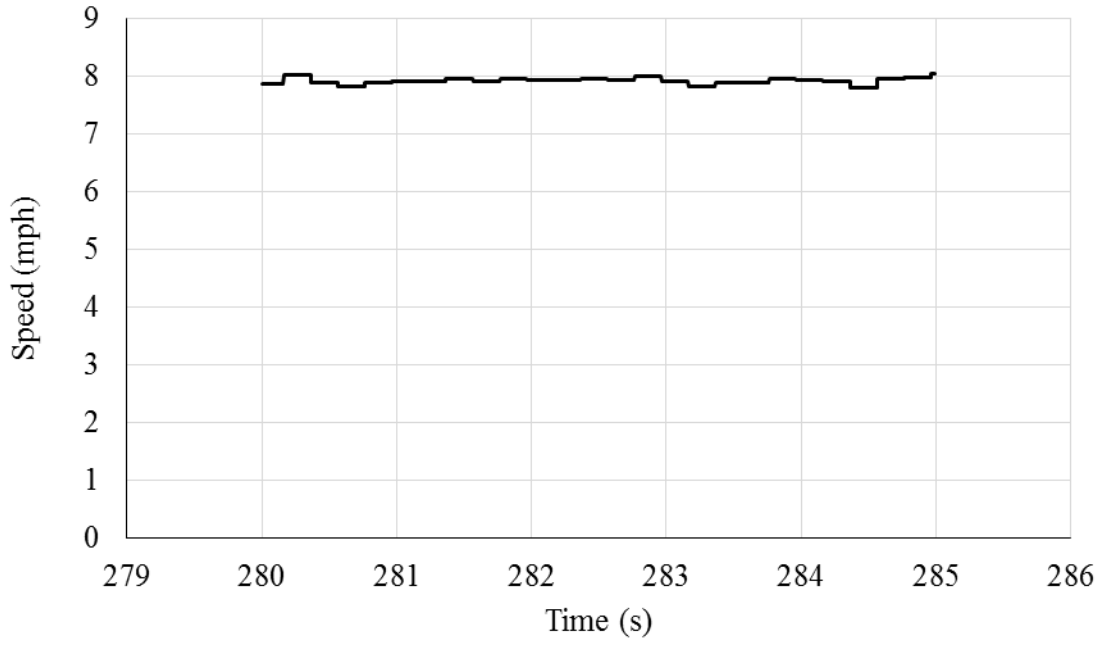

Figure 4-22 First segment of speed

Table 4-9 and Figure 4-23 compare the measured RRC via the simulations. It can be seen the simulation results are showing agreement with the measured RRC same as the previous conditions under the same loading.

Table 4-9 RRC comparison in six segments

Average Tire Load 8,871 lbs - Average Speed 8 mph - 110 psi		
RRC Results	**Virtual tests**	**Measurements**
First Segment	0.0003239	0.0003068
Second Segment	0.0003132	0.0006540
Third Segment	0.0003065	0.0008402
Fourth Segment	0.0003016	0.0002640
Fifth Segment	0.0002943	0.0004586
Sixth Segment	0.0002962	0.0002733

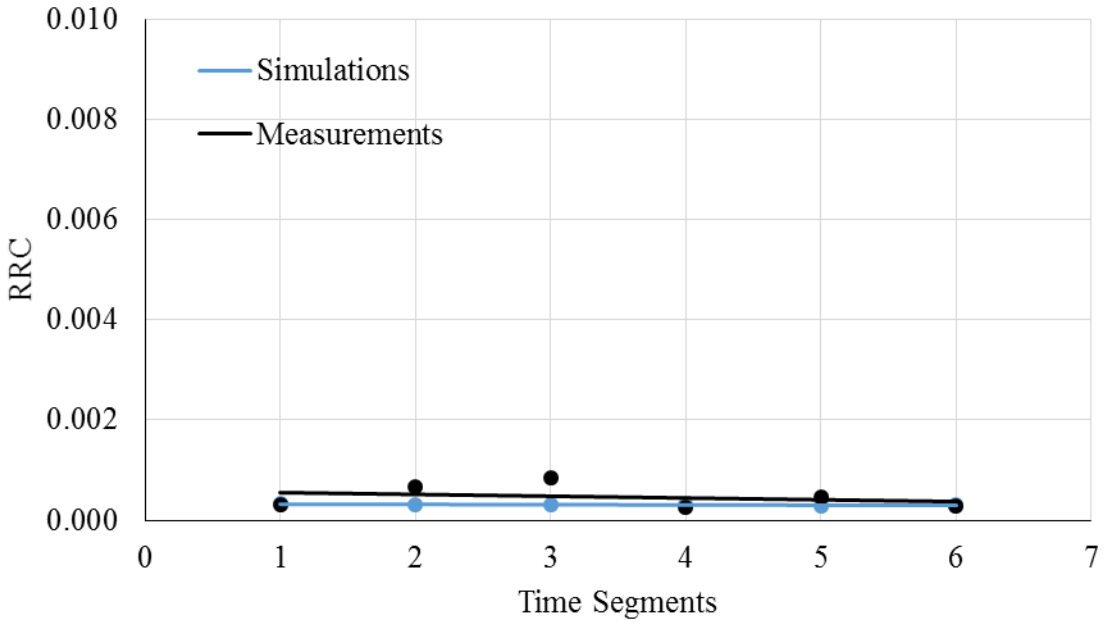

Figure 4-23 RRC comparison for each time segment between measurements and simulations

4.1.3 Tractor-Second Trailer

Second trailer is the heaviest load compared to other cases with the average tire vertical load of 8,699 lbs.The test results are conducted under 110 psi inflation pressure and the vertical load and speed as shown in Figure 4-24 and Figure 4-25 correspondingly. Table 4-10 shows the six segments of the straight movement of the truck; each one is five seconds. Figure 4-26 and Figure 4-27 show the first segment of measured vertical load and speed of the total experimental data.

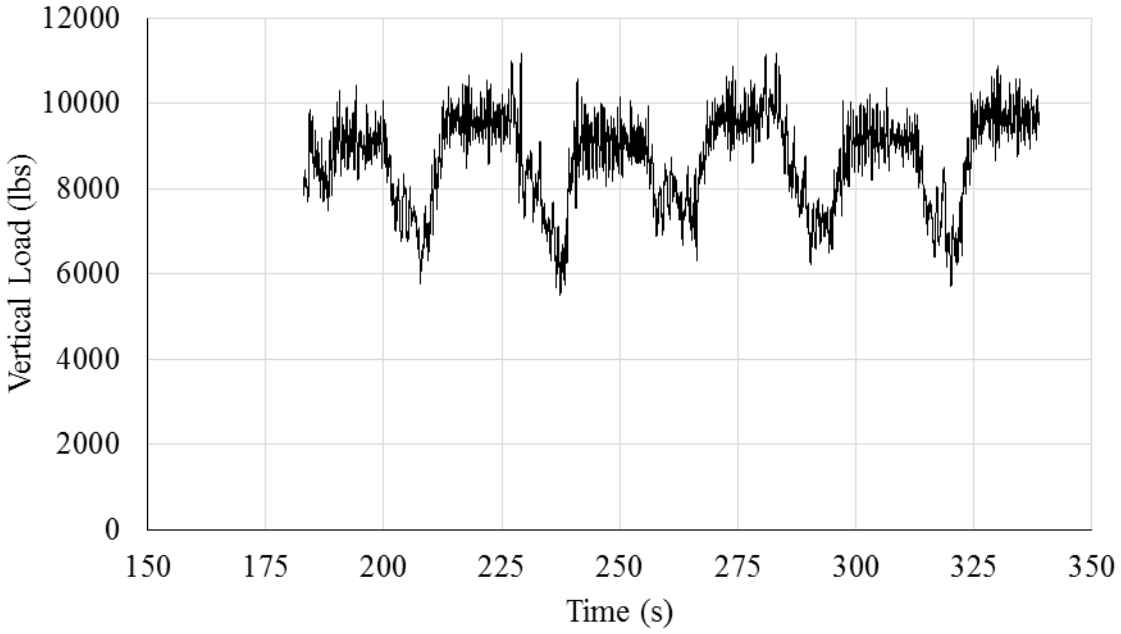

Figure 4-24 Measured tire vertical load

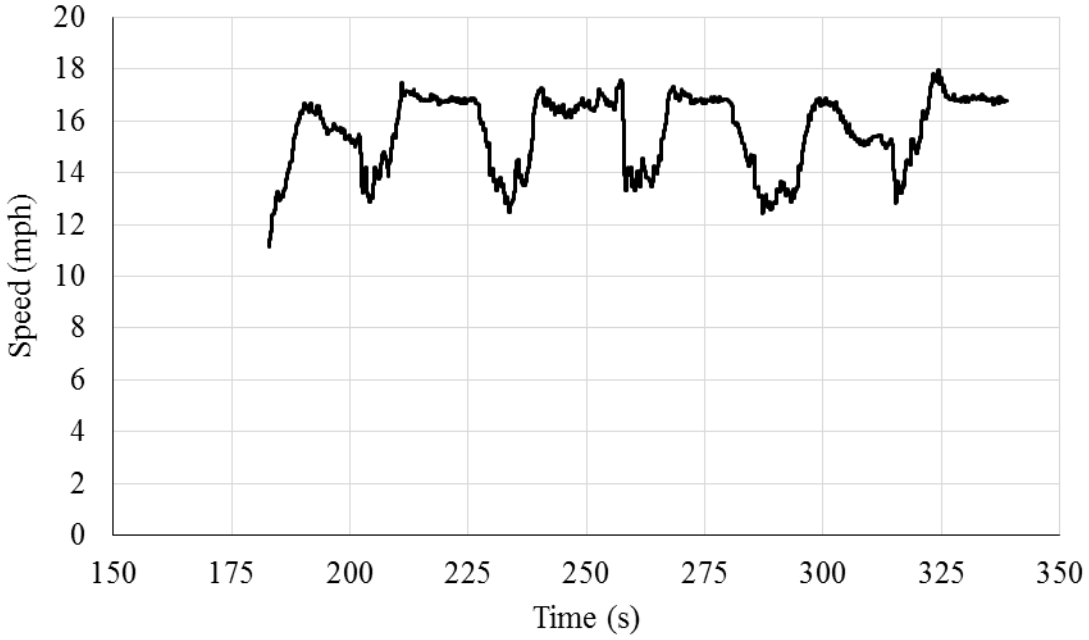

Figure 4-25 Measured speed vs. time

Table 4-11 and Figure 4-28 compare the measured RRC via the simulations. Same as previous cases, it can be seen the simulation's RRC results are corresponding to the measured RRC.

Table 4-10 Second trailer time segments

Time Segments	
1	190-195
2	220-225
3	245-250
4	275-280
5	305-310
6	330-335

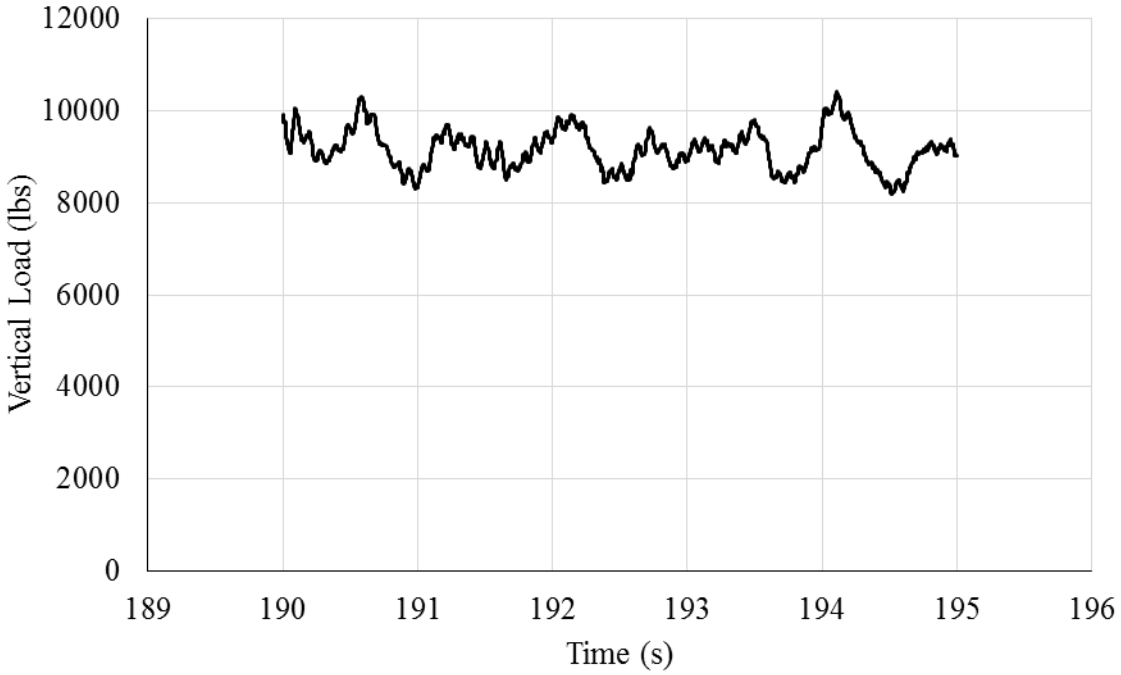

Figure 4-26 First segment of tire vertical load

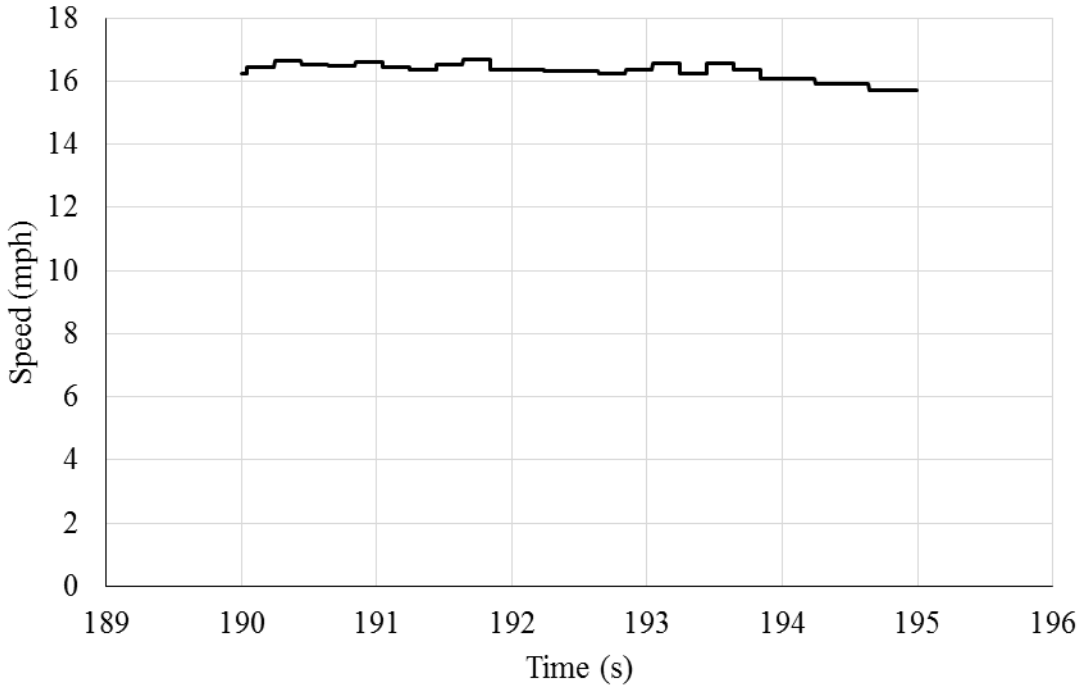

Figure 4-27 First segment of speed

Table 4-11 RRC comparison in six segments

Average Tire Load 8,699 lbs - Average Speed 15 mph - 110 psi		
RRC Results	**Virtual tests**	**Measurements**
First Segments	0.0008999	0.0010886
Second Segments	0.0008702	0.0011134
Third Segments	0.0008514	0.0008941
Fourth Segments	0.0008378	0.0010593
Fifth Segments	0.0008177	0.0008844
Sixth Segments	0.0008229	0.0009728

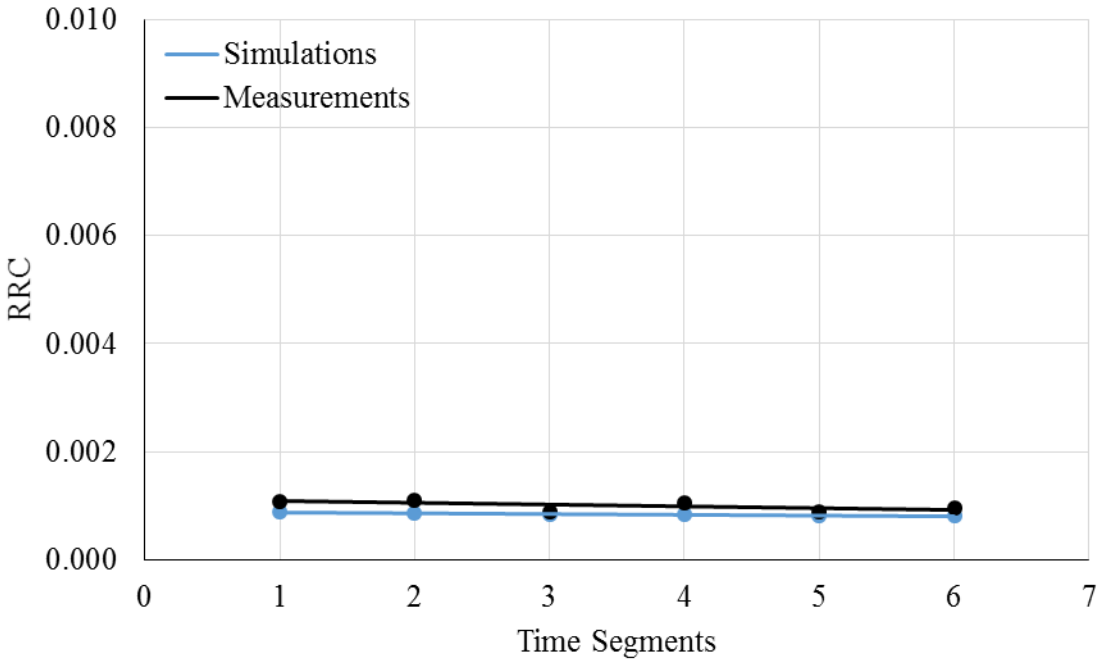

Figure 4-28 RRC comparison for each time segment between measurements and simulations

4.2 CHAPTER SUMMARY

Series of rolling resistance tests took place at Volvo facility in North Carolina. The testing environment is created as simulations in PAM-CRASH. Different simulation conditions are listed below based on the vertical load applied:

1. Bobtail (866 lbs)
    - Speed: 15 mph, Inflation pressure: 110 psi
2. Tractor-first trailer (8,723 lbs)
    - Speed: 8 mph, Inflation pressure 80 psi
    - Speed: 15 mph, Inflation pressure 80 psi
    - Speed: 8 mph, Inflation pressure 110 psi

3. Tractor-Second Trailer (8,699 lbs)

    - Speed: 15 mph, Inflation pressure 110 psi

In all mentioned cases, the results achieved from simulations are in agreement with measurements received from experimental tests, except for the lightest load (Bobtail).

CHAPTER 5

ROLLING RESISTANCE TESTS AND SIMULATIONS ON SOFT SOIL

In this chapter, the rolling resistance coefficient (RRC) of the *Michelin XOne Line Energy T* tire model is examined on all soft soil models. The efficiency of each soil model is discussed. This chapter is part of an article accepted in the International Journal of Vehicle Performance.

5.1 MEASUREMENTS

In order to validate the UOIT FEA model of the *Michelin XOne Line Energy T* tire model on soft soil, a series of tests are conducted at the Volvo Group Trucks Technology facility in Greensboro, North Carolina. The subject tire is tested under various vertical loads. Force transducers are installed onto the tire to record three-dimensional forces and moments applied to the tire as previously described in CHAPTER 4. Figure 5-1 shows the soft soil testing environment used for physical testing of the RRC.

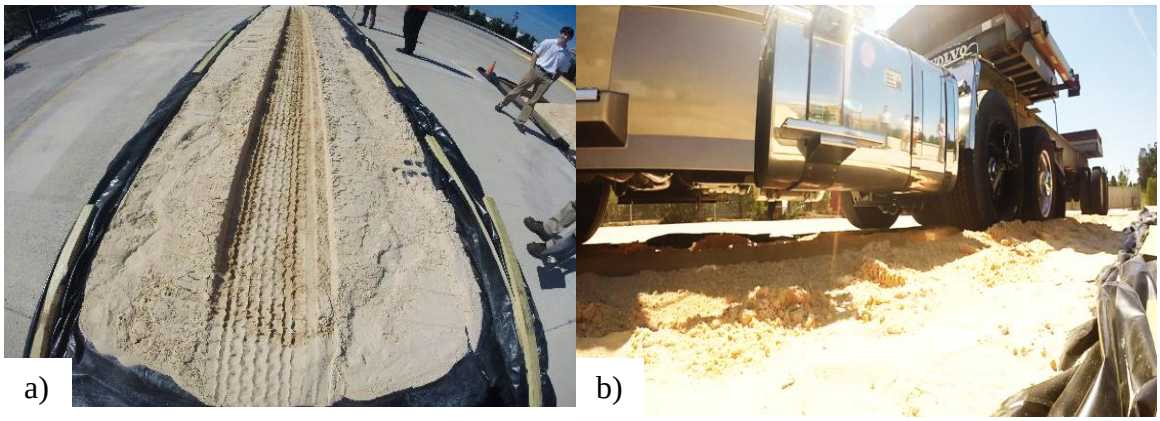

Figure 5-1 a) *Michelin XOne Line Energy T* tire dry sand test and b) tire's footprint on dry sand

5.2 ROLLING RESISTANCE VALIDATION ON SOFT SOIL

In order to validate the modeled tire's simulation result by the measurements taken from the experiments on soft soil, the full SPH, half SPH, quarter SPH, and full FEA soil models are used. The UOIT FEA *Michelin XOne Line Energy T* tire model is placed on each of the soil models. The tire is then inflated to the desired inflation pressure and loaded with a specified vertical loading applied to the center axis of the wheel. Gravity is also assigned to the model by using acceleration field card in PAM-CRASH. The constant speed of 5 mph is also assigned to the center of the tire and friction coefficient is taken as 0.6. By using Equation (5-1), RRC is then calculated for measurements and all simulation results.

$$RRC = \frac{F_x}{F_z} \tag{5-1}$$

In the rolling resistance test, four different vertical loads are applied to the tire through different trailers assigned to the tractor. One of the loads is tested both under 110 and 80 psi inflation pressure.

Simulation results are compared to measurements are shown for all soil models. Table 5-1 and Figure 5-2 show the results for full FEA soil model. The resultant RRC displays good correlation with measurements. However, as previously mentioned, the high computational time using the FEA modeling method for a wide-base tire makes for an inefficient simulation of the soil model.

Table 5-1 RRC measurements and full FEA simulation results

Dry Sand-Full FEA Model (5 mph)				
Truck Type	**Tire Vertical Load (lbs)**	**Inflation Pressure (psi)**	**RRC Measurement**	**RRC Simulation**
Bobtail	1774.97	110	0.2794	0.2178
Light	2680.94	110	0.2795	0.2337
Loaded 2-1	8184.02	110	0.3088	0.3055
Loaded 2-2	8311.40	80	0.2907	0.3014
Loaded 1	8706.17	110	0.3277	0.3109

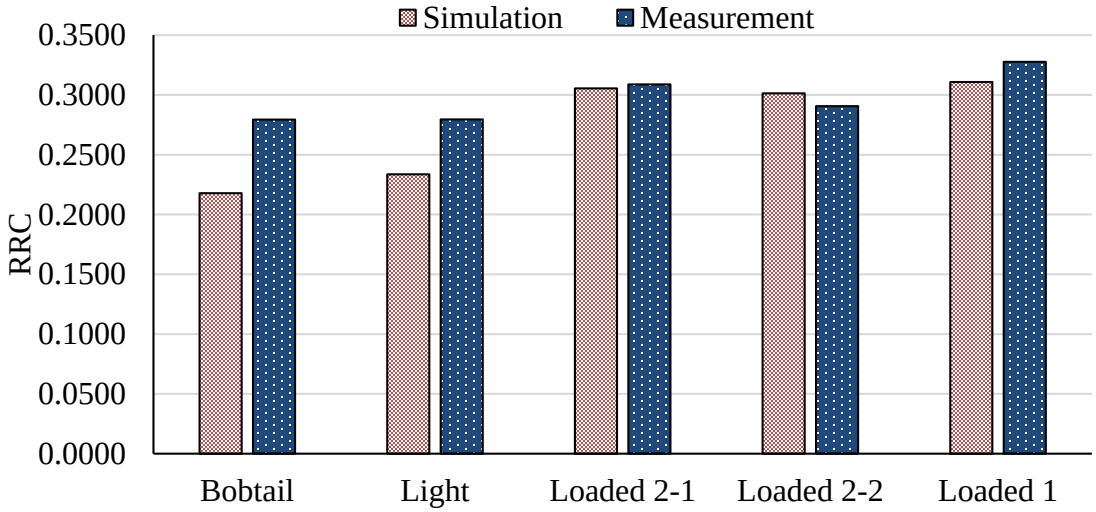

Figure 5-2 RRC measurement vs simulation bar chart of full FEA

Figure 5-3 and Table 5-2 shows the RRC comparison for full SPH soil model.

Table 5-2 RRC measurements and full SPH simulation results

Dry Sand- Full SPH Model (5 mph)				
Truck Type	**Tire Vertical Load (lbs)**	**Inflation Pressure (psi)**	**RRC Measurement**	**RRC Simulation**
Bobtail	1774.97	110	0.2794	0.2510
Light	2680.94	110	0.2795	0.2795
Loaded 2-1	8184.02	110	0.3088	0.3497
Loaded 2-2	8311.40	80	0.2907	0.3395
Loaded 1	8706.17	110	0.3277	0.3502

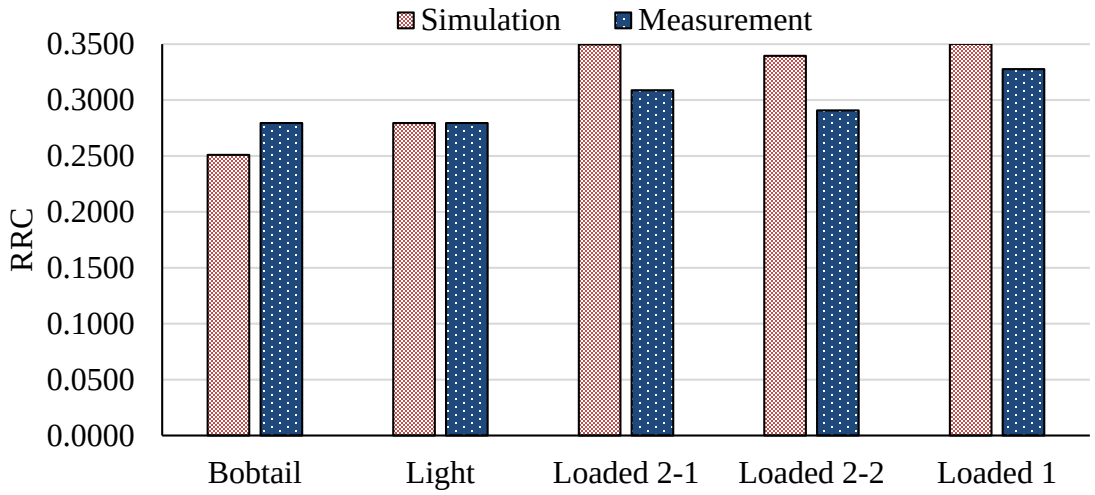

Figure 5-3 RRC measurement vs full SPH simulation results bar chart

As shown in Table 5-2 and Figure 5-3, the simulation results are in good correlation with the physical measurements, most notably on the light load (2680.9 lbs). In case of the wide-base FEA tire, the full SPH soil takes less computation time compared to full FEA and since SPH is a better representative of soil, SPH is considered more efficient compared to FEA soil. Later, half SPH and quarters SPH models are studied and RRC results are compared to determine the optimum soil.

Figure 5-4 and Table 5-3 show the RRC comparison for hybrid half SPH soil model.

Table 5-3 RRC measurements half SPH simulation results

Dry Sand-Hybrid Half SPH Model (5 mph)				
Truck Type	**Tire Vertical Load (lbs)**	**Inflation Pressure (psi)**	**RRC Measurement**	**RRC Simulation**
Bobtail	1774.97	110	0.2794	0.2654
Light	2680.94	110	0.2795	0.2699
Loaded 2-1	8184.02	110	0.3088	0.3446
Loaded 2-2	8311.40	80	0.2907	0.3445
Loaded 1	8706.17	110	0.3277	0.3485

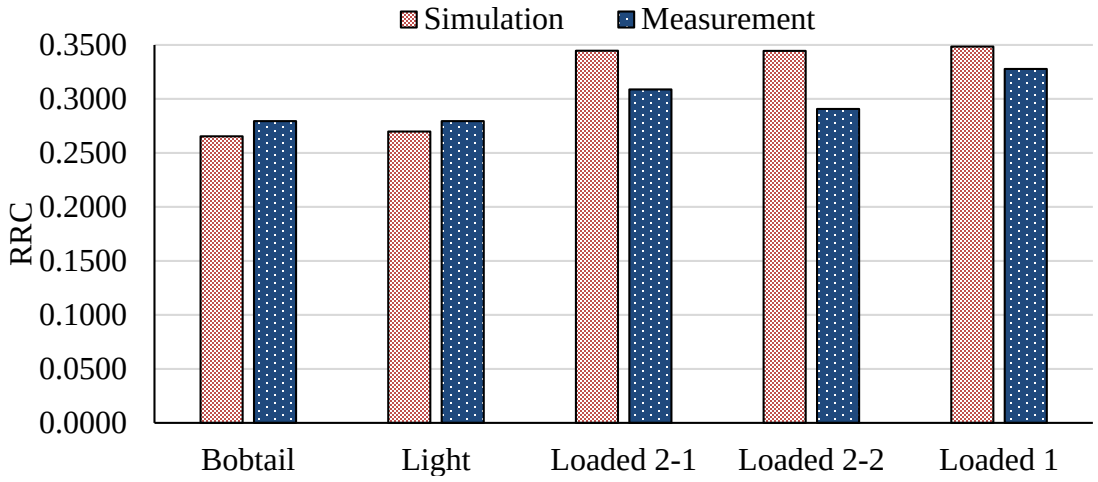

Figure 5-4 RRC measurement vs half SPH simulation results bar chart

From Table 5-3 and Figure 5-4, it can be seen that there is a good correlation between measured RRC and simulation results. This proves the accuracy of half SPH soil model. The half SPH soil model was also previously proven to require less computational time compared to the full SPH, which further emphasizes its superior efficiency over the use of full SPH.

Figure 5-5 and Table 5-4 show the RRC comparison for hybrid quarter SPH soil model.

Table 5-4 RRC measurements and quarter SPH simulation results

Dry Sand-Hybrid Quarter SPH Model (5 mph)				
Truck Type	**Tire Vertical Load (lbs)**	**Inflation Pressure (psi)**	**RRC Measurement**	**RRC Simulation**
Bobtail	1774.97	110	0.2794	0.2438
Light	2680.94	110	0.2795	0.2615
Loaded 2-1	8184.02	110	0.3088	0.3515
Loaded 2-2	8311.40	80	0.2907	0.3497
Loaded 1	8706.17	110	0.3277	0.3584

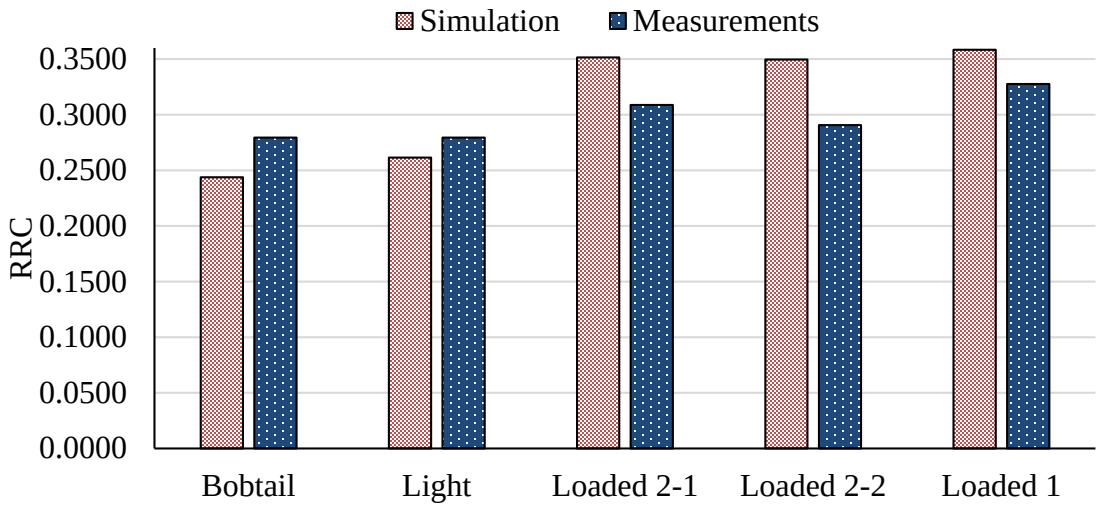

Figure 5-5 RRC measurement vs quarter SPH simulation results bar chart

RRC results for quarter SPH are also obtained as shown in Figure 5-5 and Table 5-4. Compared to all soil models quarter SPH has higher accuracy. As shown previously quarter SPH has the lowest computation time among all other models, which makes it the most efficient model among the others.

The rolling resistance coefficient (RRC) of simulations as shown above are in good agreement with measurements. The measurement received from experimental tests showed that the soil has the depth of 6 inches (152 mm). However in simulations the soil height used has the depth of 585 mm. The reason for using this height is to show that the tire sinkage in the soil under heavy loads is greater than 6 inches (152 mm), as shown in Figure 5-6. The tire in the right is loaded to 8706.17 lbs (loaded 1) whereas the tire in the left is loaded to 1774.97 lbs (Bobtail). In continuation all simulations are repeated with a soil with 6 inch height which shows poor results.

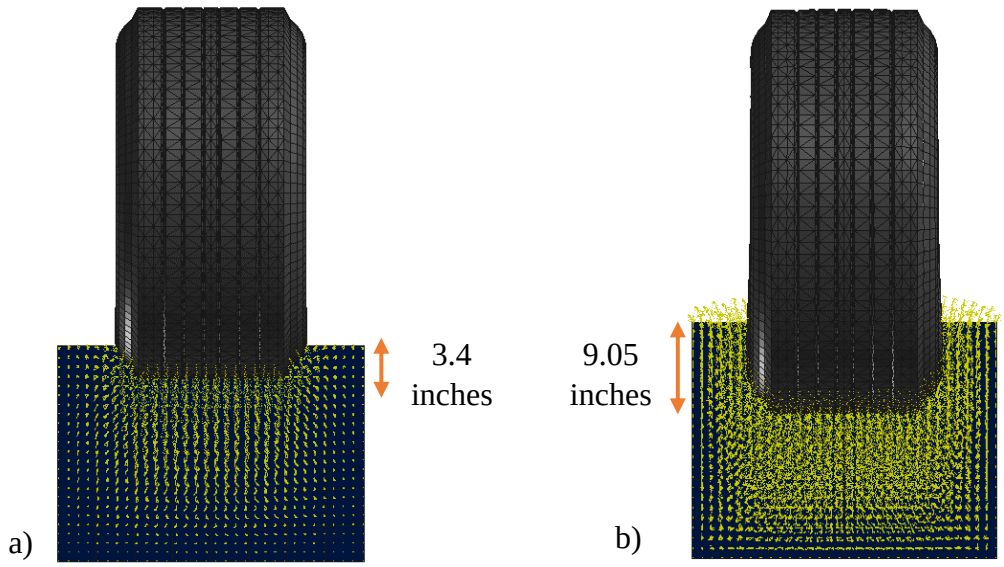

Figure 5-6 a) UOIT FEA *Michelin XOne Line Energy T* Tire model sinkage for 8706 lbs (loaded 1) and b) 1775 lbs (Bobtail) on left

When the tire is rolling on 6-inch height soil, the tire will contact the concrete beneath the soil (or the rigid soil box in the simulation which is the same as running the tire on concrete). In order to prove this, series of tests are conducted to simulate the tire rolling on 6 inch dry sand in a rigid container with same width and height as the measurements, shown in Figure 5-7.

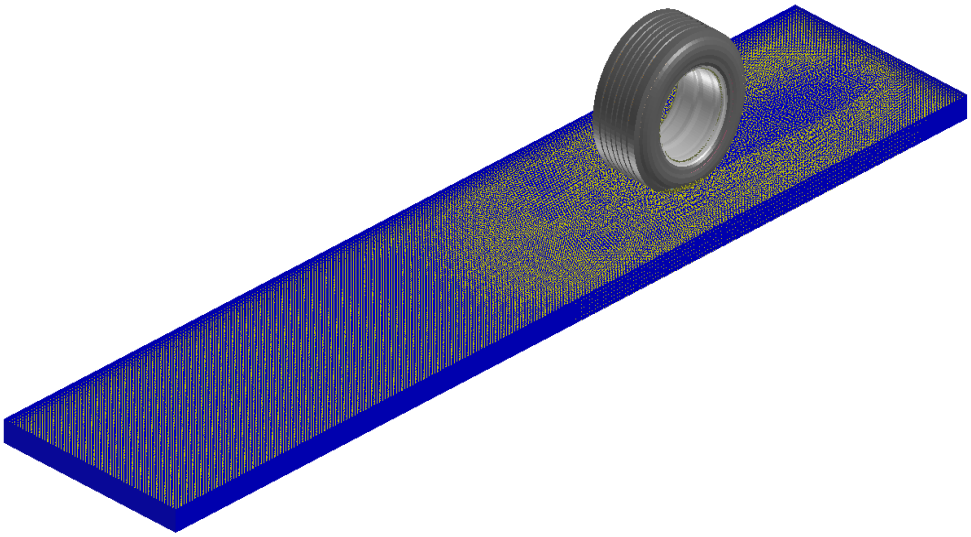

Figure 5-7 UOIT FEA *Michelin XOne Line Energy T* tire model rolling on 6 inch dry sand

Rolling resistance coefficient for 6 inch dry sand is shown in Table 5-5 and

Figure 5-8. As it can be seen the results are showing much lower RRC values due to the low thickness of the soil compared to what sinkage the tire may have.

Table 5-5 6-inch dry sand simulation results

Dry Sand (5 mph)- 6 inch Full SPH				
Truck Type	**Tire Vertical Load (lbs)**	**Inflation Pressure (psi)**	**RRC Measurement**	**RRC Simulation**
Bobtail	1774.97	110	0.2794	0.1727
Light	2680.94	110	0.2795	0.1798
Loaded 2-1	8184.02	110	0.3088	0.2004
Loaded 2-2	8311.40	80	0.2907	0.1955
Loaded 1	8706.17	110	0.3277	0.2049

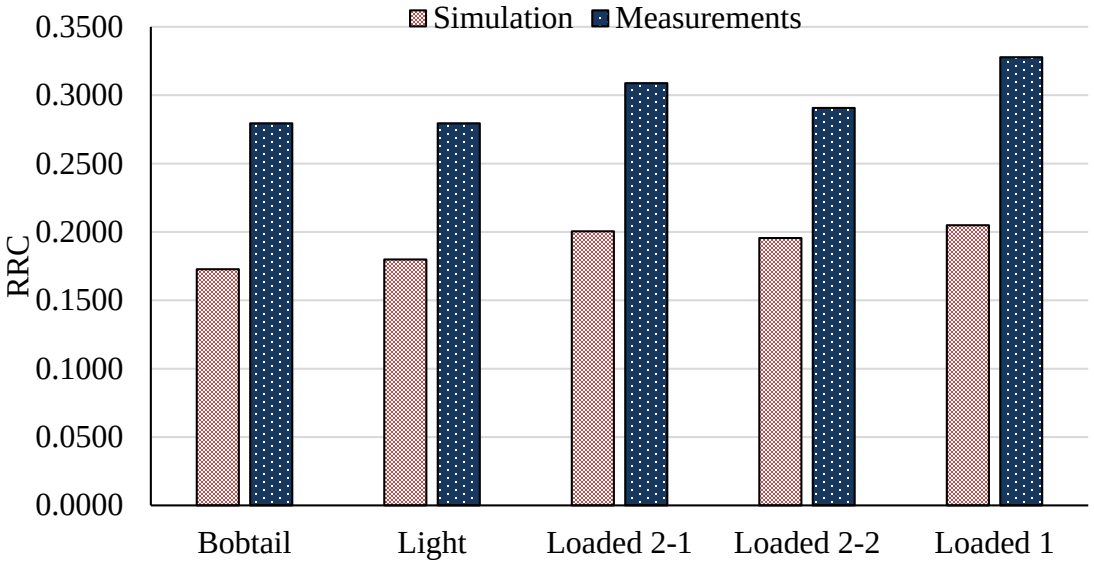

Figure 5-8 RRC comparison of modeled tire on 6 inch sand

In the end the total error of each soil models results are compared to one another in Table 5-6. As it can be seen in Table 5-6, quarter SPH model has the least error percentage which makes it the most accurate. Also as shown previously it has the lowest computation time.

.

Table 5-6 Total error percentage of each soil model

Soil Model	Total Error %
FEA Model	7.86%
Full SPH	5.36%
Hybrid Half SPH	5.84%
Hybrid Quarter SPH	5.30%
6 inch SPH	35.85%

5.3 CHAPTER SUMMARY

In this chapter, tire is validated on soft soil models based on the measurements of rolling resistance on soft soil obtained from the Volvo testing facility in North Carolina and the efficiency of different soil models are discussed.

The tests had been done for all soil models. RRC of simulations are compared with measurements for full FEA, full SPH, hybrid half SPH, hybrid quarter SPH, and 6 inch SPH soil for all loads known as:

1. Bobtail (1774.97 lbs)
    - Speed: 5 mph, Inflation pressure: 110 psi
2. Light (2680.94 lbs)
    - Speed: 5 mph, Inflation pressure: 110 psi
3. Tractor-first trailer (8706.17 lbs)
    - Speed: 5 mph, Inflation pressure: 110 psi
4. Tractor-second trailer (8184.02 lbs)
    - Speed: 5 mph, Inflation pressure: 110 psi

5. Tractor-second trailer (8311.40 lbs)

    - Speed: 5 mph, Inflation pressure: 80 psi

The total error for each soil is calculated in the end. The hybrid quarter SPH has the highest accuracy by 5.30% total error and the 6 inch SPH soil model has the lowest accuracy by having total error of 35.85%.

CHAPTER 6

CONCLUSION AND SUGGESTIONS FOR FUTURE WORK

6.1 ACHIEVEMENTS

FEA as the strongest application for solving nonlinear problems has been used in this thesis to model tire characteristics. In this thesis by using FEA methodology a wide-base *Michelin XOne Line Energy T* tire is modeled. The tire is validated through different tests and the results obtained from simulations are compared with published data. Vertical stiffness test is effective by having less than 5% error. Static footprint length and width has less than 4 mm difference between simulation results and published data. Also the first mode of vibration happened at 74 Hz which is a good achievement since it is in a reasonable range for truck tires as revealed previously.

By getting satisfactory results from tire validation, the new phase of thesis begins which is modeling dry sand soil. In order to create soil models that can be a representative of dry sand, two steps are needed to be taken to calibrate the soil: pressure-sinkage relationship test and shear strength test. Pressure-sinkage relationship test is implemented both to FEA, and SPH soil models and shear strength test is implemented to SPH only. Afterward by using FEA and SPH methodologies, four soil models are successfully created; full FEA, full SPH, hybrid half SPH, and hybrid quarter SPH. Each soil model is compared in same situations and simulation setups in order to find the most efficient soil regarding to CPU solving time. It is proved that hybrid quarter SPH model is able to reduce the computational time by almost 50%.

Series of tests have taken place at Volvo Facility in North Carolina regarding to rolling resistance of the modeled tire. Fine transducer is assigned to the actual *Michelin XOne Line Energy T* tire and is recorded all forces and moments applied to it. The rolling resistance of desired tire is tested both on hard surface and soft soil through series of tests under various loads, inflation pressure, and speed. All tests are replicated in PAM-CRASH as shown in CHAPTER 4 and CHAPTER 5.

In most of the cases, rolling resistance simulations on hard surface shows good correlation with measurements. Soft soil tests are simulated in PAM-CRASH using all soil models. The hybrid quarter SPH soil model has the highest accuracy among all the other models by having 5.3% error in total.

6.2 FUTURE CONSIDERATIONS

The work done to accomplish the goals of this thesis consists of various areas of engineering and science. The best effort has been put in the certain amount of time through the work to simulate each test in the most accurate way possible. However, there is always room for improvement and modification to the methodologies, modeling and testing set up, and physical experiments.

Material of the tire is one factor that there is no possible access to it. The material used is the experimental achievements by previous researchers using optimization methods to have the material properties as accurate as possible. In order to have more realistic tire model material is one thing to be considered.

Another factor which needs consideration is the mesh sensitivity analysis for tire model. As it is known, by having smaller mesh the accuracy of the model will increase, however,

on the other hand the CPU computational time will increase. The results obtained from this specific tire model is satisfactory and the solving time is reasonable, however, by implementing mesh sensitivity analysis the tire model may have the opportunity to become more accurate and efficient at the same time.

In soil modeling, calibration methodologies can be a very good field to be studied in future. By reading various papers, setups for shear strength test is accomplished. Even though the results achieved from shear strength test has a good angle of internal friction, there is still room for modification to reach more accurate results for cohesion.

In the end, this research has opened the floor for rigid ring model simulations. The rigid ring parameters of this tire can be determined both on hard surface and soft soil.

PUBLICATIONS

Marjani, M., El-Gindy, M., Philipps, D., Öijer, F., & Johansson, I. "FEA Tire Modeling and Validation Techniques." *ASME 2015 International Design Engineering Technical Conferences and Computers and Information in Engineering Conference*. American Society of Mechanical Engineers, 2015.

Marjani, M., El-Gindy, M., Philipps, D., Öijer, F., & Johansson, I. “Development of FEA tire/soil interaction model using SPH and hybrid SPH/FEA technique” International Journal of Vehicle Performance. (Accepted)

Note: Some portions of the mentioned publications are used in this thesis. All writing, simulation setups, models, and results are conducted by the author. Revisions, advices and technical support are recived from the co-authors through the work.

REFERENCES

[1] J. Y. Wong, Theory of Ground Vehicles, Ottawa: John Wiley & Sons, Inc., 2008.

[2] R. S. Dhillon, Development of Truck Tire-Terrain Finite Element Analysis Models, Master Thesis, University of Ontario Institute of Technology, 2013.

[3] T. Tires, "www.trazano.be," [Online]. Available: http://www.trazano.be/tire-construction.html.

[4] A. C. Reid, Development and optimization of a wide base FEA truck tire model for prediction of tire-road interactions, Master Thesis, University of Ontario Institute of Technology, 2015.

[5] P. Altidis, B. Warner and V. Adams, "Analyzing Hyperelastic Materials," IMPACT Engineering Solutions, Inc., 2005.

[6] "Michelin Media," 27 03 2014. [Online]. Available: http://michelinmedia.com/c0/michelin-reaches-millionth-michelin-milestone-north-america/.

[7] NASFE, "Executive Report-Wide Base Tires," Driving Innovations-NASFE, 2010.

[8] M. X. Bruchure, "www.michelinb2b.com," Michelin, 2014. [Online]. Available: https://www.michelinb2b.com/wps/b2bcontent/PDF/MICHELIN_X_One_Brochure.pdf.

[9] T. D. Gillespie, Fundamentals of vehicle dynamics, Warrendale, PA: Society of Automotive Engineers, 1992.

[10] H. Rakha, I. Lucic, S. H. Demarchi, J. R. Setti and M. V. Aerde, "Vehicle dynamics model for predicting maximum truck acceleration levels," *Journal of transportation engineering,* vol. 127, no. 5, pp. 418-425, 2001.

[11] K. M. Captain, A. B. Boghani and D. N. Wormley, "Analytical Tire Models for Dynamic Vehicle," *Vehicle System Dynamics,* vol. 8, no. 1, pp. 1-32, 1979.

[12] D. C. Davis, "A radial-spring terrain-enveloping tire model," *Vehicle System Dynamics,* vol. 4, no. 1, pp. 55-69, 1975.

[13] P. W. Zegelaar and H. B. Pacejka, "Dynamic tyre responses to brake torque variations," *Vehicle System Dynamics,* vol. 27, no. S1, pp. 65-79, 1997.

[14] R. N. Yong, E. A. Fattah and P. Brunsinsuk, "Analysis and Prediction of Tyre-Soil Interaction Performance Using Finite Elements," *Journal of Terramechanics,* vol. 15, no. 1, pp. 43-63, 1978.

[15] Y. Nakajima and J. Padovan, "Numerical simulation of tire sliding events involving impacts with holes and bumps," *Tire Science and Technology,* vol. 14.2, pp. 125-136, 1986.

[16] E. Gelosa, "FEA Simulations for Tire Tests: descriptions and validations," in *"Workshop on Tires" at Deutches Institute fur kautschuktechnologie*, Hannover, May 25th-26th,1998.

[17] Y. P. Chang and M. El-Gindy, "Virtual prediction of a radial-ply tire's in-plane free vibration modes transmissibility," *International Journal of Automotive Technology,* vol. 6.2, pp. 149-159, 2005.

[18] R. Ali, M. El-Gindy, R. Dhillon, T. Mukesh, F. Öijer and I. Johansson, "Prediction of Tire Ground Interaction Using FEA Truck Tire Models," in *ASME 2012 International Design Engineering Technical Conferences and Computers and Information in Engineering Conference,* 2012.

[19] S. Chae, Nonlinear finite element modeling and analysis of a truck tire, PhD Thesis, The Pennsylvania State University, 2006.

[20] J. Y. Wong, Terramechanics and off-road vehicles, Amsterdam: Butterworth-Heinemann, 2010.

[21] M. G. Bekker, Theory of land locomotion, 1956.

[22] M. G. Bekker, Off-the-road locomotion: Research and Development in Terramechanics, Ann Arbor: University of Michigan Press, 1960.

[23] M. G. Bekker, Introduction to Terrain-Vehicle Systems. Part I: The Terrain. Part II: The Vehicle, Ann arbor: The University of Michegan, 1969.

[24] Z. Janosi and B. Hanamoto, "The analytical determination of drawbar pull as a function of slip for tracked vehicles in deformable soils," in *Terrain-Vehicle Systems,* Turin, Italy, 1961.

[25] M. S. Osman, "The Measurement of Soil Shear Strength," *Journal of Terramechanics,* vol. 1, no. 3, pp. 54-60, 1964.

[26] R. D. Wismer and H. J. Luth, "Off-road traction prediction for wheeled vehicles," *Journal of Terramechanics,* vol. 10, no. 2, pp. 49-61, 1973.

[27] R. N. Yong, A. F. Youssef and E. A. Fattah, "Vane-cone measurements for assessment of tractive performance in wheel-soil interaction.," in *5th International Conference of the ISTVS,* Detroit, USA, 1975.

[28] T. Hiroma, S. Wanjii, T. Kataoka and Y. Ota, "Stress analysis using FEM on stress distribution under a wheel considering friction with adhesion between a

wheel and soil," *Journal of terramechanics,* vol. 34, no. 4, pp. 225-233, 1997.

[29] S. A. Shoop, "Finite element modeling of tire-terrain interaction," U.S. Army Engineer Research and Development Center, Hanover, 2001.

[30] R. C. Chiroux, W. A. Foster, C. E. Johnson, S. A. Shoop and R. L. Raper, "Three-dimensional finite element analysis of soil interaction with a rigid wheel," *Applied Mathematics and Computation,* vol. 162, no. 2, pp. 707-722, 2005.

[31] J. L. Slade, Development of a New Off-Road Rigid Ring Model for Truck Tires Using Finite Element Analy, Master Thesis, The Pennsylvania State University, 2009.

[32] B. Schlatter, A pedagogical tool using smoothed particle hydrodynamics to model fluid flow past a system of cylinders, Dual MS Project, Oregon State University., 1999.

[33] H. H. Bui, K. Sako and R. Fukagawa, "Numerical simulation of soil–water interaction using smoothed particle hydrodynamics (SPH) method," *Journal of Terramechanics,* vol. 44, pp. 339-346, 2007.

[34] H. H. Bui, R. Fukagawa, K. Sako and S. Ohno, "Lagrangian meshfree particles method (SPH) for large deformation and failure flows of geomaterial using elastic–plastic soil constitutive model," *International Journal for Numerical and Analytical Methods in Geomechanics,* vol. 32, pp. 1537-1570, 2008.

[35] P. H. Groenenboom, "Numerical simulation of 2D and 3D hypervelocity impact using the SPH option in PAM-SHOCK™.," *International Journal of Impact Engineering,* vol. 20.1, pp. 309-323, 1997.

[36] P. H. Groenenboom and B. K. Cartwright, "Hydrodynamics and fluid-structure interaction by coupled SPH-FE method," *Journal of Hydraulic Research,* vol. 48, no. S1, pp. 61-73, 2010.

[37] R. Lescoe, Improvement of Soil Modeling in a Tire-soil Interaction Using Finite Element Analysis and Smoothed Particle Hydrodynamics, Master Thesis, The Pennsylvania State University, 2010.

[38] M. Marjani, M. El-Gindy, D. Philipps, O. Fredrik and J. Inge, "FEA Tire Modeling and Validation Techniques," in *ASME,* Boston, MA, USA, 2015.

[39] R. S. Dhillon, R. Ali, M. El-Gindy, D. Philipps, F. Oijer and I. Johansson, "Development of Truck Tire-Soil Interaction Model using FEA and SPH," in *SAE International,* 2013.

[40] A.-H. M. Sharaf, Investigation of All-Wheel-Drive Off-Road Vehicle Dynamics Augmented by Visco-Lock Devices, PhD Thesis, Loughborough University, 2007.

[41] M. A. McCarthy, J. R. Xiao, C. T. McCarthy, A. Kamoulakos, J. Ramos, J. P. Gallard and V. Melito, "Modelling of bird strike on an aircraft wing leading edge made from fibre metal laminates–Part 2: modelling of impact with SPH bird model.," *Applied Composite Materials*, vol. 11(5), pp. 317-340, 2004.

[42] L.-M. Chu and J.-H. Yin, "Comparison of interface shear strength of soil nails measured by both direct shear box tests and pullout tests," *Journal of geotechnical and geoenvironmental engineering*, vol. 131.9, pp. 1097-1107, 2005.

[43] M. S. Corporation, Wheel Load Measurement System, Milford, MI: http://www.michsci.com/, 2013.

[44] S. K. Clark, Mechanics of Pneumatic Tires, US Department of Transportaion, National Highway Traffic Safety Administration, 1981.

[45] A. L. Priest, D. H. Timm and W. E. Barrett, "Mechanistic comparison of wide-base single vs. standard dual tire configurations," NCAT Report, 05-03, Auburn, AL, 2005.